XI School on Synchrotron Radiation:
Fundamentals, Methods and Applications
Duino Castle / Trieste, Italy / 5-16 September 2011

SiLS
SOCIETA' ITALIANA DI
LUCE DI SINCROTRONE

elettra

Powder Diffraction & Synchrotron Radiation

P. Scardi

Department of Materials Engineering and Industrial Technologies
University of Trento

PRESENTATION OUTLINE

PART I

- Some advantages and peculiarities of synchrotron radiation X-ray powder diffraction (SR-XRPD)
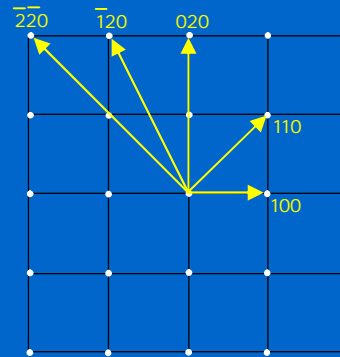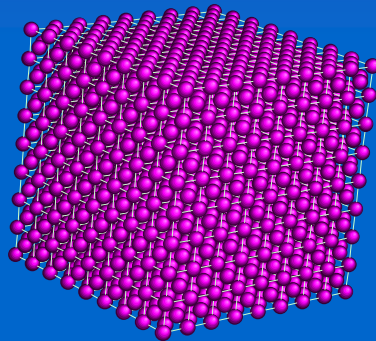
- Main applications of XRPD and SR-XRPD

PART II

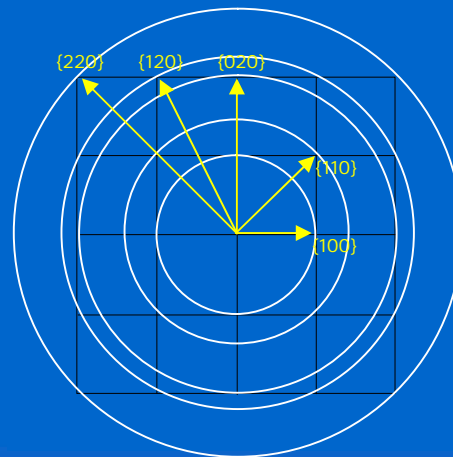- Diffraction from nanocrystalline and highly deformed materials

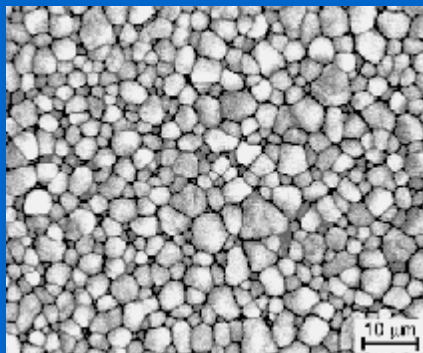single crystal

powder
(bulk polycrystalline)

FIGURE 10.11 Diffraction of monochromatic x-rays from (a) a single crystal and (b) an aggregate of small mineral fragments. (c) Diffraction cones produced by the powder method.
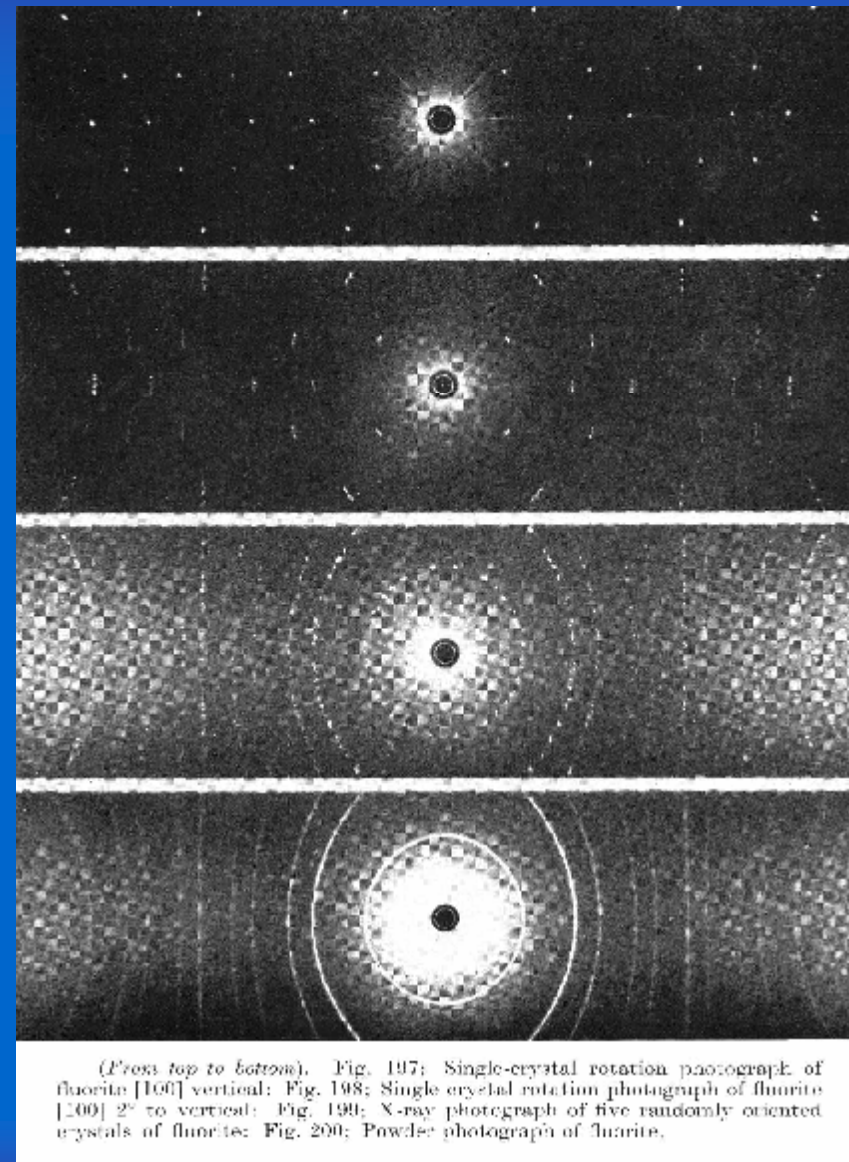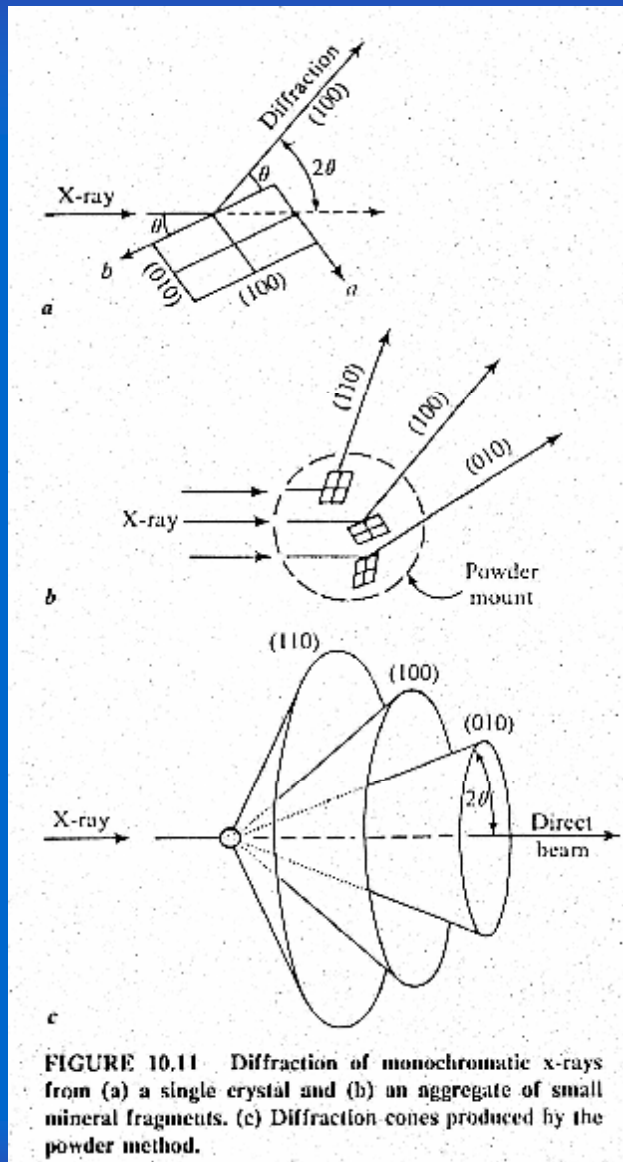
(From top to bottom). Fig. 197; Single-crystal rotation photograph of fluorite [100] vertical: Fig. 198; Single crystal rotation photograph of fluorite [100] 2° to vertical: Fig. 199; X-ray photograph of five randomly oriented crystals of fluorite: Fig. 200; Powder photograph of fluorite.
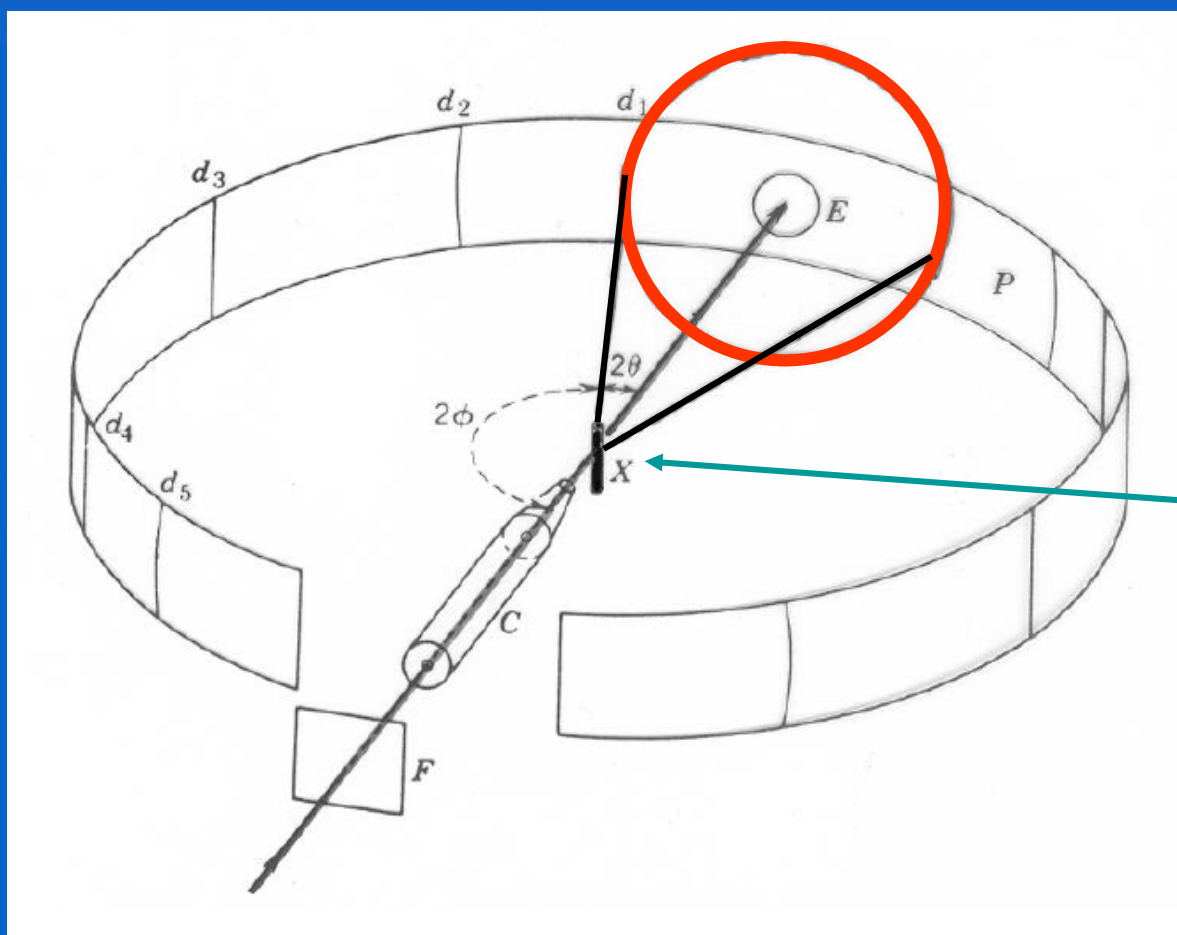
POWDER

ID31 Goniometer and nine-crystal analyzer

Parallel beam geometry at ID31 (ESRF)
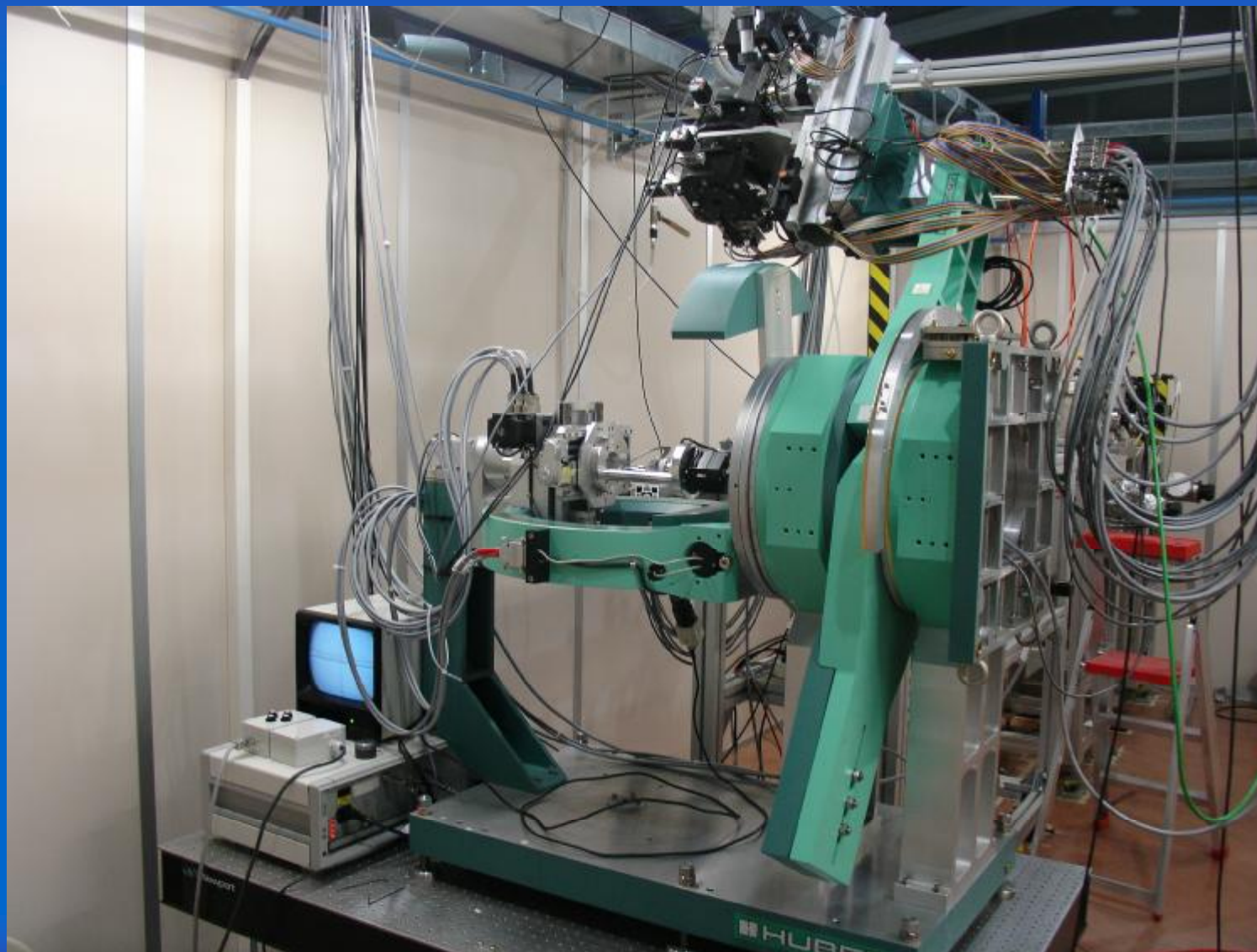### capillary holder / high temperature blower
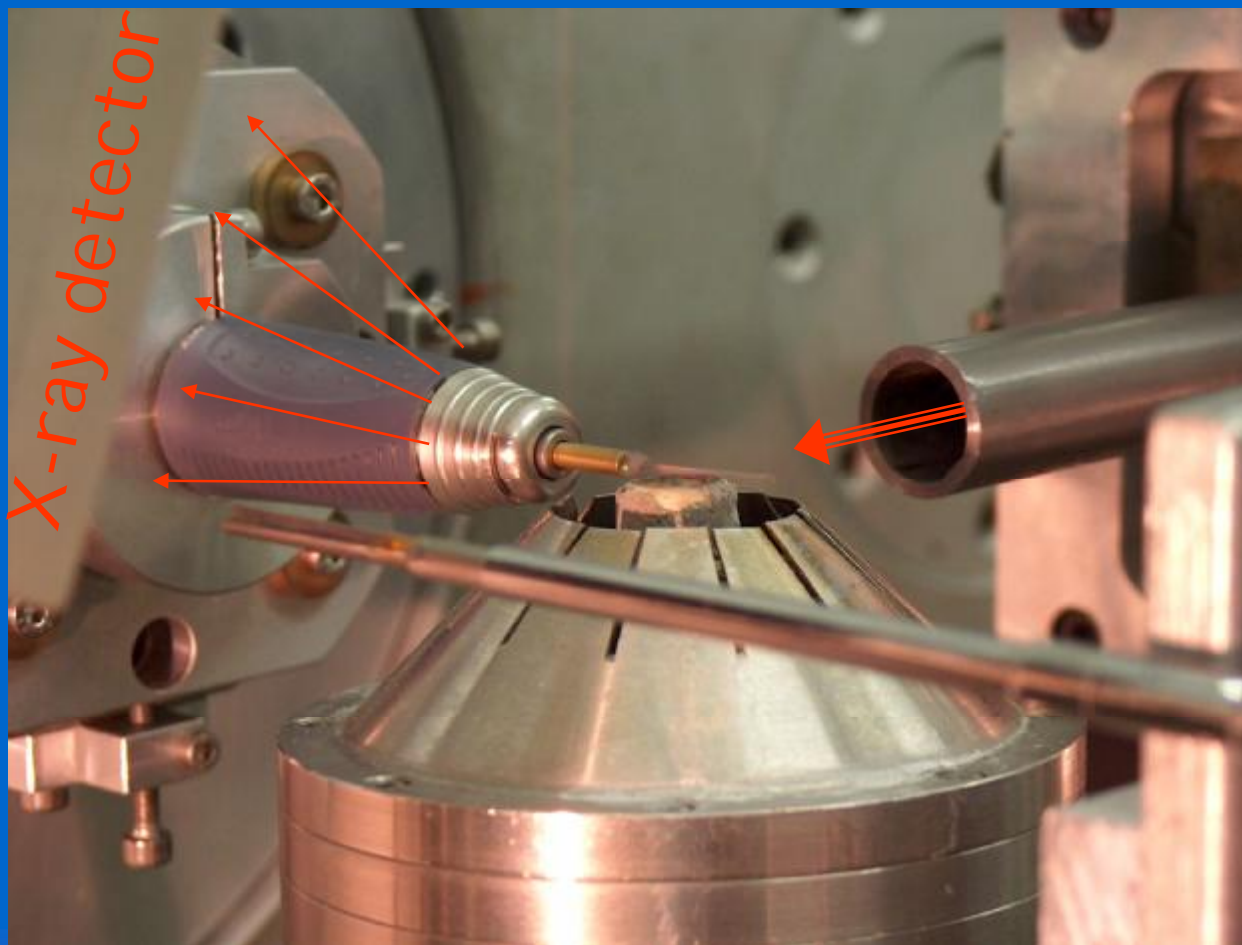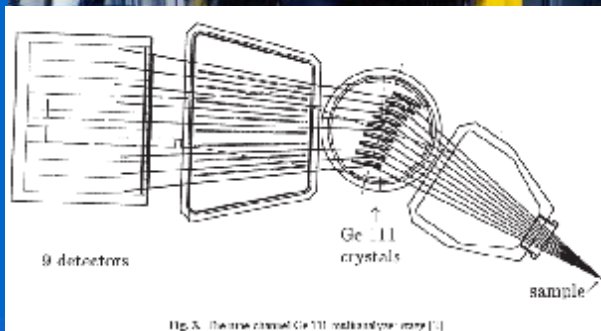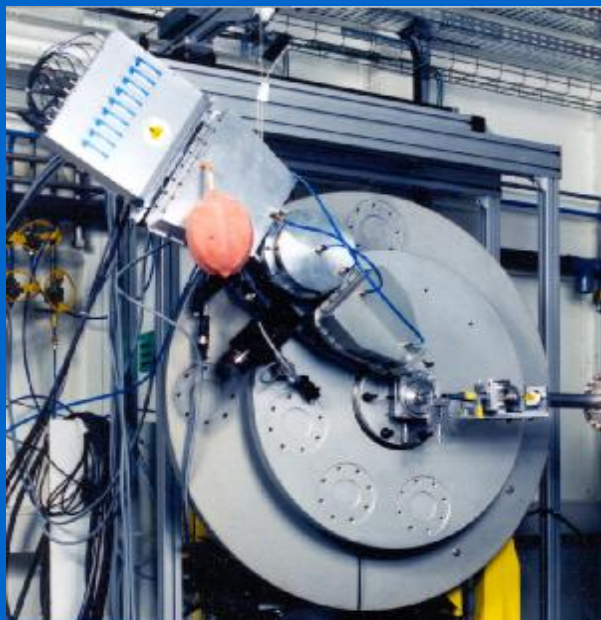
Parallel beam geometry of MCX (Elettra)
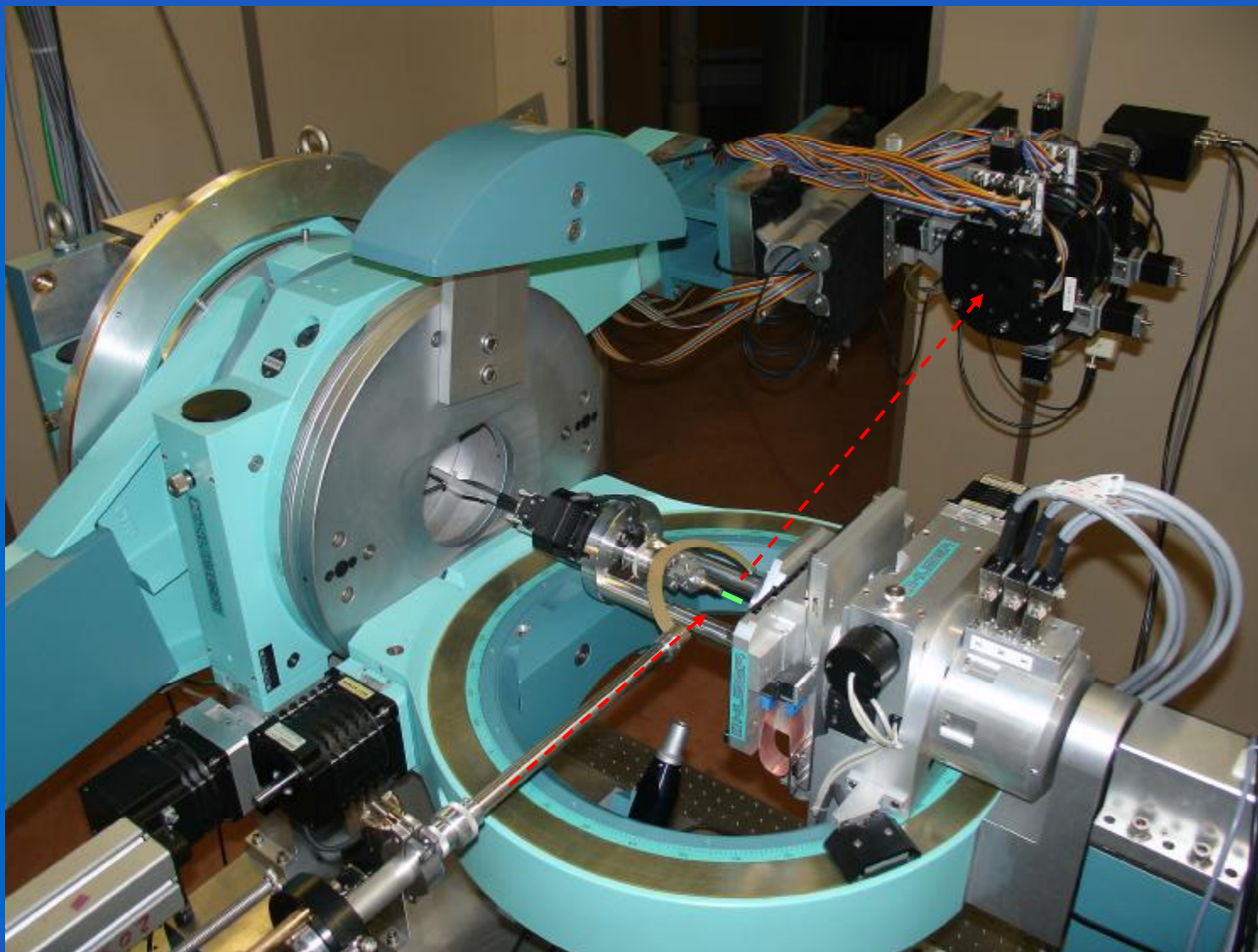
Parallel beam geometry of MCX (Elettra)

Parallel beam geometry of MCX (Elettra)

BEAMTIME APPLICATIONS:
DEADLINE IS SEPTEMBER 15th
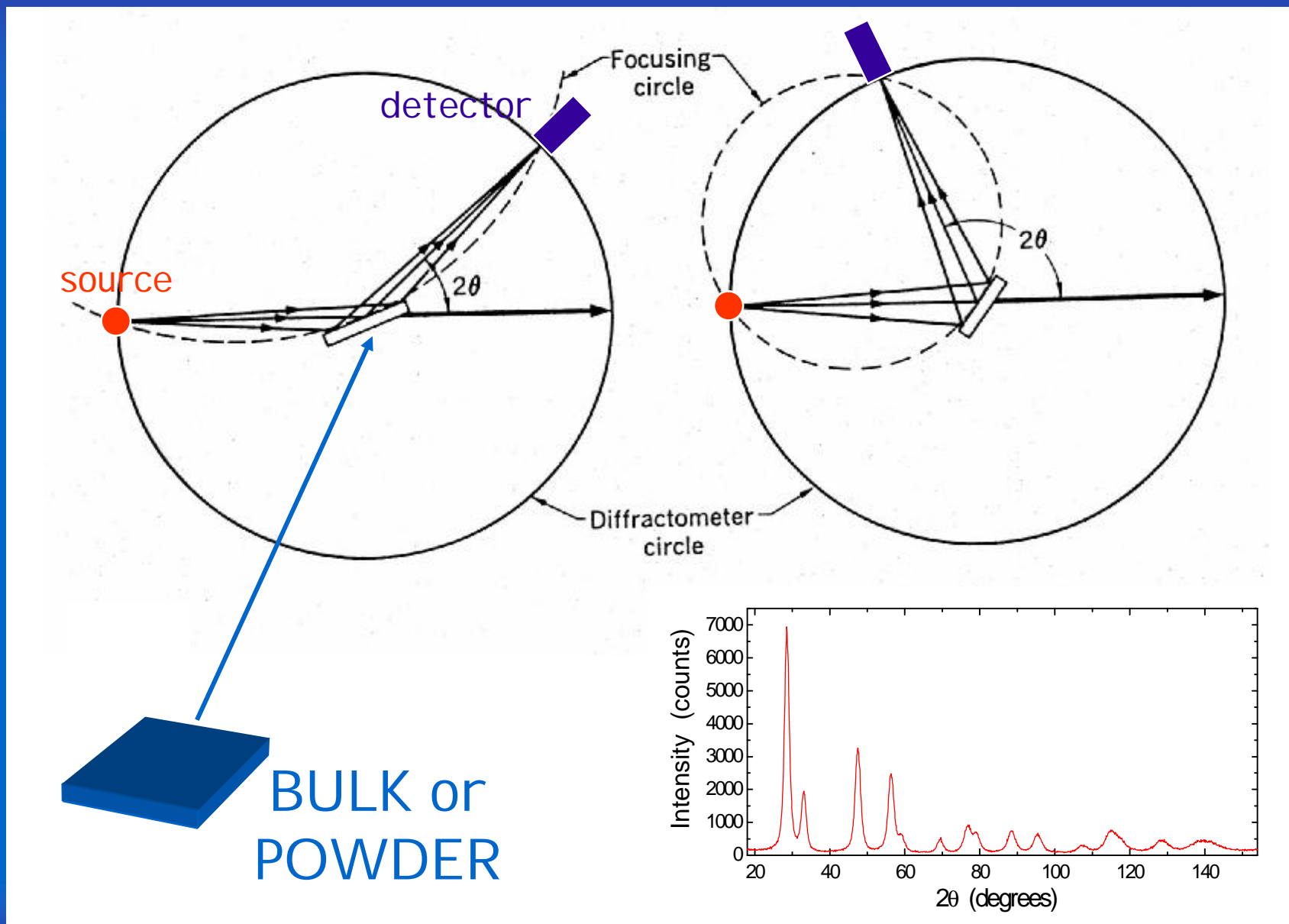
(why) do we need synchrotron radiation?

Early microscope
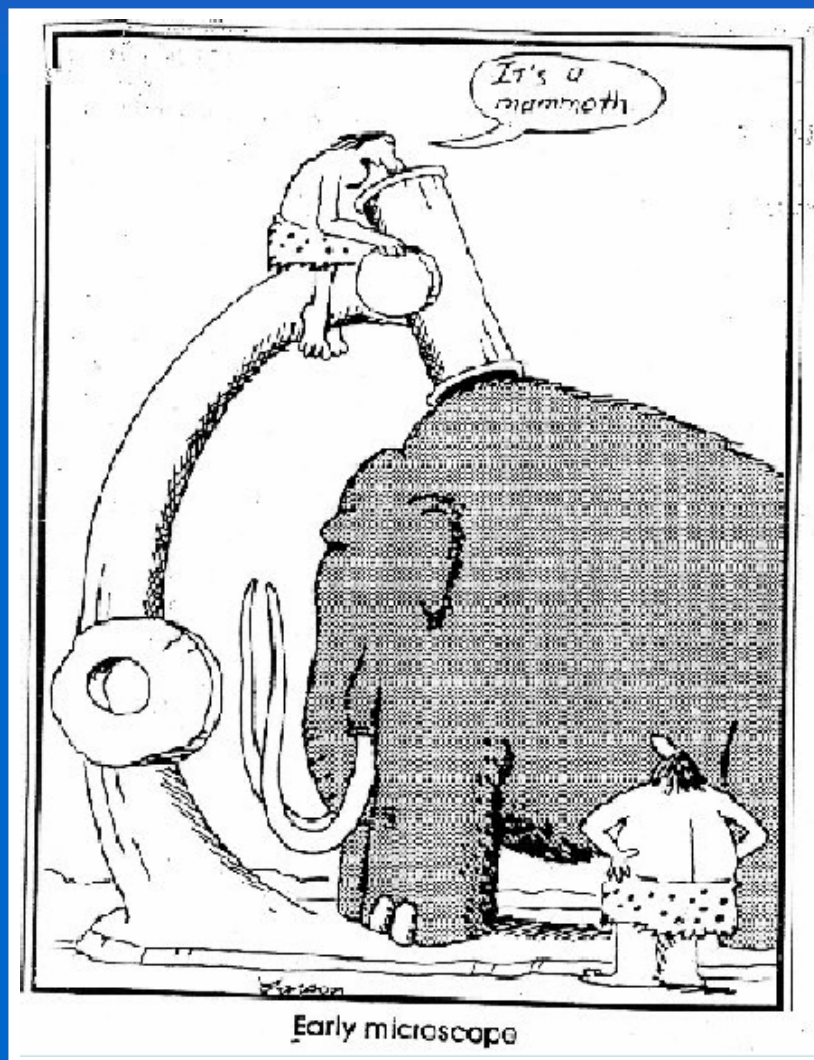
quoted by G. Artioli

... never use a cannon
to kill a fly !

1) High brillance, much better counting statistics / shorter data collection time (à fast kinetics, in situ studies)

Lab instrument: ~80.000s

9-crystal analyzer: 1.500s! (x100 counts)

$$\frac{counts \cdot N° \text{ of peaks}}{time} = 1$$

=25.000
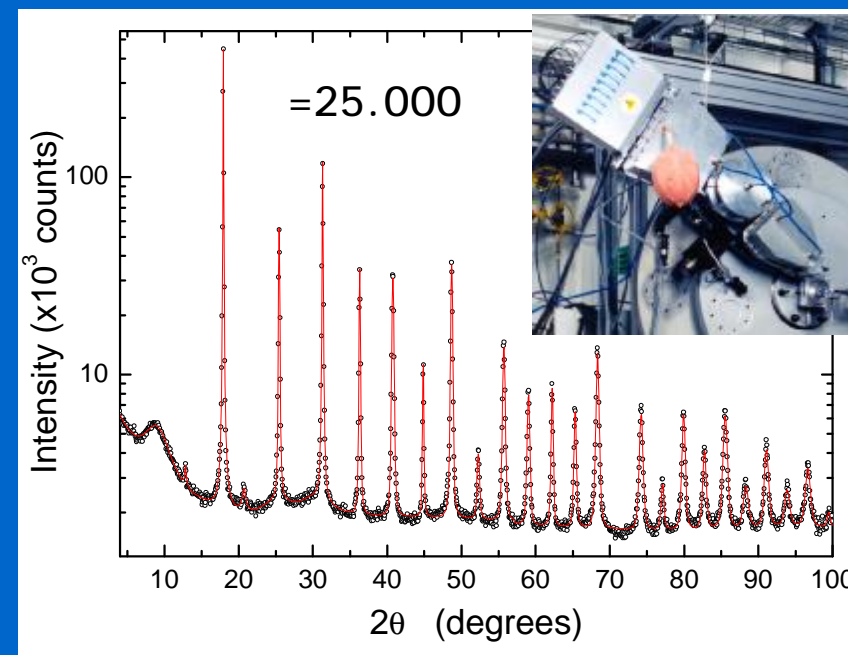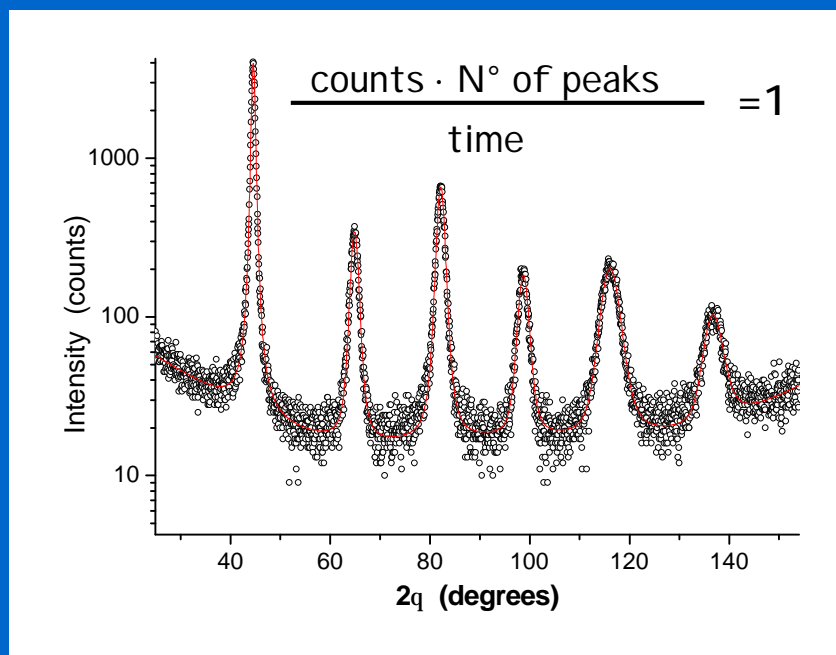
CuKα λ=0.15406 nm   ESRF ID31 λ=0.0632 nm

iron powder (ball milled)

1) High brillance, much better counting statistics / shorter data collection time (à fast kinetics, in situ studies)

Lab instrument: ~80.000s

Mythen detector: 100 s !! (x100 counts)

$$\frac{counts \cdot N° \text{ of peaks}}{time} = 1$$

=350.000
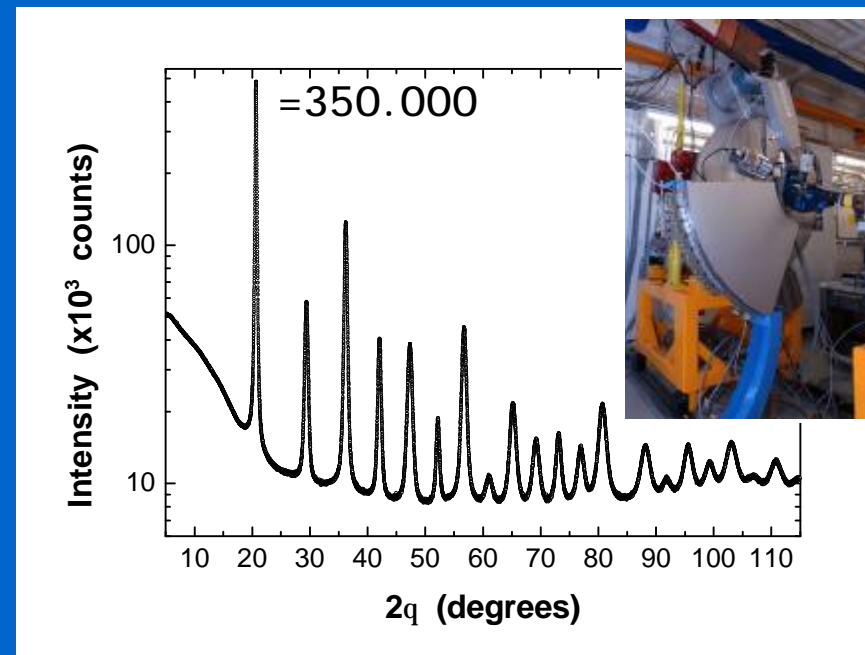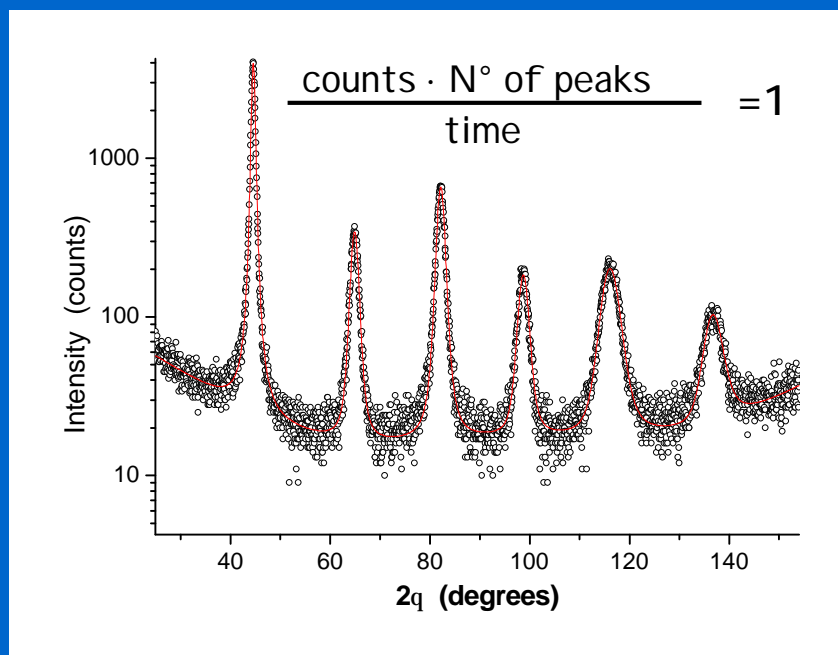
CuKα λ=0.15406 nm   PSI MS-X04SA λ=0.072929 nm

iron powder (ball milled)

2) With proper selection of optics, very narrow instrumental profile: increased resolution and accuracy in the measurement of peak position, intensity and profile width/shape.
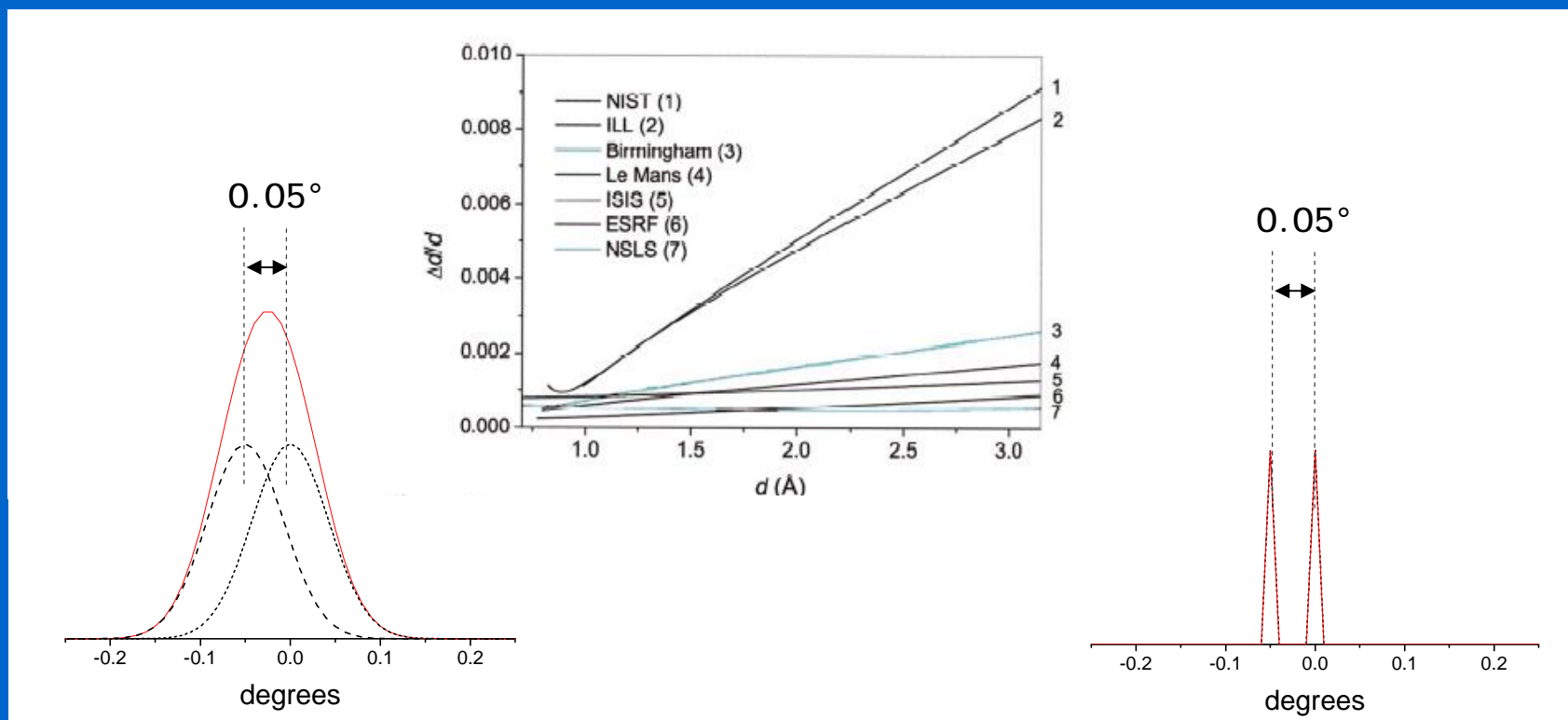
Lab instrument:
FWHM≈0.05-0.1°

ID31 @ESRF:
FWHM≈0.003-0.004°

3) Extending the accessible region of reciprocal space well beyond what traditional lab instruments can make

$$\lambda_1 \qquad\qquad \lambda_2 < \lambda_1$$

3) Extending the accessible region of reciprocal space well beyond what
   traditional lab instruments can make

Lab instrument: ~80.000s   9-crystal analyzer: 1.500s ! (x100 counts)
            : 6 peaks   : 28 peaks
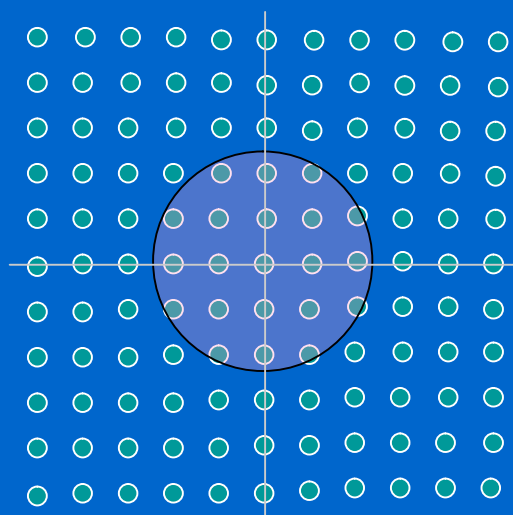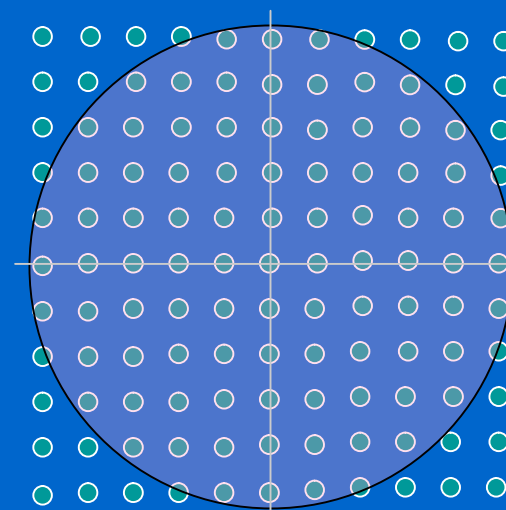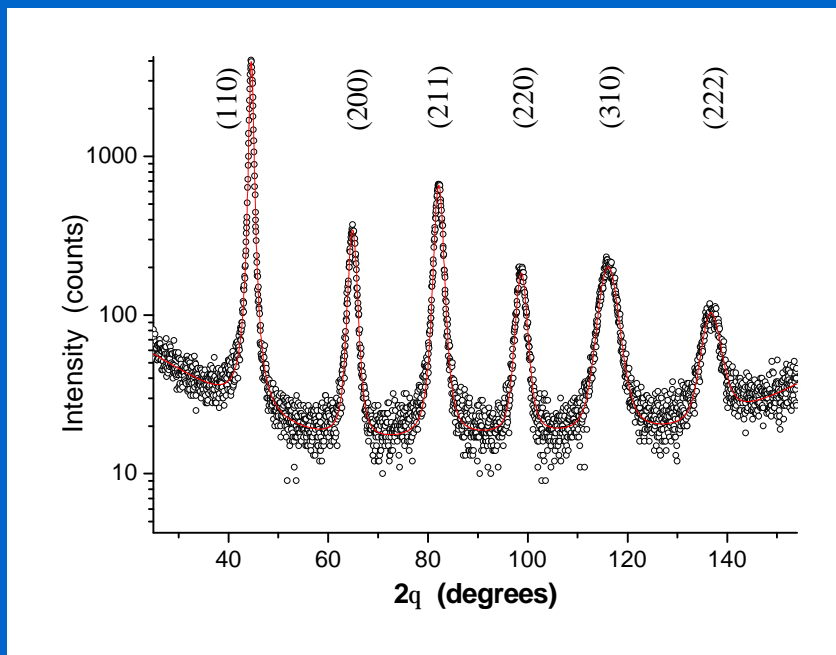

CuKα λ=0.15406 nm   ESRF ID31 λ=0.0632 nm
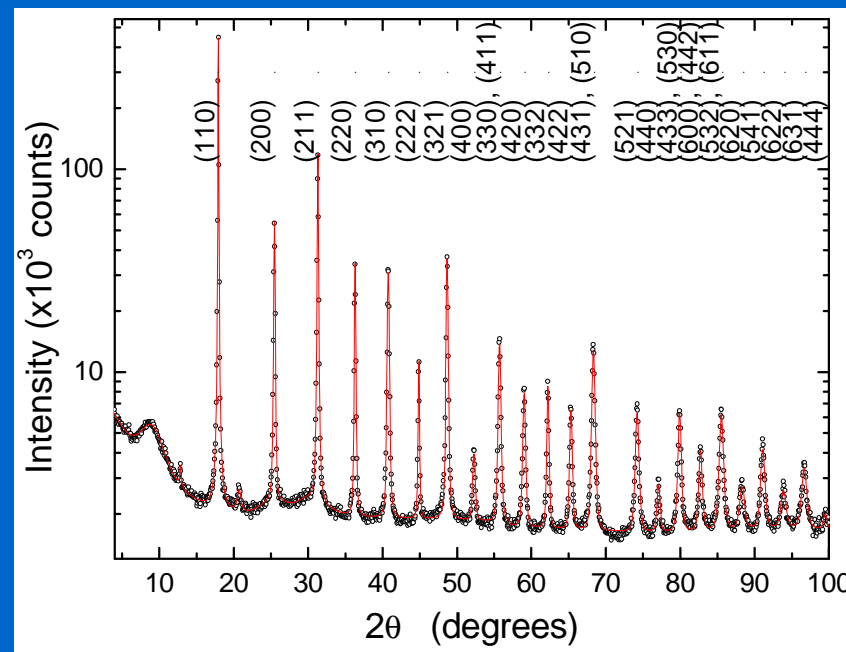
4) Tuning the energy according to adsorption edges. Resonant scattering, control of fluorescence emission and depth of analysis.

$$I = I_0 e^{-\left(\frac{m}{r}\right)rt}$$

QUESTIONS ??

P. Scardi – Powder Diffraction & Synchrotron Radiation

X-RAY POWDER DIFFRACTION

most frequent applications

- Crystal structure determination
  (Powder diffraction structure solution and refinement)

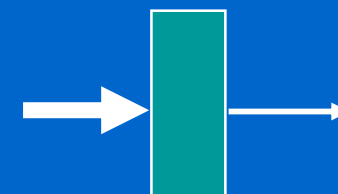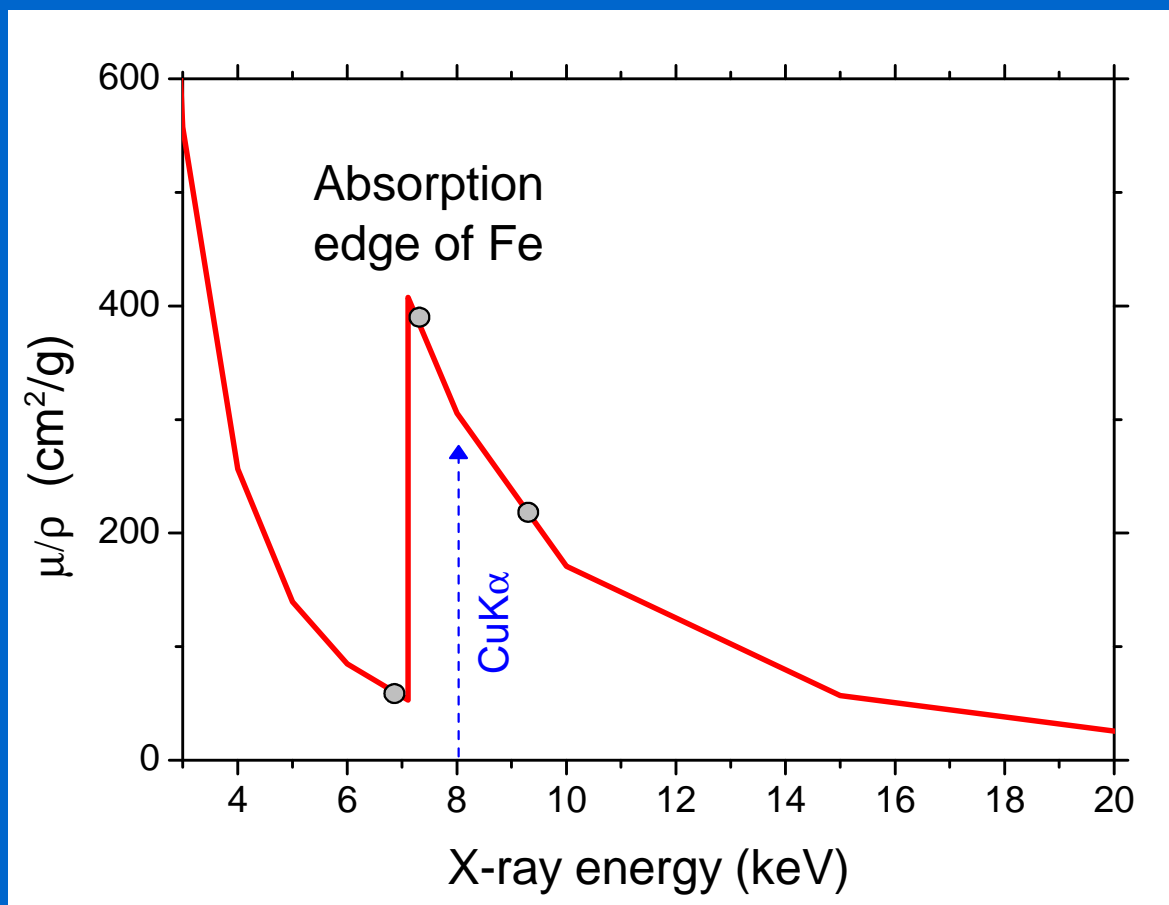- Phase Identification – pure crystalline phases or mixtures
  (Search-Match procedures)

- Phase Quantification - Quantitative Phase Analysis (QPA)

- Amorphous phase analysis (radial distribution function)
  and Total Scattering – PDF analysis

- Crystalline domain size/shape and lattice defect analysis
  (Line Profile Analysis - LPA)

- Determination of preferred orientations (Texture Analysis)

- Determination of residual stress field   (Residual Stress Analysis)

Selected examples
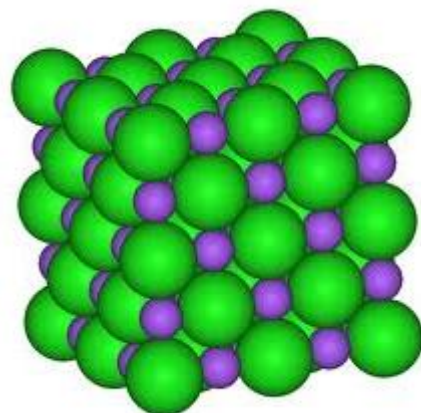
hollow microsphere

Halite – NaCl

J. Zhang et al.
Angew. Chem. Ind. Ed. 50 (2011) 6044

single crystal

powder

Structure solution of heptamethylene-1,7-bis(diphenylphosphane oxide)

Structural formula

$Ph_2P(O)(CH_2)_7P(O)Ph_2$
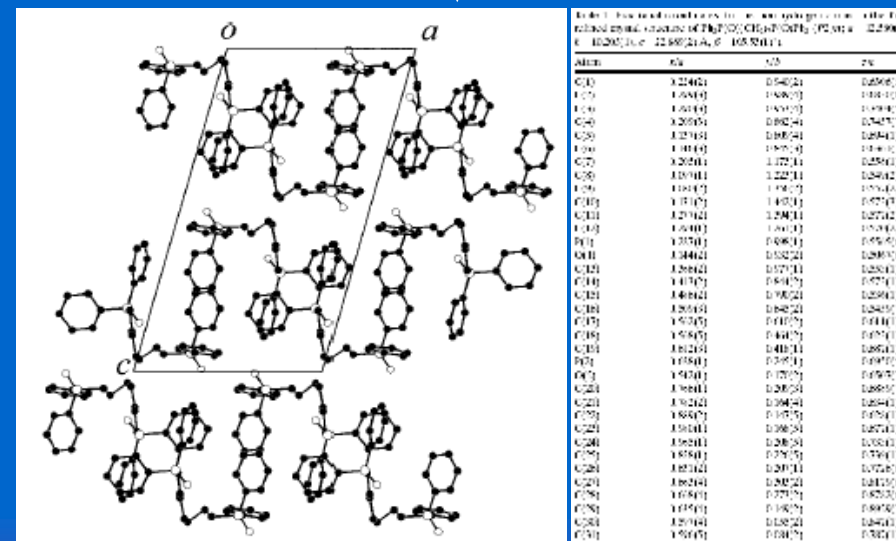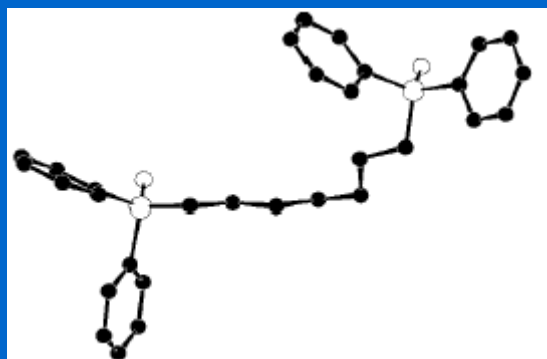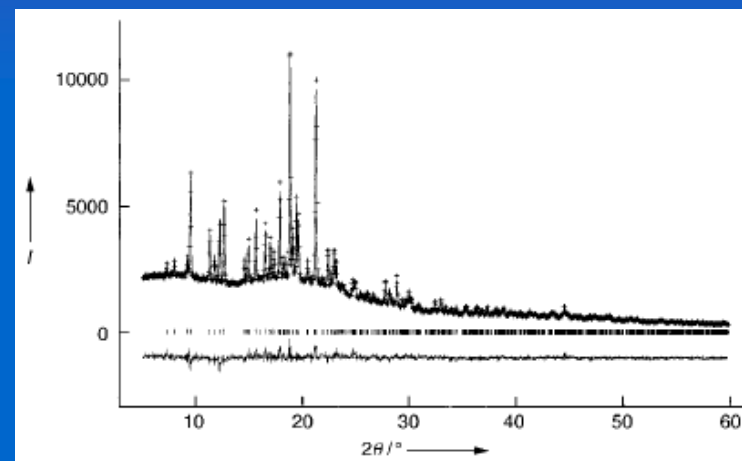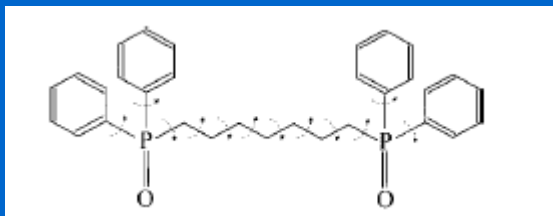
B.M. Kariuki, P. Calcagno, K. D. M. Harris, D. Philp and R.L. Johnston, Angew. Chem. Int. Ed. 1999, 38, No. 6, 831-835.

Structure solution/refinement of a complex triclinic organic compound ($C_{24}H_{16}O_7$)

K. D. Knudsen *et al.*, Angew. Chem. Int. Ed., 37 (1998) 2340

Fluorescein diacetate
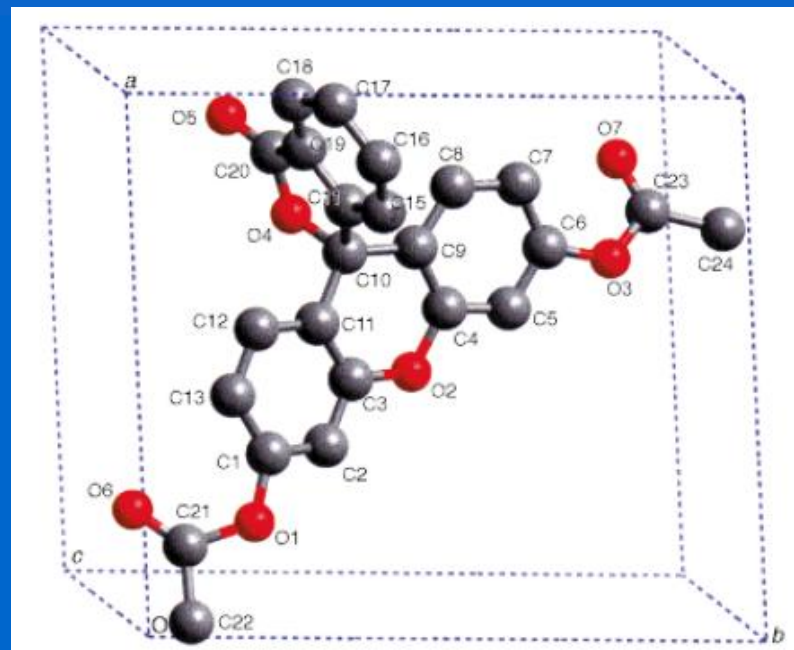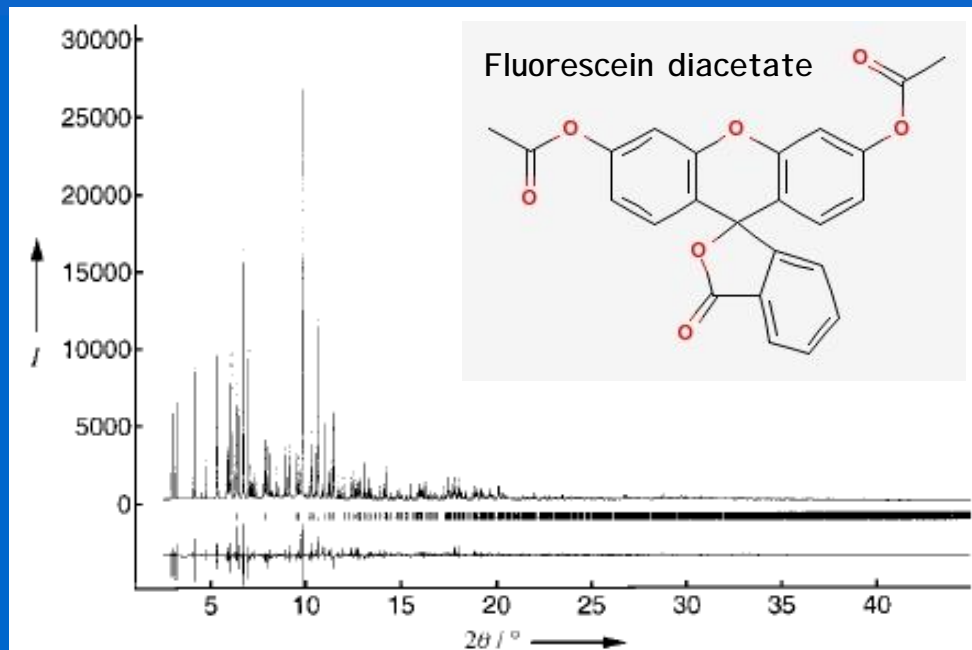
- Narrow peak profiles
- Large number of measurable peaks
- Accurate peak position/intensity
- X-ray energy tuning to adsorption edges

Crystalline
structure

↓

long-range order

Crystalline SiO₂   Amorphous SiO₂
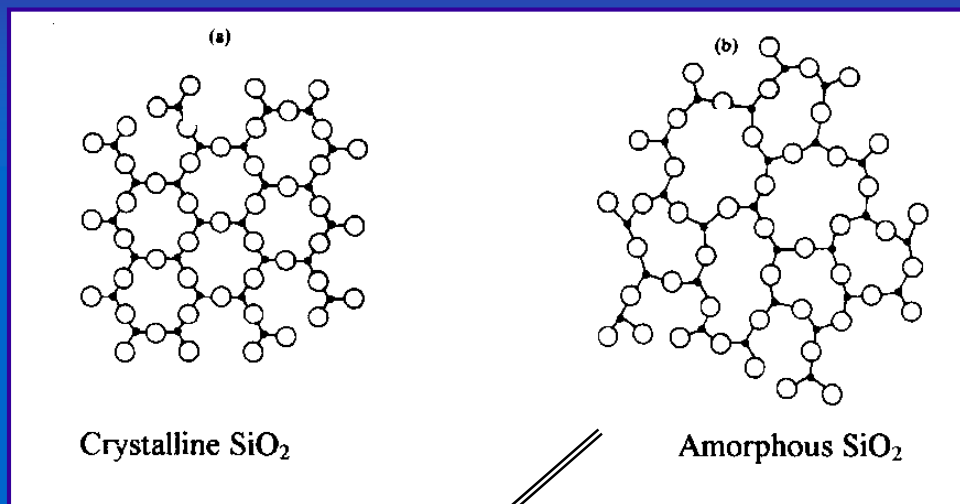
Amorphous
phase

↓

short-range order

Amorphous specimen of volume V (N atoms with scattering factor f_i):

$$I(s) \cong Nf^2 \left\{ 1 + \frac{1}{q} \int_V 4pr\left[r(r) - r_0 \right] \sin(qr) dr \right\} \quad (q = 2ps = 4p\sin q/1)$$

By Fourier inversion:

$$RDF(r) \equiv 4pr^2 r(r) \cong 4pr^2 r_0 + \frac{2r}{p} \int_0^\infty q\left[\frac{I(q)}{Nf^2} - 1 \right] \sin(qr) dq$$

RDF – Radial Distribution Function

Structure of nanocrystalline materials using atomic Pair Distribution Function (PDF) analysis: study of LiMoS$_2$. (V. Petkov *et al.*, Phys. Rev. B 65 (2002) 092105)

$$reduced\ PDF:\ G(r) = 4pr[r(r) - r_0] = \frac{RDF(r)}{r} - 4prr_0$$

FIG. 1. Experimental structure functions of (a) LiMoS$_2$ and (b) MoS$_2$. Note the different scale between (a) and (b). The data are shown in an expanded scale in the insets.
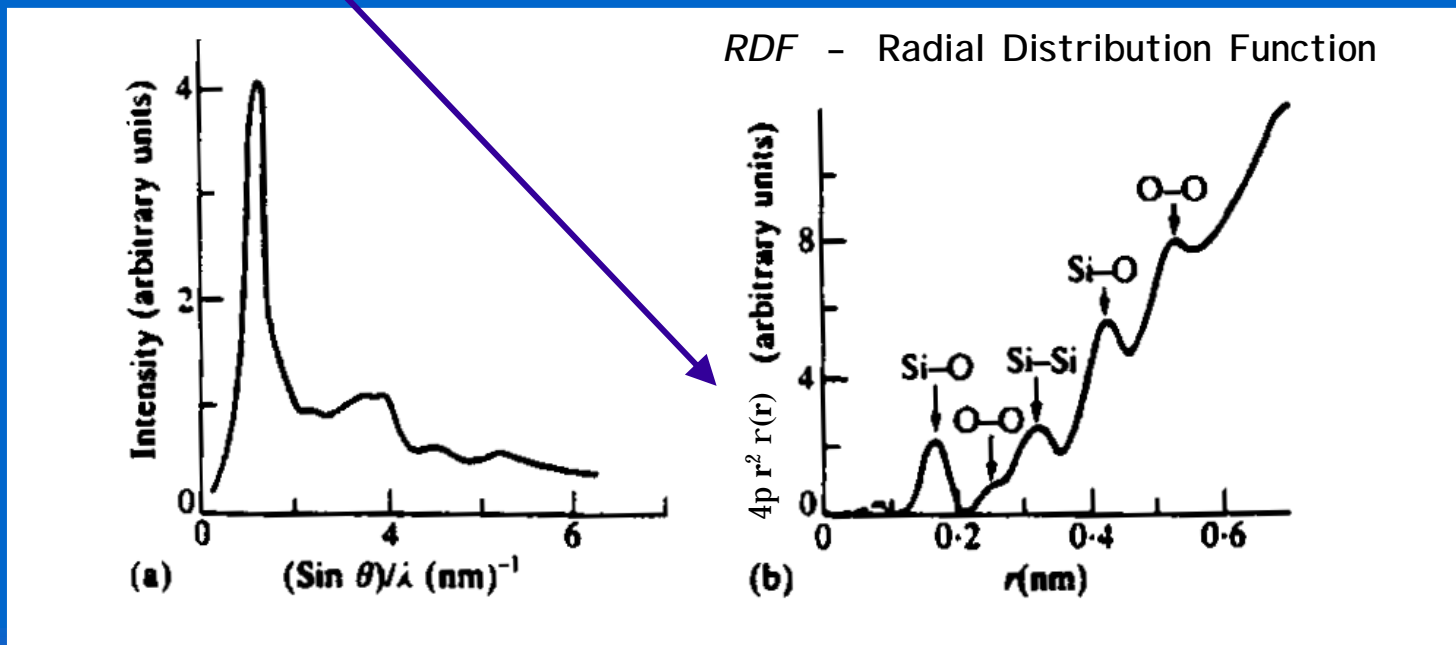
FIG. 2. Experimental (dots) and fitted (solid line) PDF's for LiMoS$_2$ (a) and MoS$_2$ (b). Note the different scale between (a) and (b). The first two peaks in the PDF's are labeled with the corresponding atomic pairs. The experimental data are shown in an expanded scale in the insets.

Structure of nanocrystalline materials using atomic Pair Distribution Function (PDF) analysis: study of LiMoS$_2$. (V. Petkov *et al.*, Phys. Rev. B 65 (2002) 092105)

$$reduced\ PDF : \quad G(r) = 4pr\left[r(r) - r_0 \right] = \frac{RDF(r)}{r} - 4prr_0$$

TABLE I. Structural parameters for MoS$_2$. Space group is $P6_3/mmc$. Mo is at $(\tfrac{1}{3}, \tfrac{2}{3}, \tfrac{1}{4})$ and S at $(\tfrac{1}{3}, \tfrac{2}{3}, z)$.

	PDF	Rietveld	Single crystal[a]
a (Å)	3.169(1)	3.168(1)	3.1604(2)
c (Å)	12.324(1)	12.322(1)	12.295(2)
z	0.623(1)	0.625(1)	0.629(1)

FIG. 4. Projection down the c axis of the crystal structures of hexagonal MoS$_2$ (up) and triclinic LiMoS$_2$ (down). The large black circles are Mo atoms and the small gray circles are the S atoms. Li atoms are not shown for the sake of clarity.
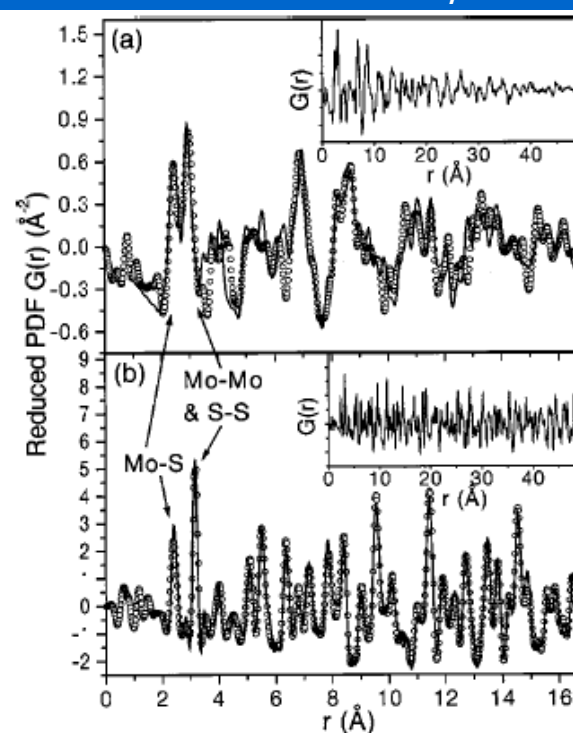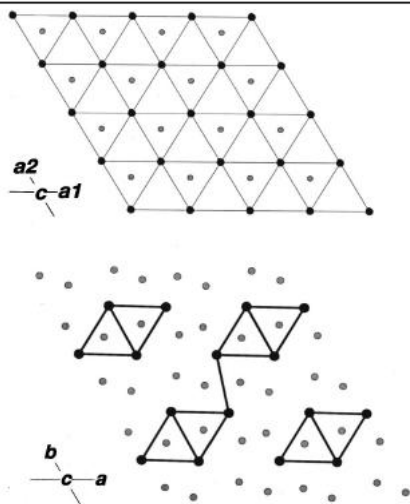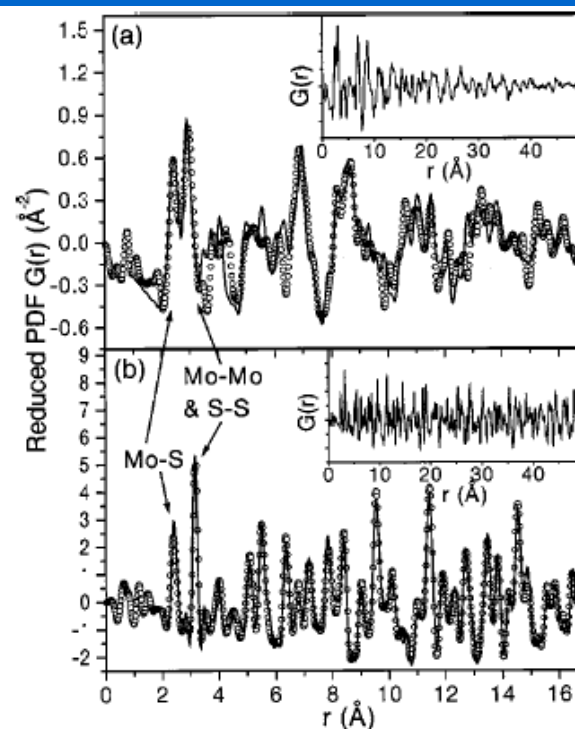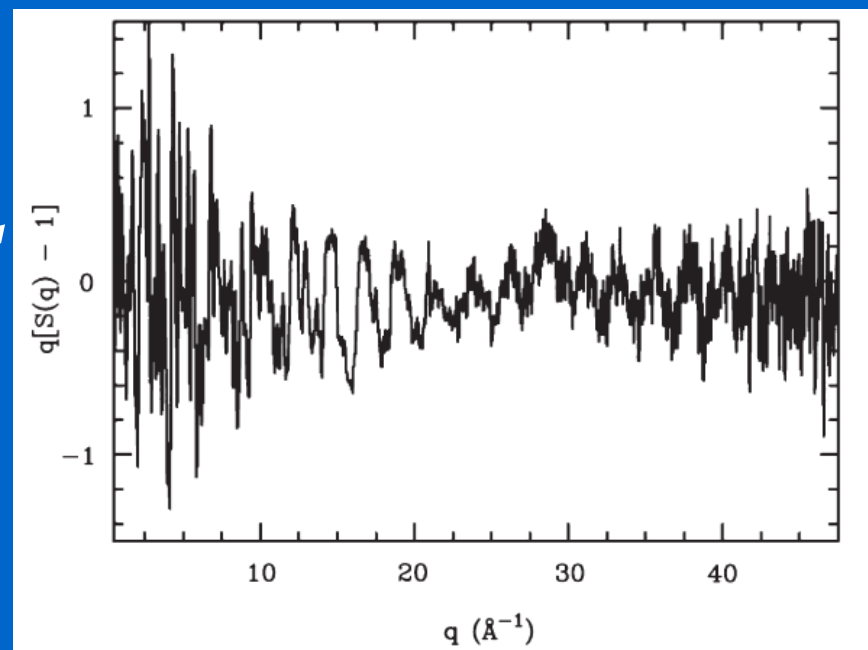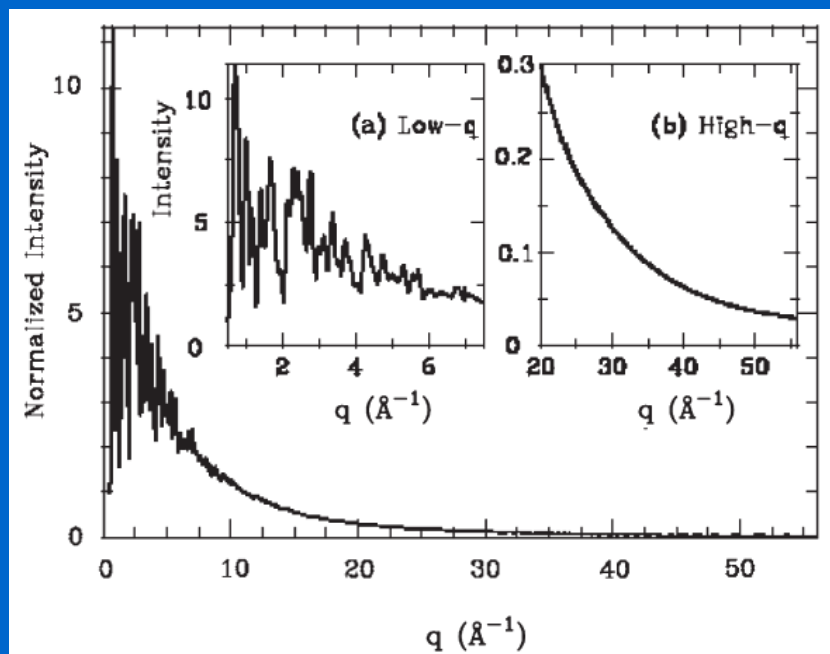

FIG. 2. Experimental (dots) and fitted (solid line) PDF's for LiMoS$_2$ (a) and MoS$_2$ (b). Note the different scale between (a) and (b). The first two peaks in the PDF's are labeled with the corresponding atomic pairs. The experimental data are shown in an expanded scale in the insets.

Bragg and diffuse scattering analysis to high q values

$$G(r) = 4pr\left[r(r) - r_0\right] \cong \frac{2}{p}\int_0^\infty q\left[\frac{I(q)}{Nf^2} - 1\right]\sin(qr)\,dq \quad (q = 2ps = 4p\sin q/l)$$

X-ray energy as high as 100 keV (!)
e.g., APS 11-ID-B, 90-91 keV

$$q\left[\frac{I(q)}{Nf^2} - 1\right] = q\left[S(q) - 1\right]$$

total scattering function

Eulerian cradle for stress/texture measurement

Zirconia thin film with non-uniform microstructure across thickness

fibre texture

Top layer

Interface layer

CaSZ

SiO$_2$

Si

720 nm
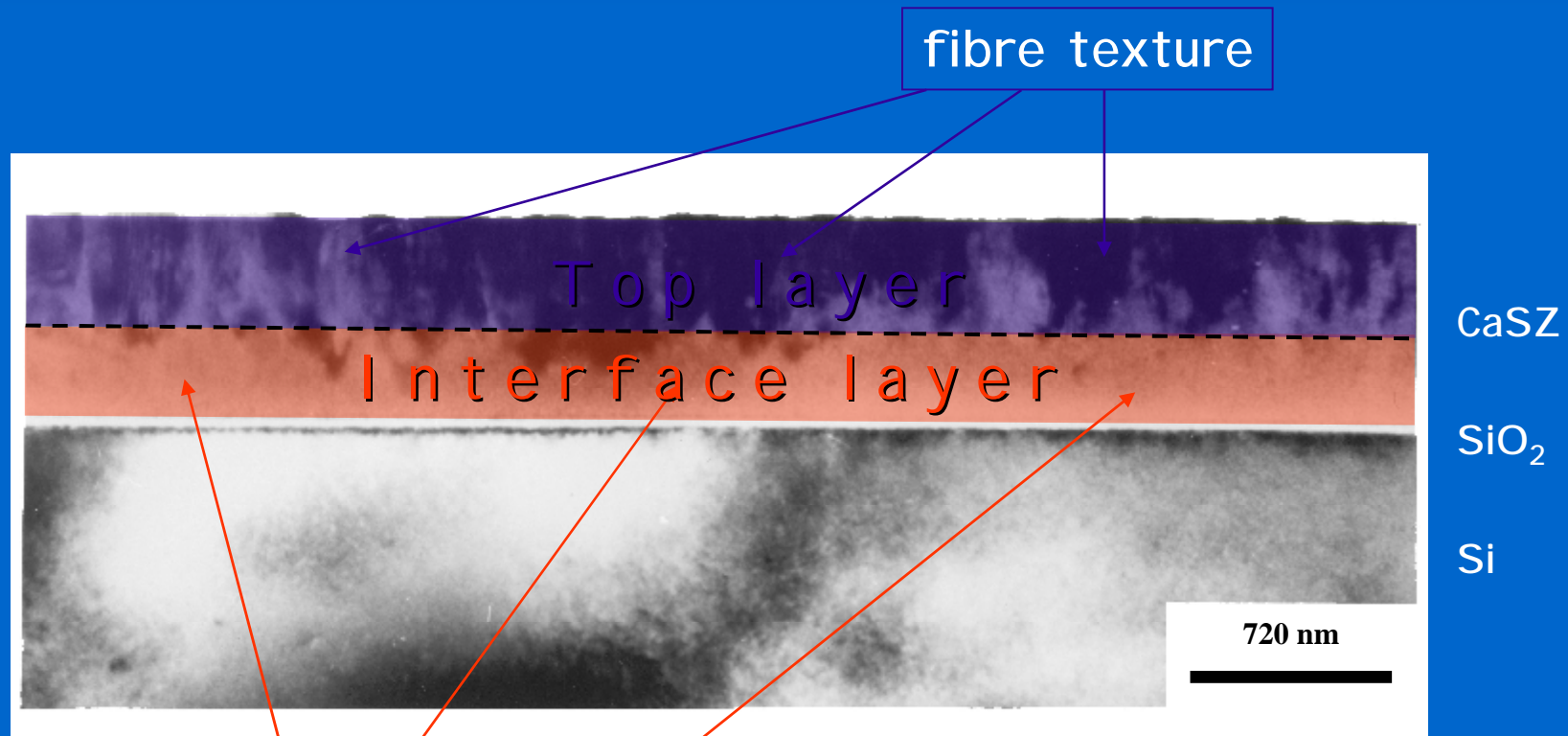
polycristalline (random oriented grains)

Zirconia thin film with non-uniform microstructure across thickness

Below ZrKa edge

Above ZrKa edge

Top layer

Interface layer

CaSZ

SiO
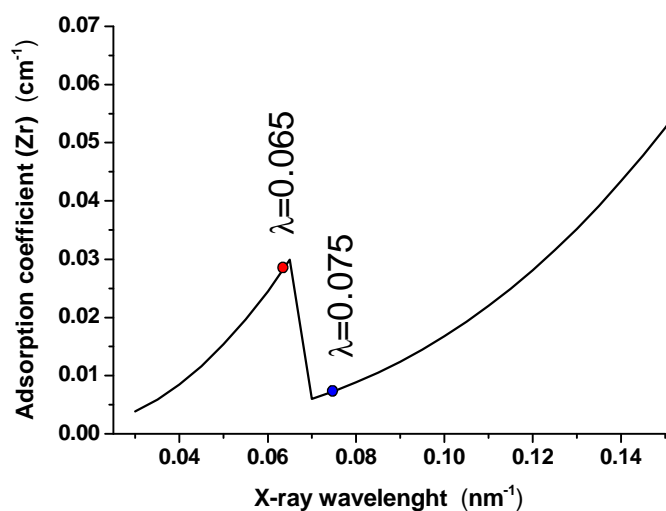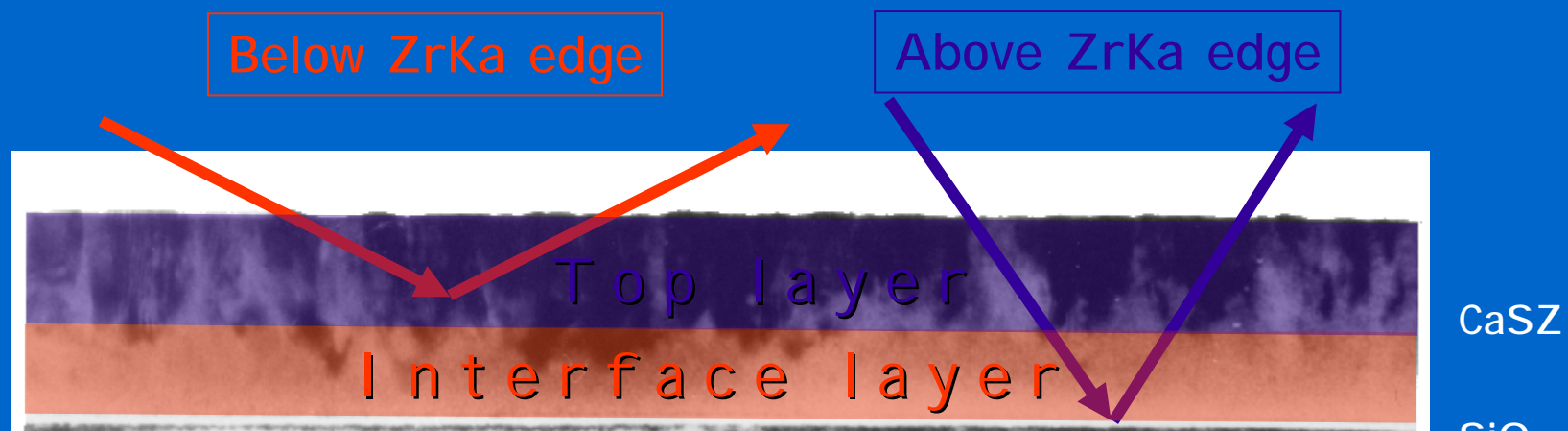
P. Scardi, Leoni, M. D'Incau, Thin Solid Films, 467 (2004) 326.
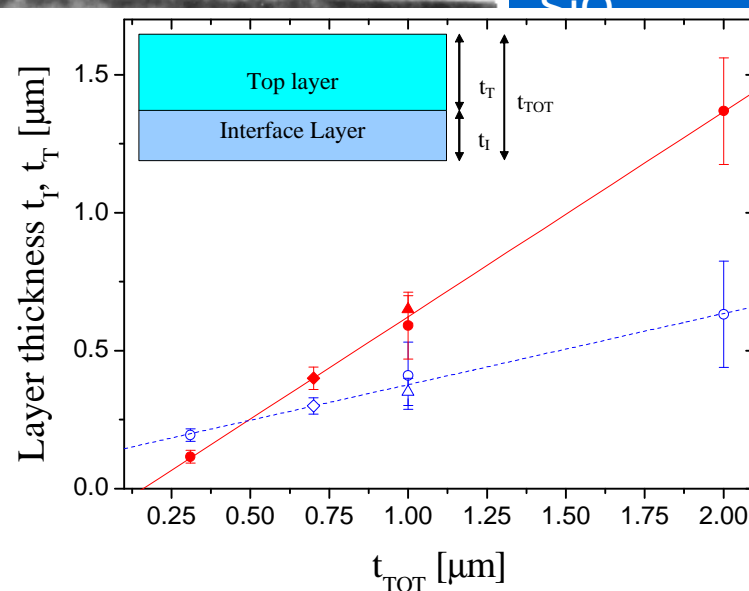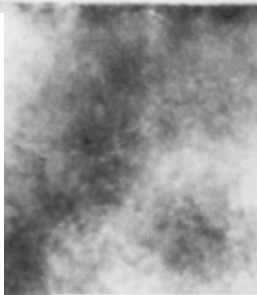
diamond coated Ti-alloy tools: multiple energy (wavelength) analysis

compression
λ = 1.66 Å

(024) TiC

compression
λ = 2.15 Å

(220) diamond

tension
λ = 1.68 Å

α-Ti (121)

Diamond — −6.37(1) GPa

TiC — −1.36(2) GPa

a-Ti(C) — +68(7) MPa

+97(10) MPa

P. Scardi – Powder Diffraction & Synchrotron Radiation

QUESTIONS ??

P. Scardi – Powder Diffraction & Synchrotron Radiation
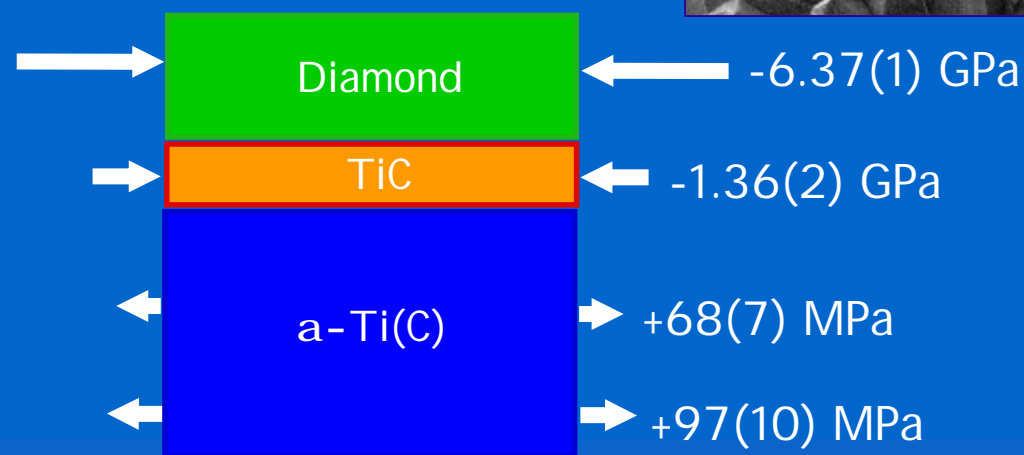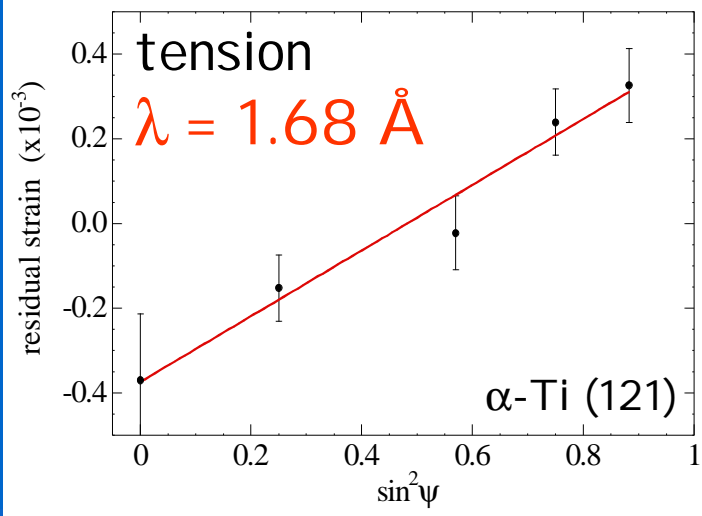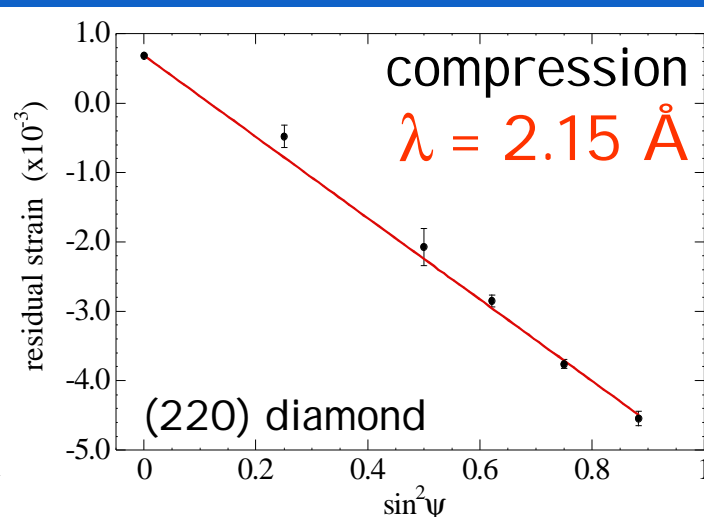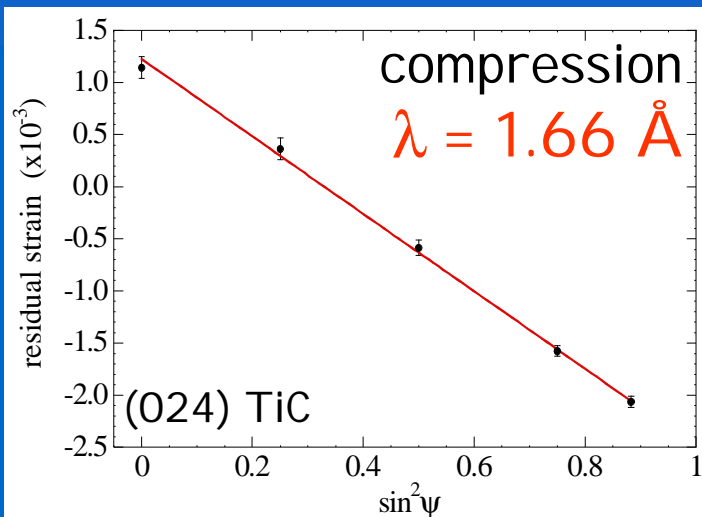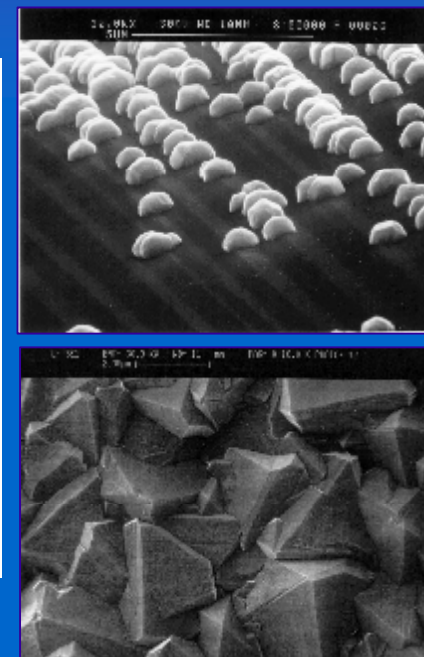
SCATTERING FROM NANOCRYSTALS

Scattering from a small crystal of Cu (*fcc*)

$s_0/1$

$\underline{d}^*$

$s/1$

$\underline{r}_m$

O

$\underline{r}_n$
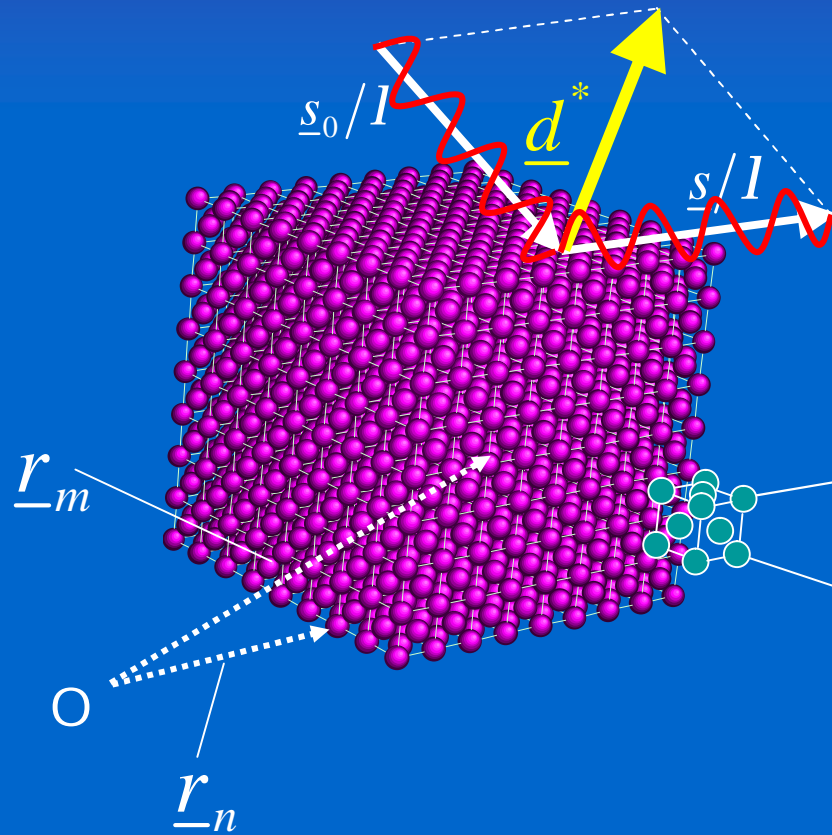
One scattering centre
(electron, atom, unit cell)

$$I \propto \left|A\right|^2 = AA^*$$

$$I_c \propto \sum_m A_m \sum_n A_n^* = \sum_m f_m e^{2pi\left(\underline{d}^* \cdot \underline{r}_m\right)} \sum_n f_n e^{-2pi\left(\underline{d}^* \cdot \underline{r}_n\right)}$$

Scattering from a unit cell of Cu (*fcc*)

$$O \qquad \underline{r}_m \qquad \underline{r}_n$$

$$I_{uc} \propto \sum_m f_m e^{2pi\left(\underline{d}^* \cdot \underline{r}_m\right)} \sum_n f_n e^{-2pi\left(\underline{d}^* \cdot \underline{r}_n\right)}$$

Scattering from two atoms in a Cu (*fcc*) unit cell

$$\underline{r}_{mn} = \underline{r}_m - \underline{r}_n$$

$\underline{r}_m$

$\underline{r}_n$

O

$$I_{uc} \propto \sum_m f_m e^{2pi\left(\underline{d}^* \cdot \underline{r}_m\right)} \sum_n f_n e^{-2pi\left(\underline{d}^* \cdot \underline{r}_n\right)} = \sum_m \sum_n f_m f_n e^{2pi\left(\underline{d}^* \cdot \underline{r}_{mn}\right)}$$

Scattering from two atoms in a Cu (*fcc*) unit cell

$$\underline{d}^* = \frac{\underline{s} - \underline{s}_0}{l} = \frac{2\sin q}{l}$$
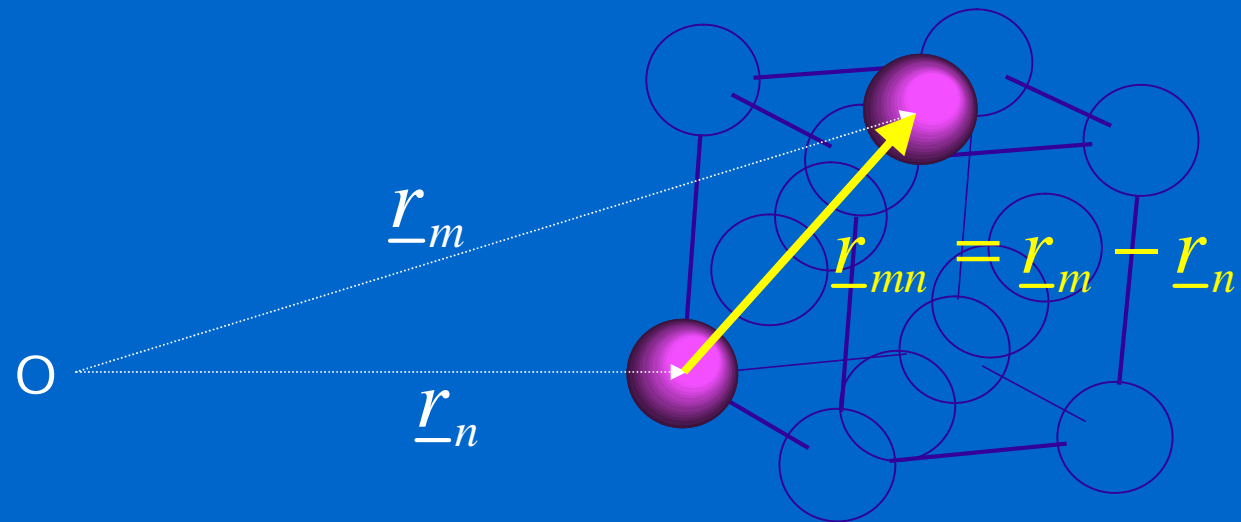

$$I_{uc} \propto \sum_m f_m e^{2pi\left(\underline{d}^* \cdot \underline{r}_m\right)} \sum_n f_n e^{-2pi\left(\underline{d}^* \cdot \underline{r}_n\right)} = \sum_m \sum_n f_m f_n e^{2pi\left(\underline{d}^* \cdot \underline{r}_{mn}\right)}$$
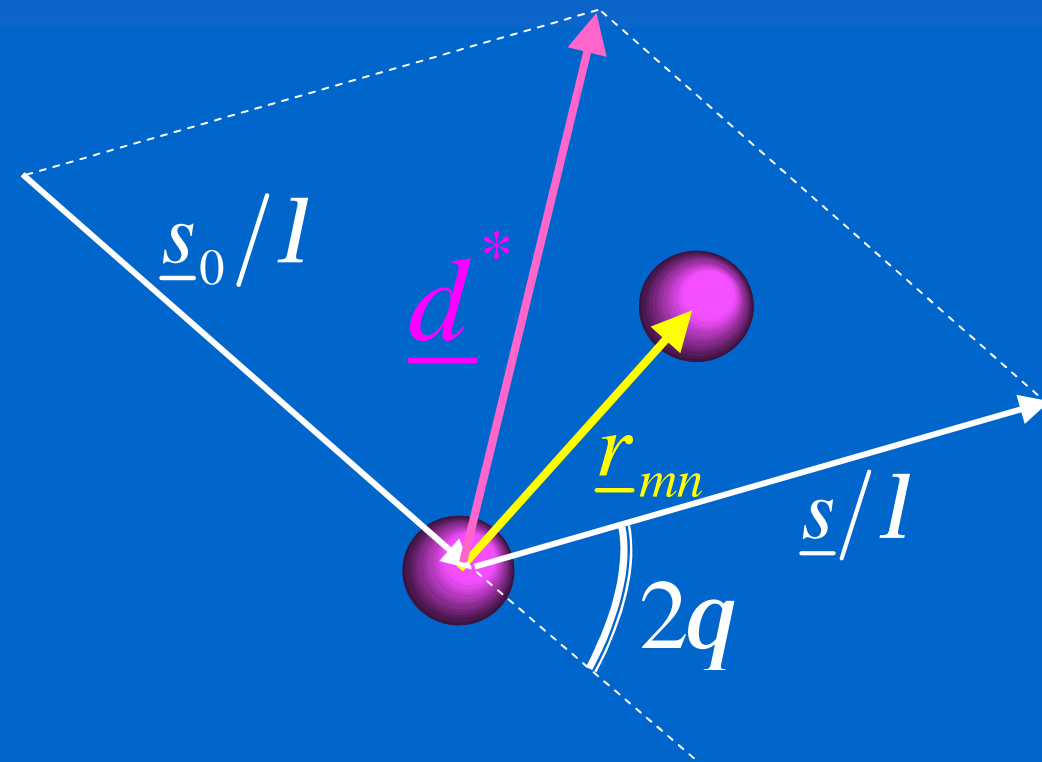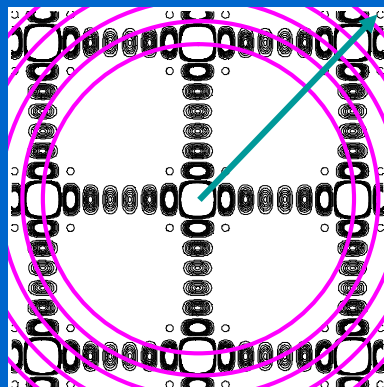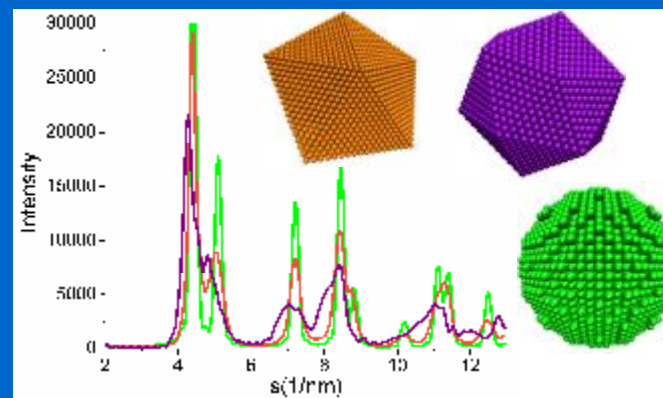
SCATTERING FROM A POWDER
Two possible approaches

1. Reciprocal space approach
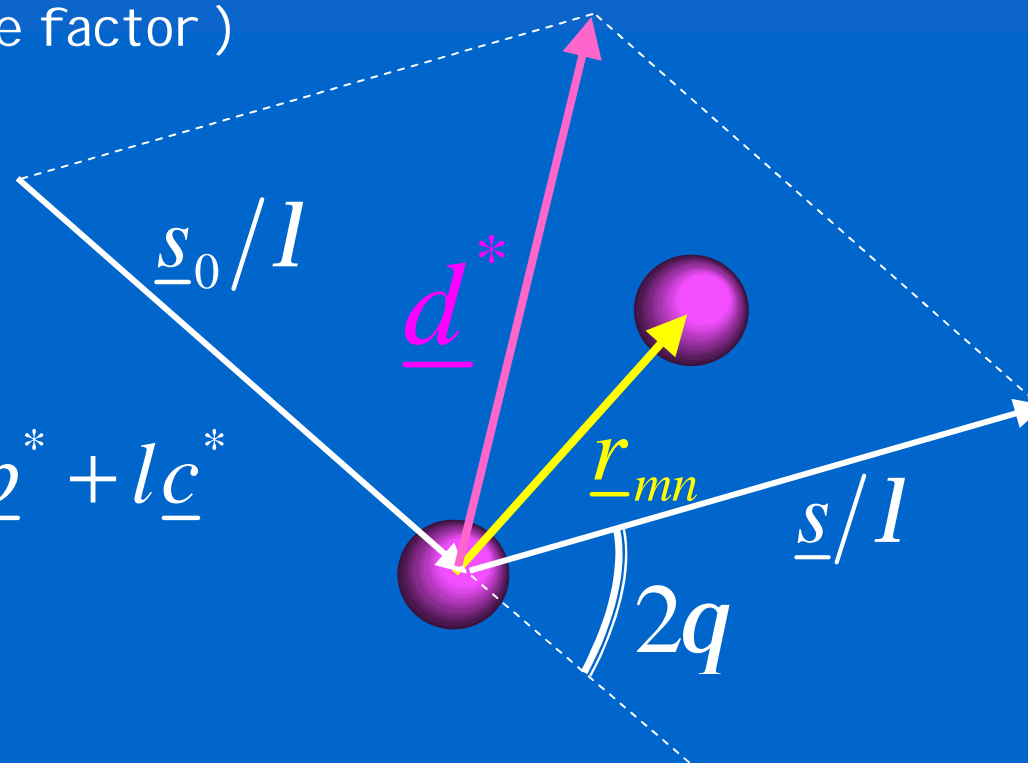(Laue – Wilson)

2. Direct (Real) space approach
(Debye)

Two possible approaches - #1 reciprocal space

1. Factorize the contribution from a unit cell ($|F|^2$ – F, structure factor)

$$\underline{d}^* = \frac{\underline{s} - \underline{s}_0}{l} = h\underline{a}^* + k\underline{b}^* + l\underline{c}^*$$

$$\underline{r}_n = u_n\underline{a} + v_n\underline{b} + w_n\underline{c}$$

$$\underline{s}_0/l \qquad \underline{d}^* \qquad \underline{r}_{mn} \qquad \underline{s}/l \qquad 2q$$

$$I_{uc} \propto \sum_m f_m e^{2pi\left(\underline{d}^*\cdot\underline{r}_m\right)} \sum_n f_n e^{-2pi\left(\underline{d}^*\cdot\underline{r}_n\right)} = \left|\sum_{n=1}^{N} f_n e^{2pi(u_nh+v_nk+w_nl)}\right|^2 = \left|F\right|^2$$

Two possible approaches - #1 reciprocal space

1. Factorize the contribution from a unit cell ($|F|^2$ – F, structure factor)

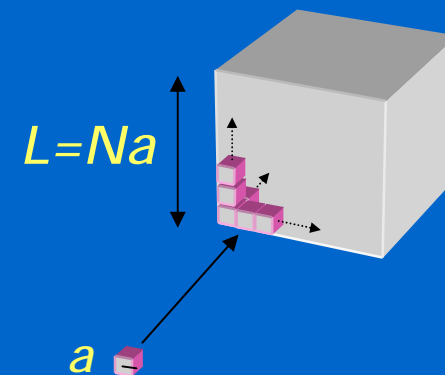$$I_{uc} \propto |F|^2 = \left| \sum_{n=1}^{N} f_n e^{2pi(u_n h + v_n k + w_n l)} \right|^2$$

Then build the diffraction signal
for a small crystal (unit cell volume, V_{uc})

(Interference function) à see ZANOTTI's lecture

$$I_{sc} \propto \frac{|F|^2}{V_{uc}^2} \frac{\sin^2(pNh)}{\sin^2(ph)} \frac{\sin^2(pNk)}{\sin^2(pk)} \frac{\sin^2(pNl)}{\sin^2(pl)}$$

L=Na

a

$$I_{sc} \propto \frac{|F|^2}{V_{uc}^2} \sum_{h'=-\infty}^{\infty} \sum_{k'=-\infty}^{\infty} \sum_{l'=-\infty}^{\infty} \frac{\sin^2(pNh)}{p^2(h-h')^2} \frac{\sin^2(pNk)}{p^2(k-k')^2} \frac{\sin^2(pNl)}{p^2(l-l')^2}$$

SCATTERING FROM A POWDER

Two possible approaches - #1 reciprocal space

1. Factorize the contribution from a
    unit cell ($|F|^2 – F$, structure factor)
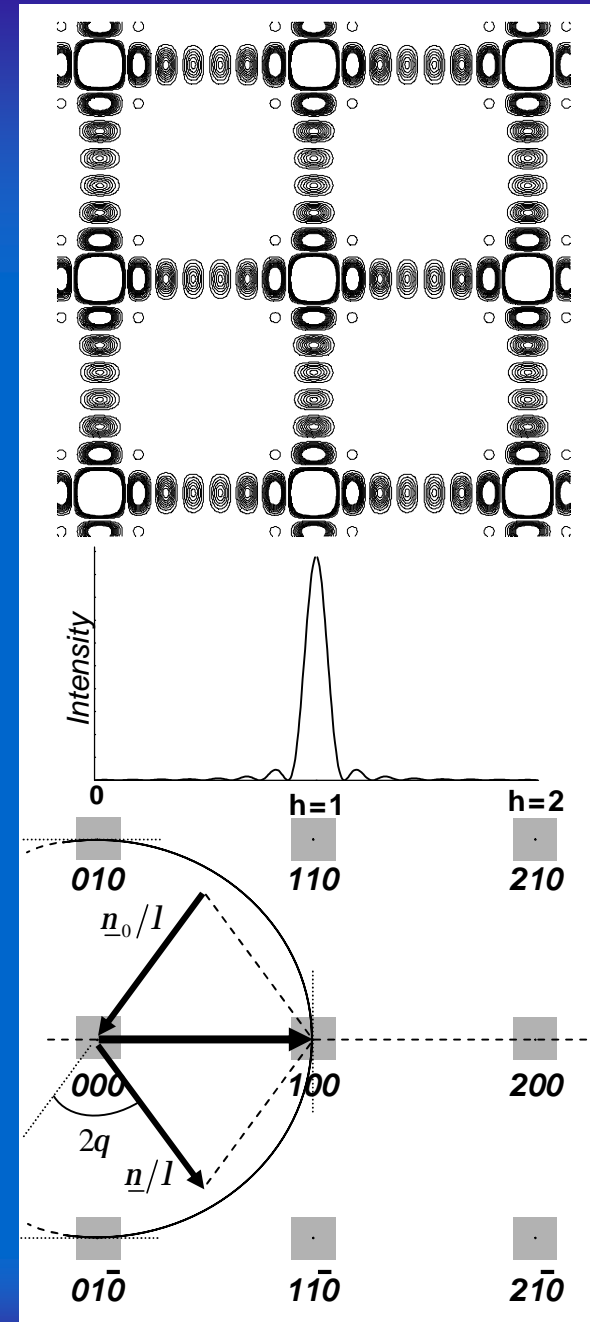
    Then build the diffraction signal
    for a small crystal (unit cell volume, V_{uc})

    (Interference function)

$$I_{sc} \propto \frac{|F|^2}{V_{uc}^2} \frac{\sin^2(pNh)}{\sin^2(ph)} \frac{\sin^2(pNk)}{\sin^2(pk)} \frac{\sin^2(pNl)}{\sin^2(pl)}$$

$$I_{sc} \propto \frac{|F|^2}{V_{uc}^2} \sum_{h'=-\infty}^{\infty} \sum_{k'=-\infty}^{\infty} \sum_{l'=-\infty}^{\infty} \frac{\sin^2(pNh)}{p^2(h-h')^2} \frac{\sin^2(pNk)}{p^2(k-k')^2} \frac{\sin^2(pNl)}{p^2(l-l')^2}$$

SCATTERING FROM A POWDER

Two possible approaches - #1 reciprocal space

1. Factorize the contribution from a
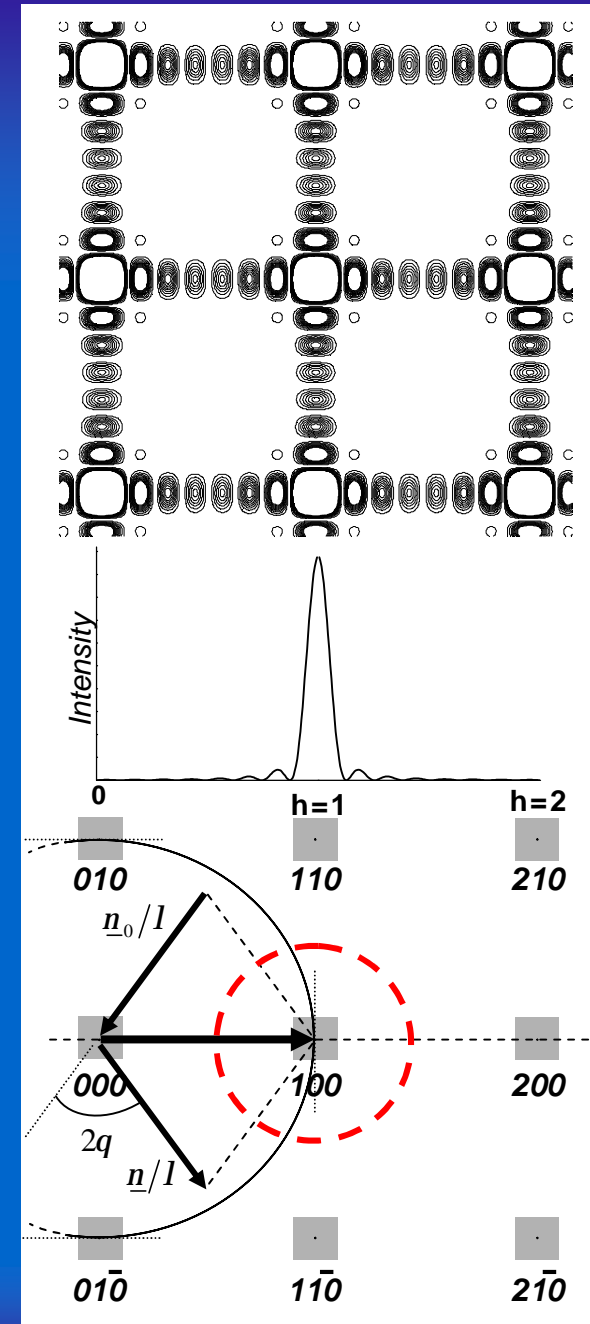   unit cell ($|F|^2$ – F, structure factor)

   Then build the diffraction signal
   for a small crystal (unit cell volume, V_{uc})

   (Interference function)

$$I_{sc} \propto \frac{|F|^2}{V_{uc}^2} \sum_{h'=-\infty}^{\infty} \sum_{k'=-\infty}^{\infty} \sum_{l'=-\infty}^{\infty} \frac{\sin^2(pNh)}{p^2(h-h')^2} \frac{\sin^2(pNk)}{p^2(k-k')^2} \frac{\sin^2(pNl)}{p^2(l-l')^2}$$
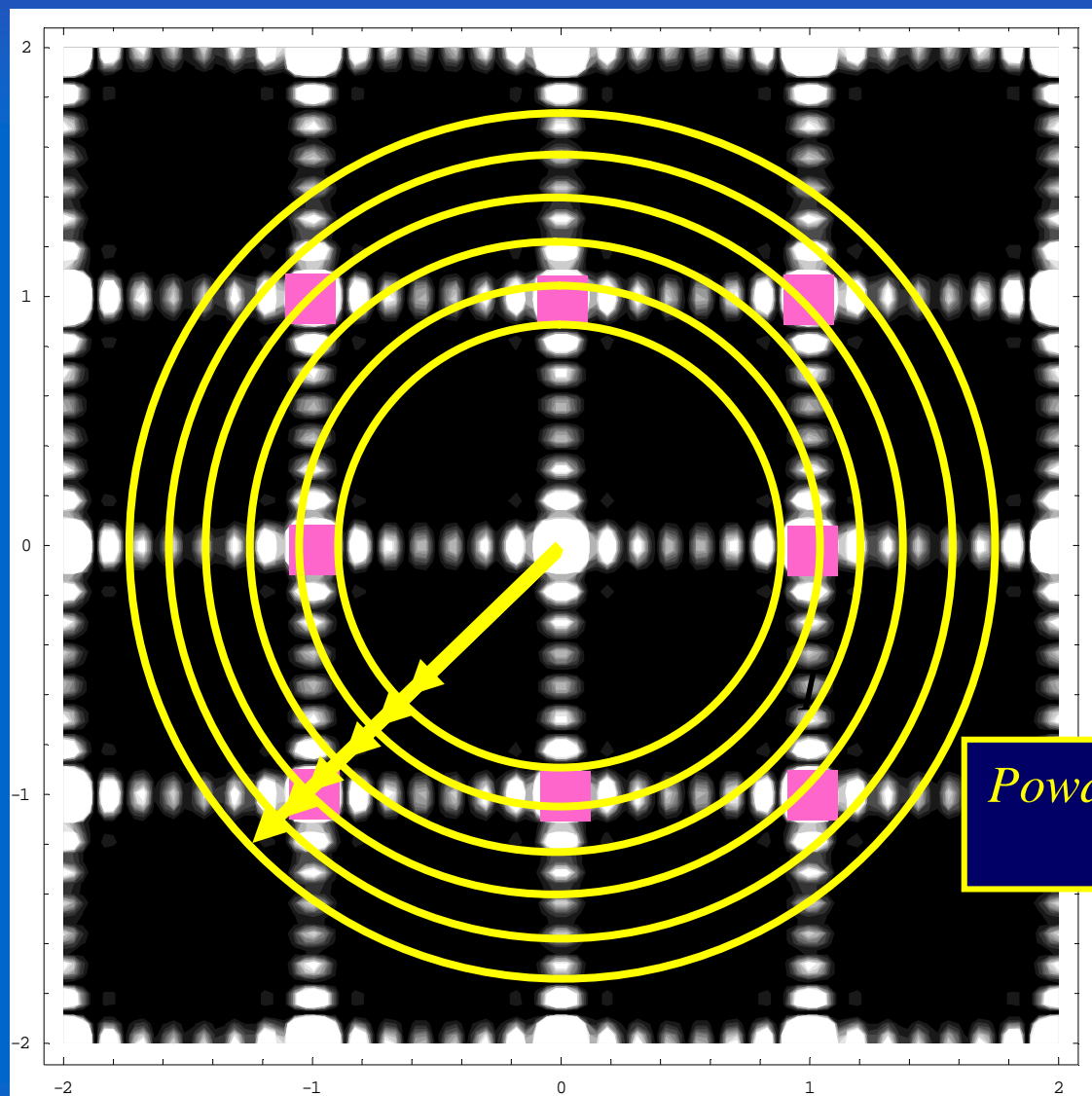
Example:

(100) point

$$I_{sc}^{100} \propto \frac{\sin^2(pNh)}{p^2(h-1)^2}$$

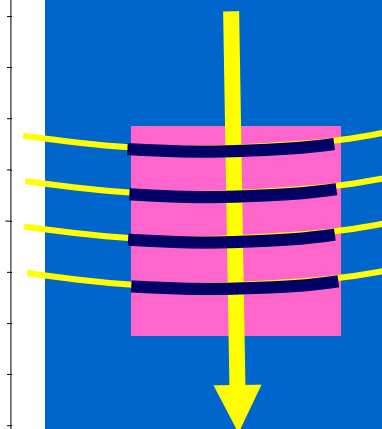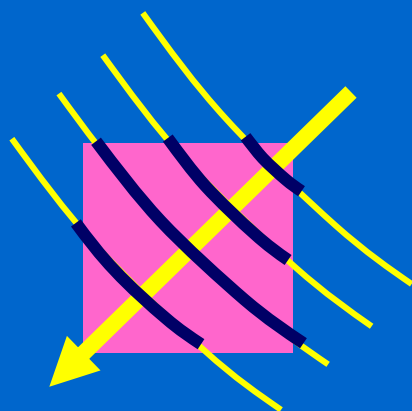## Two possible approaches - #1 reciprocal space

Powder Diffraction sphere

NANOCRYSTAL à POWDER
Two possible approaches - #1 reciprocal space

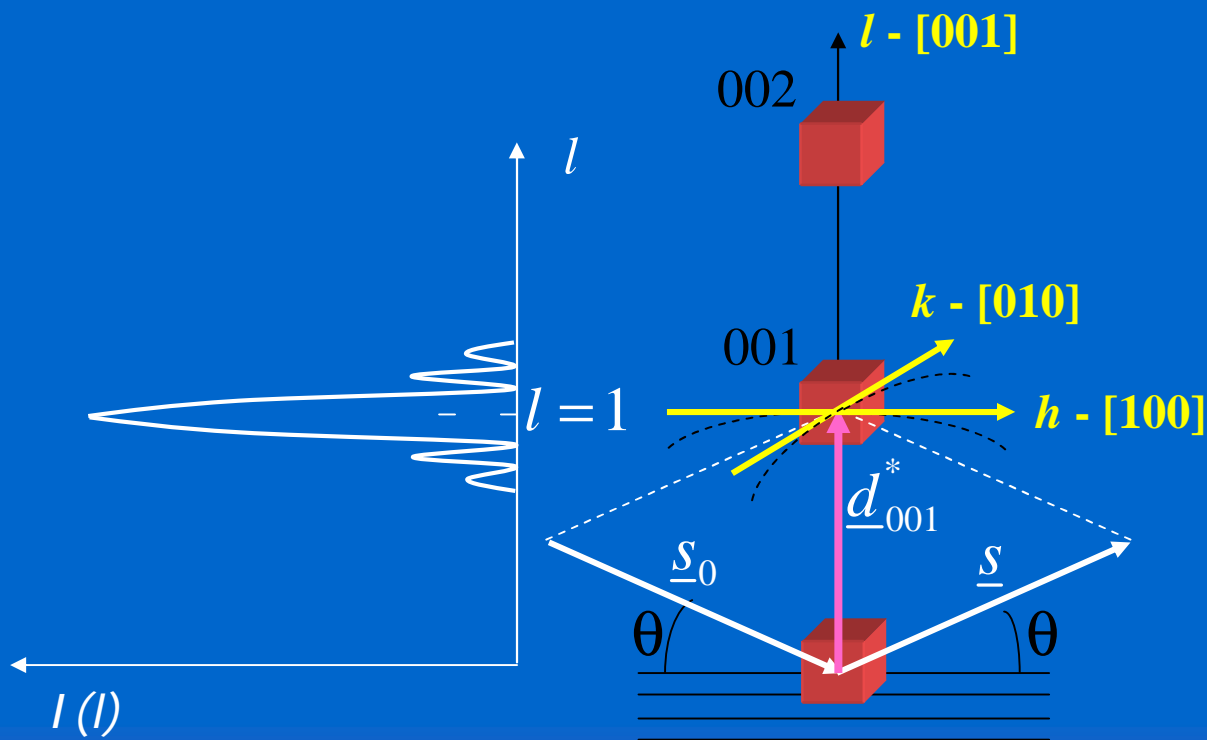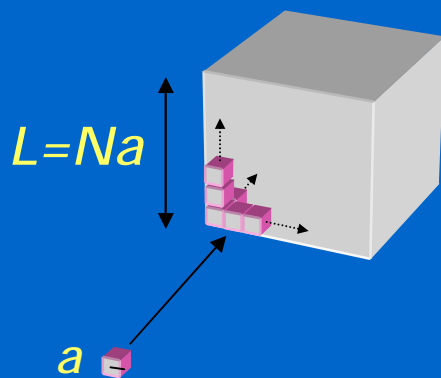*P. Scardi – Powder Diffraction & Synchrotron Radiation*
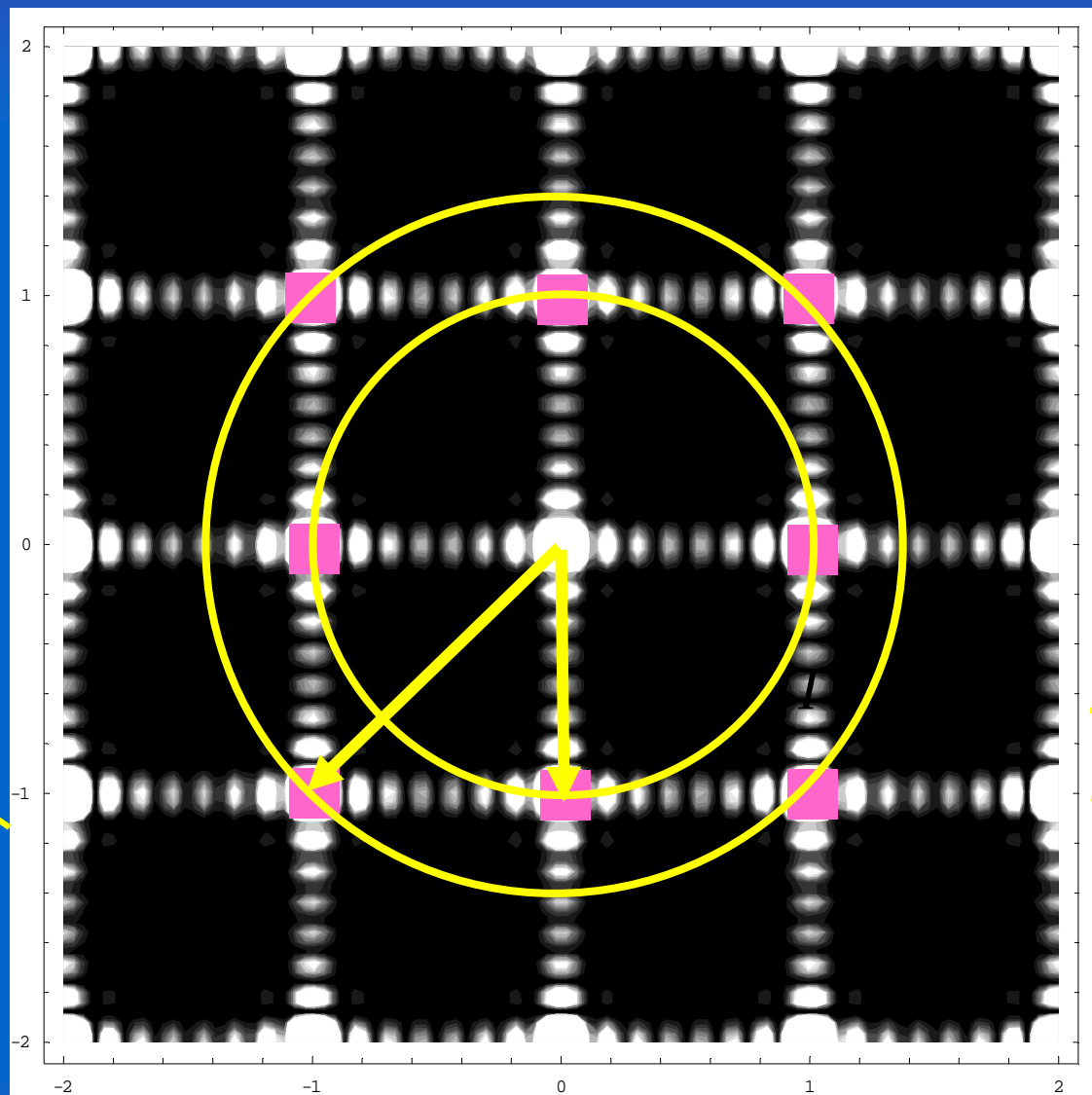
NANOCRYSTAL à POWDER

Two possible approaches - #1 reciprocal space

Example: (001) peak, powder made of cubic crystallites, cube edge L

$$I \propto |F|^2 \iint \frac{\sin^2(pNh)}{(ph)^2} \frac{\sin^2(pNk)}{(pk)^2} \frac{\sin^2(pNl)}{(pl)^2} dh \cdot dk \rightarrow |F|^2 \frac{\sin^2(pNl)}{(pl)^2}$$

$$\frac{\int_{-\infty}^{\infty} \frac{\sin^2(pNl)}{(pl)^2} dl}{I(0)} = \frac{1}{N}$$

$L = Na$

a

l

$l = 1$

$I(l)$

l - [001]

002

001

k - [010]

h - [100]

$\underline{d}^*_{001}$

$\underline{S}_0$

$\underline{S}$

θ

θ

P. Scardi – Powder Diffraction & Synchrotron Radiation
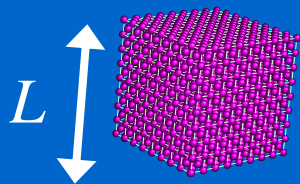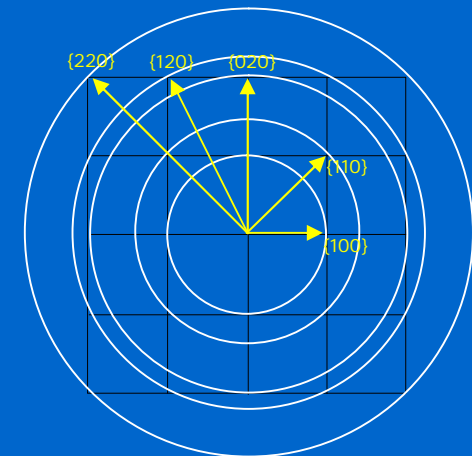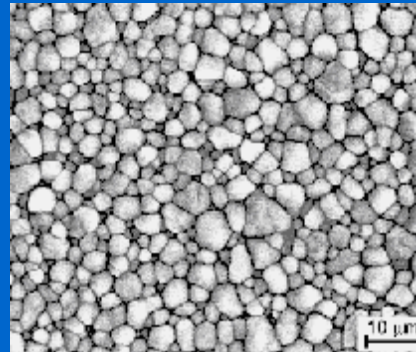
Two possible approaches - #1 reciprocal space

1. Factorize the contribution from a unit cell ($|F|^2$ – F, structure factor)

Then build the diffraction signal for a small crystal,

$$\frac{\sin^2(pNh)}{\sin^2(ph)} \frac{\sin^2(pNk)}{\sin^2(pk)} \frac{\sin^2(pNl)}{\sin^2(pl)}$$

and integrate over the powder diffraction sphere for calculating the signal from all domains in the powder

{220} {120} {020}

{110}

{100}

L

standard Powder Diffraction approach
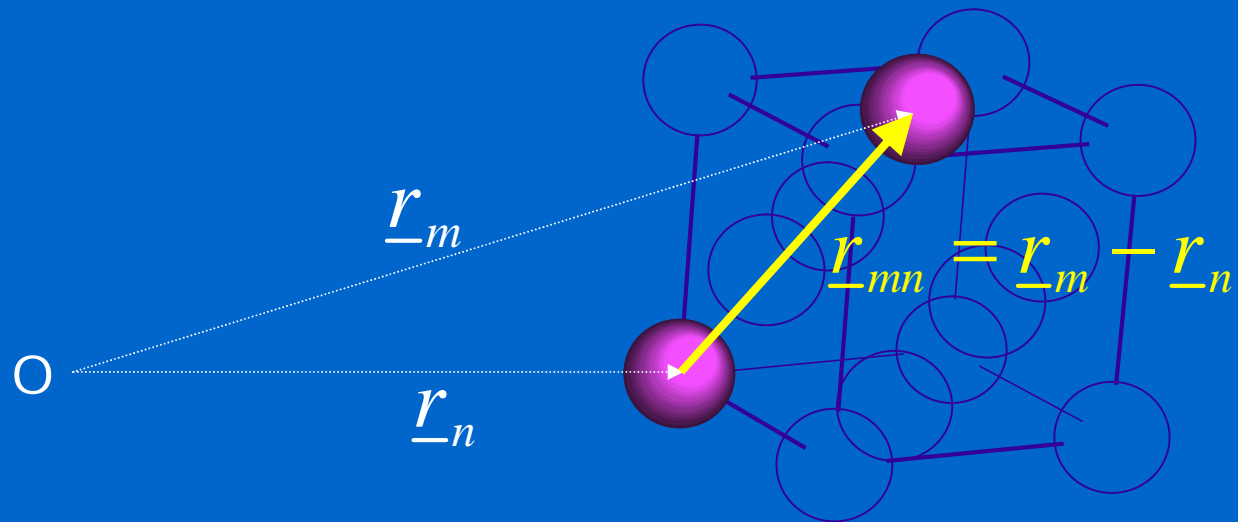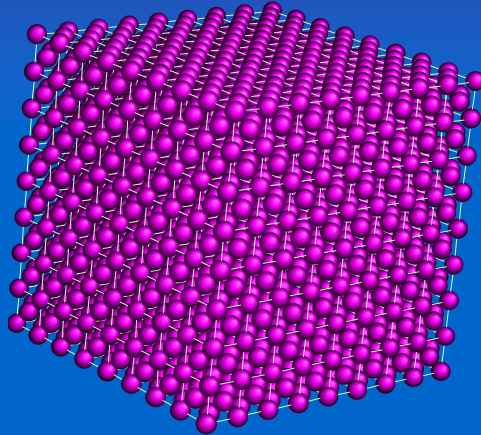
$$I_{PD} \propto |F|^2 \Phi(d^*, D)$$

Two possible approaches - #2 real space

2. Average over all possible orientations of r_{mn} in space

$$\underline{r}_{mn} = \underline{r}_m - \underline{r}_n$$

$\underline{r}_m$

$\underline{r}_n$

O

$$I_{uc} \propto \sum_m f_m e^{2pi\left(\underline{d}^* \cdot \underline{r}_m\right)} \sum_n f_n e^{-2pi\left(\underline{d}^* \cdot \underline{r}_n\right)} = \sum_m \sum_n f_m f_n e^{2pi\left(\underline{d}^* \cdot \underline{r}_{mn}\right)}$$
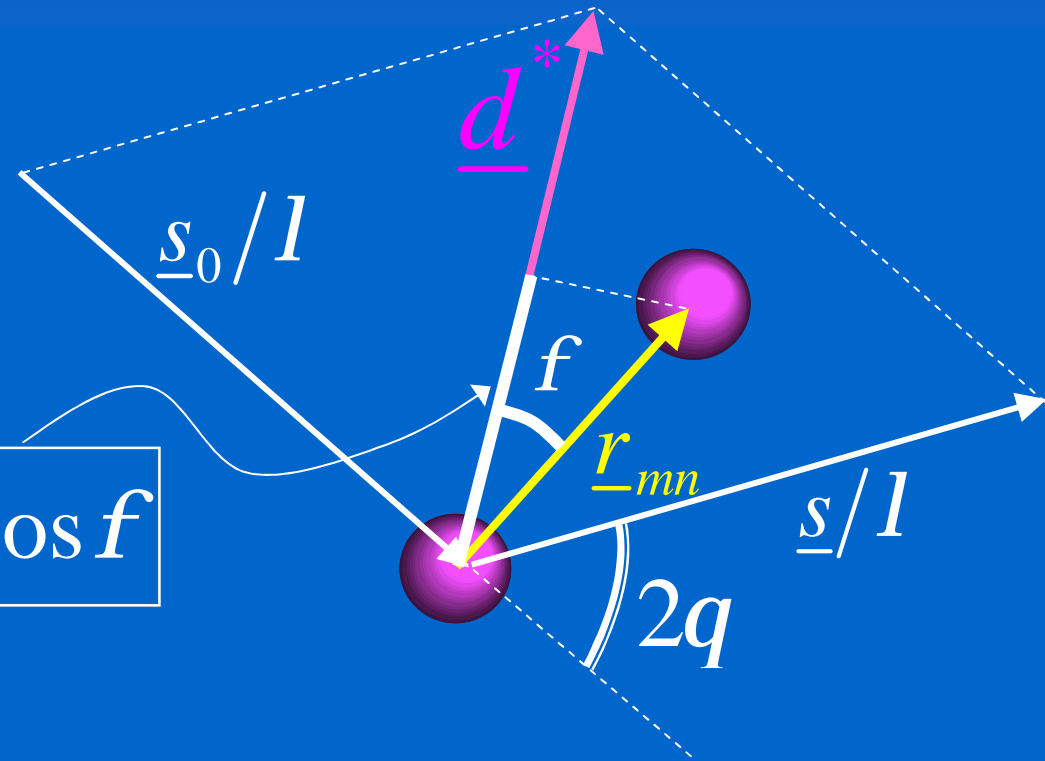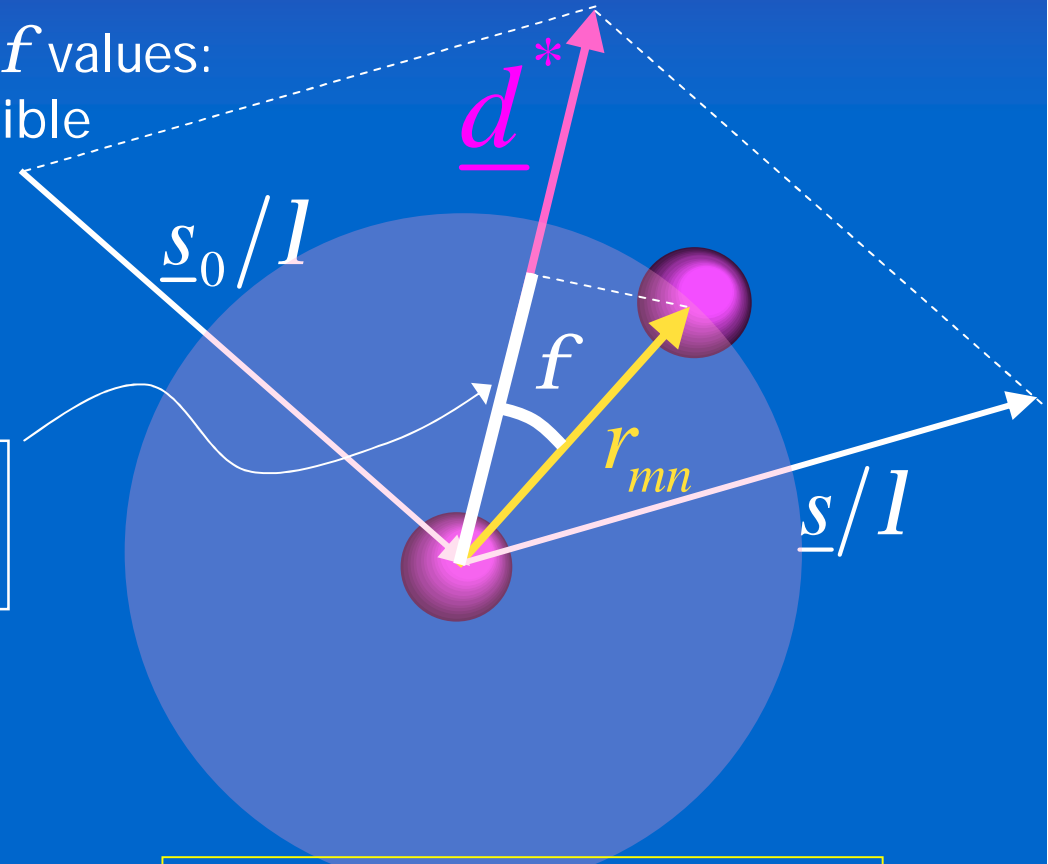
Two possible approaches - #2 real space

2. Average over all possible orientations of r_{mn} in space

$$d^* = \frac{s - s_0}{l} = \frac{2\sin q}{l}$$

$$\boxed{d^* \cdot r_{mn} = d^* \, r_{mn} \cos f}$$

$$I_{sc} \propto \sum_m f_m e^{2pi\left(d^* \cdot r_m\right)} \sum_n f_n e^{-2pi\left(d^* \cdot r_n\right)} = \sum_m \sum_n f_m f_n e^{2pi\left(d^* \cdot r_{mn}\right)}$$

Two possible approaches - #2 real space

2. Average over all possible $\cos f$ values: r_{mn} is allowed to take all possible orientations in space

$$\underline{d}^* \cdot \underline{r}_{mn} = d\, r_{mn} \cos f$$

$\underline{d}^*$

$\underline{s}_0/l$

f

r_{mn}

$\underline{s}/l$

$$I_D \propto \sum_m \sum_n f_m f_n \left\langle e^{2pi\left(\underline{d}^* \cdot \underline{r}_{mn}\right)} \right\rangle$$

Debye formula
$$= \sum_m \sum_n f_m f_n \frac{\sin\left(2p\,d^*\,r_{mn}\right)}{2p\,d^*\,r_{mn}}$$

Debye formula for one (fcc) unit cell

$$I_D = \sum_m \sum_n f_m f_n \frac{\sin 2p d^* r_{mn}}{2p d^* r_{mn}}$$

a

$$r_{mn} = 0 \qquad a/\sqrt{2} \qquad a \qquad a\sqrt{3/2} \qquad a\sqrt{2} \qquad a\sqrt{3}$$

14   72   30   48   24   8
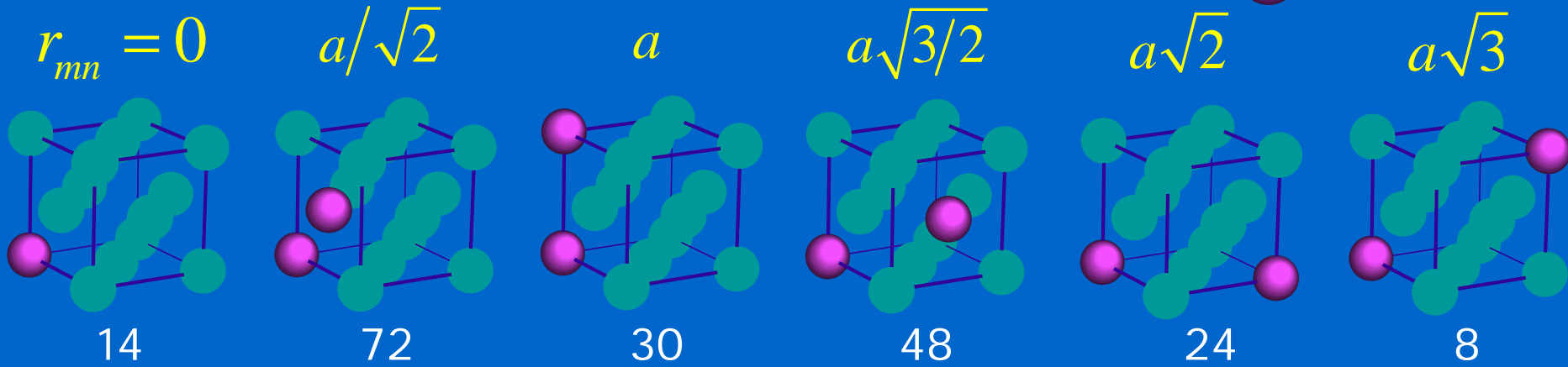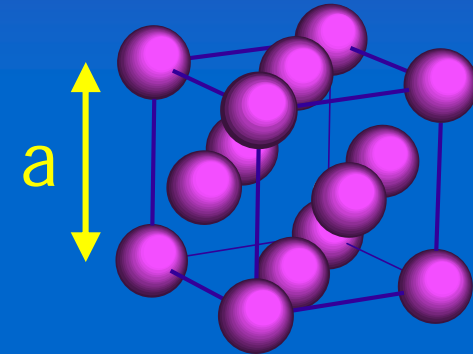
$$I_D = 14 + \frac{72\sin\left(ka/\sqrt{2}\right)}{ka/\sqrt{2}} + \frac{30\sin ka}{ka} + \frac{48\sin\left(ka\sqrt{3/2}\right)}{ka\sqrt{3/2}} + \frac{24\sin\left(ka\sqrt{2}\right)}{ka\sqrt{2}} + \frac{8\sin\left(ka\sqrt{3}\right)}{ka\sqrt{3}}$$

Scattering from (random oriented) Cu unit cells . Mo Kα (0.07093 nm)

$$I_D = 14 + \frac{72\sin\left(ka\big/\sqrt{2}\right)}{ka\big/\sqrt{2}} + \frac{30\sin ka}{ka} + \frac{48\sin\left(ka\sqrt{3/2}\right)}{ka\sqrt{3/2}} + \frac{24\sin\left(ka\sqrt{2}\right)}{ka\sqrt{2}} + \frac{8\sin\left(ka\sqrt{3}\right)}{ka\sqrt{3}}$$
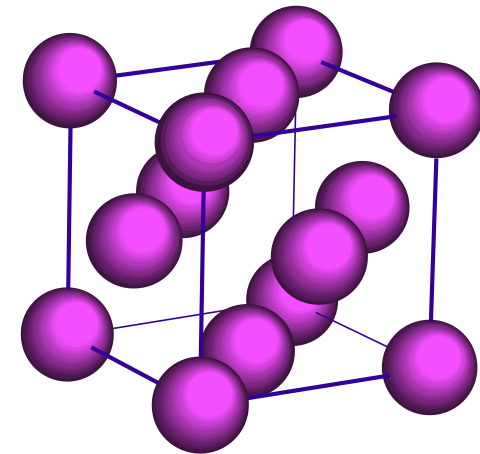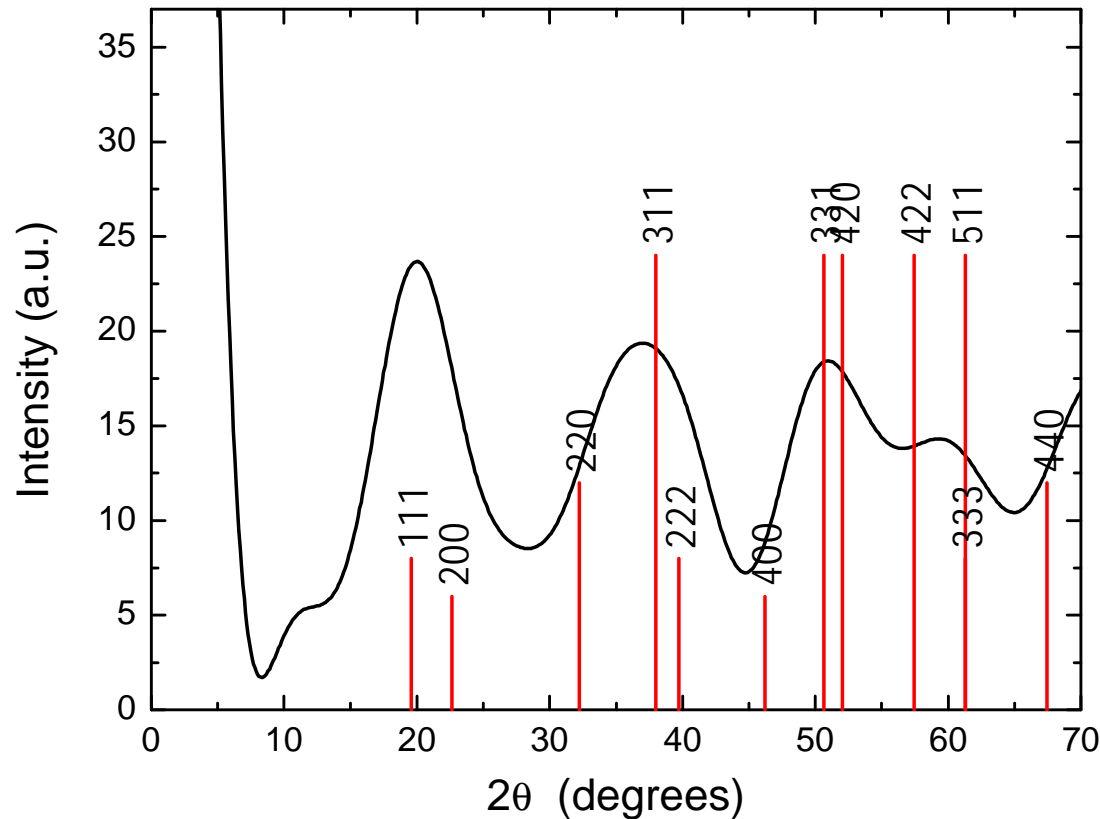
Cu bars: multiplicity

Scattering from (random oriented) Cu unit cells . Mo Kα (0.07093 nm)
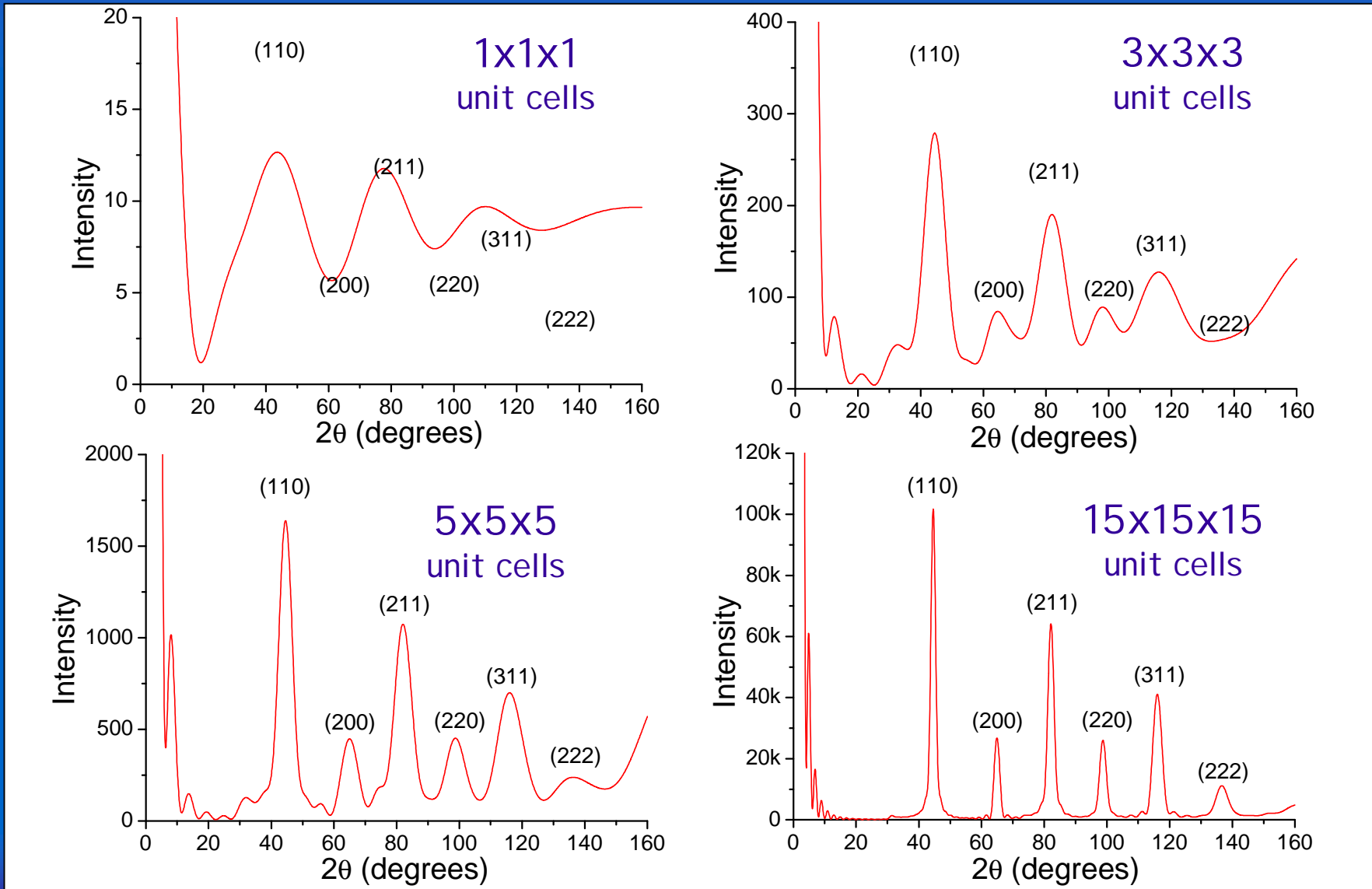
$$I_D \cdot LP \cdot e^{-k^2 \left\langle u_{d*}^2 \right\rangle}$$
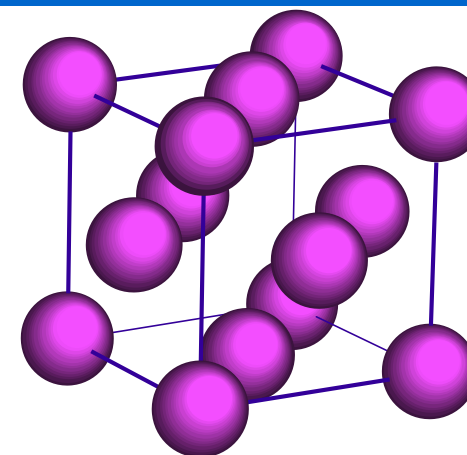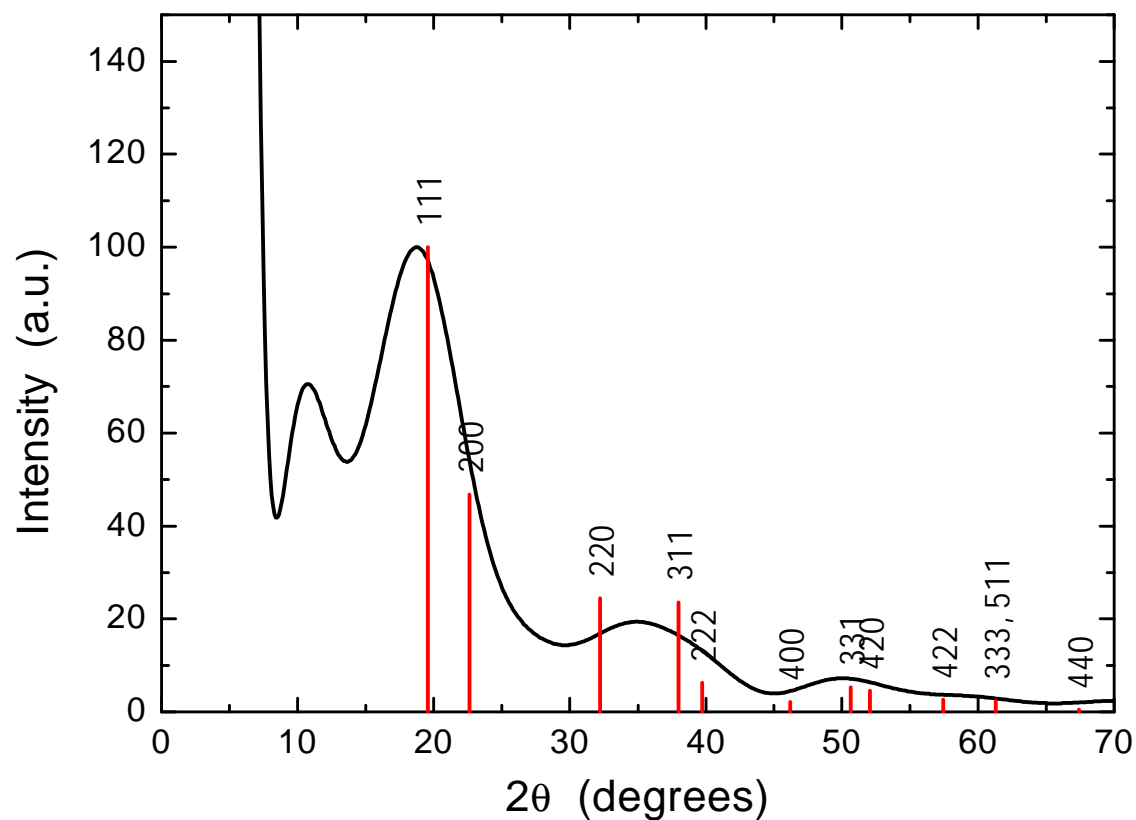
Cu bars: ICSD #46699

Scattering from bcc-Fe cubic crystals . Cu Kα (0.15406 nm)

Scattering from bcc-Fe cubic crystals . Cu Kα (0.15406 nm)

15x15x15
unit cells
7471 atoms

Scattering from bcc-Fe cubic crystals . Cu Kα (0.15406 nm)

15x15x15
unit cells
7471 atoms

Scattering from bcc-Fe cubic crystals . Cu Kα (0.15406 nm)

15x15x15
unit cells
7471 atoms

$I(0) = 55.815.841 = 7471^2$

(Small Angle X-ray Scattering)
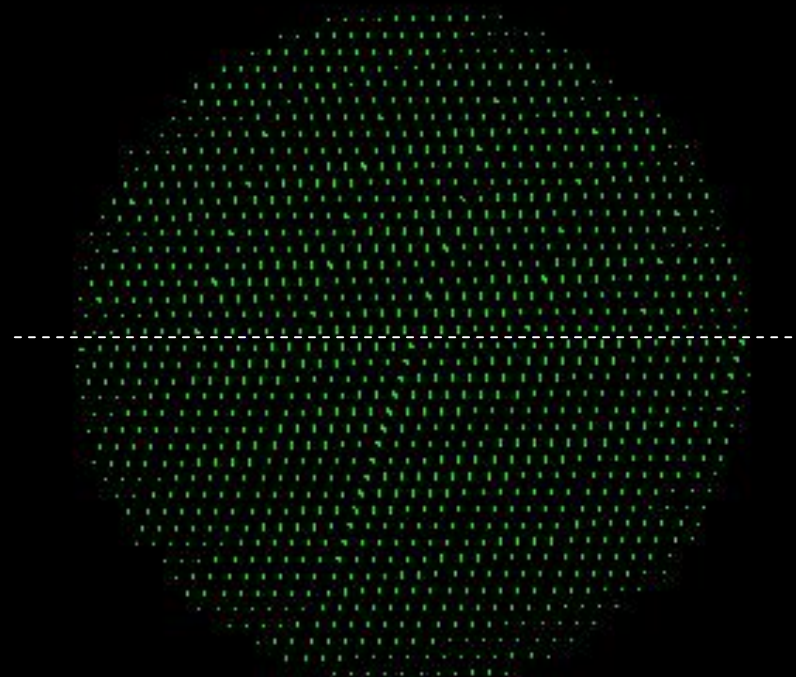à see POLIZZI's lecture
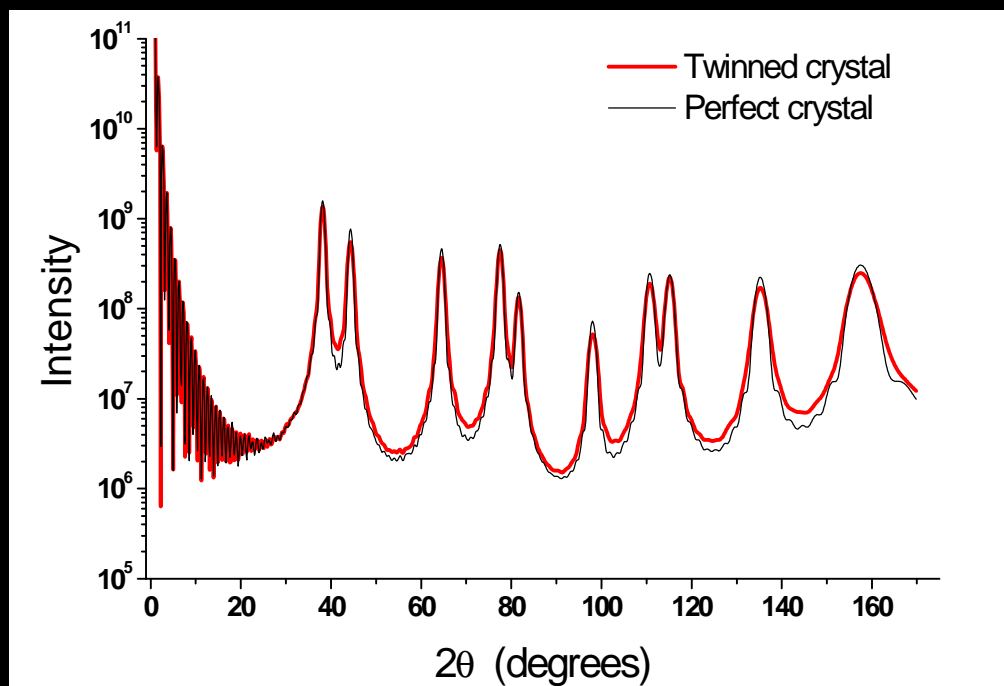
Intensity

2θ (degrees)
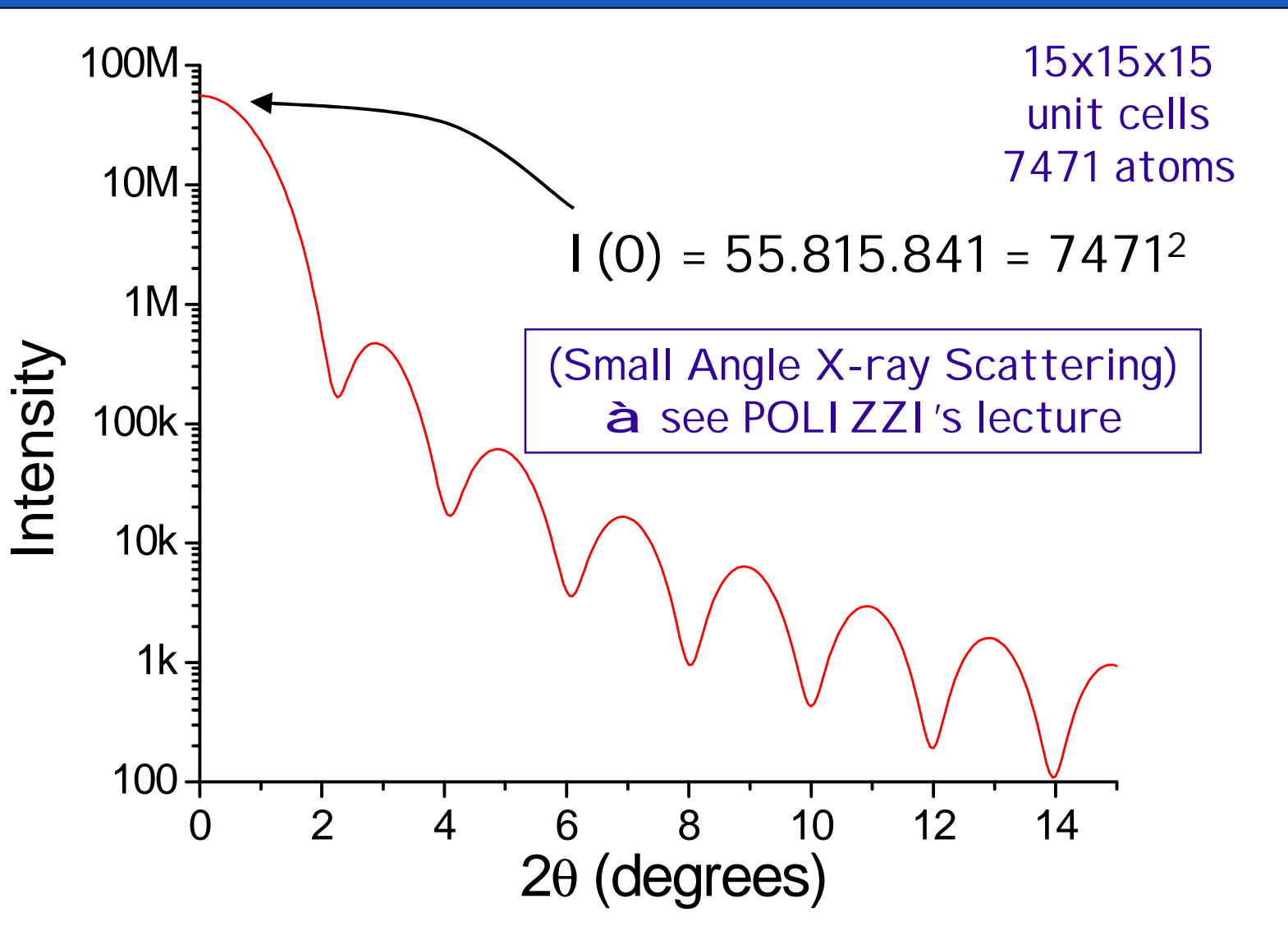
Debye formula: non crystallographic nanoparticles
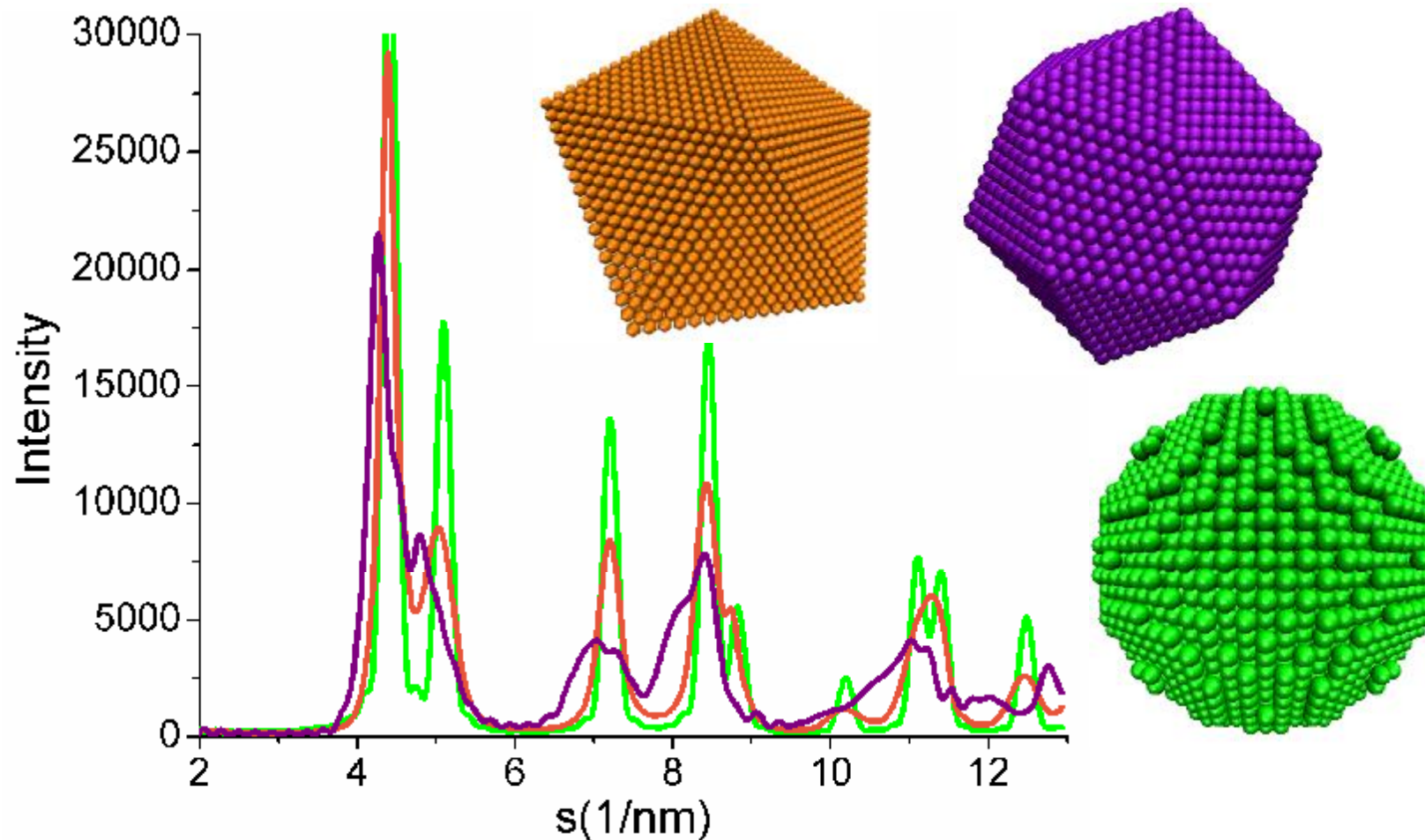
P. Scardi, M. Leoni, K.R. Beyerlein, Z. Kristallogr. (2011). In press.

Debye formula: twinned nanoparticles
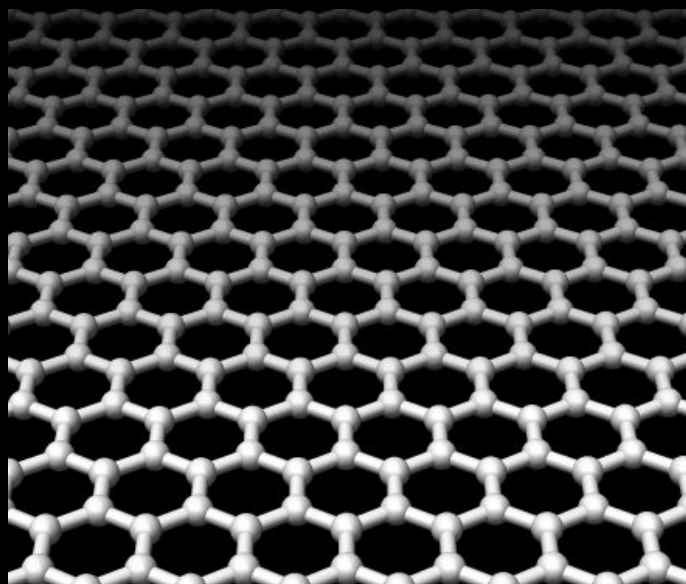

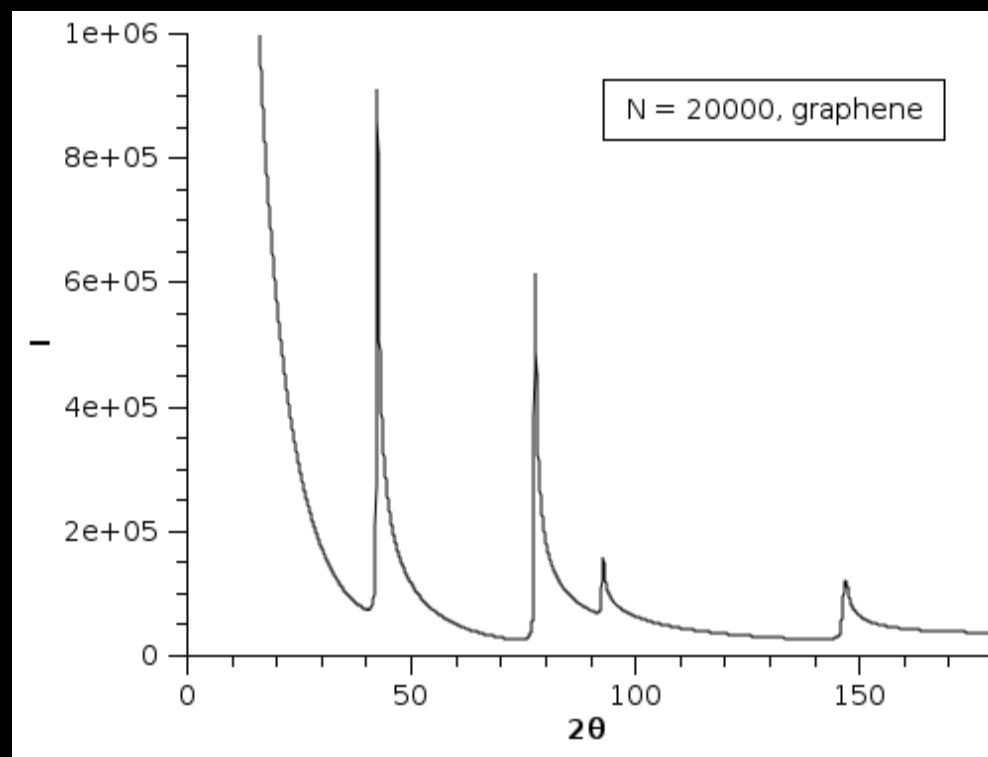Twinned spherical domains (fcc, 28897 Au atoms, nominal size 9.8 nm)

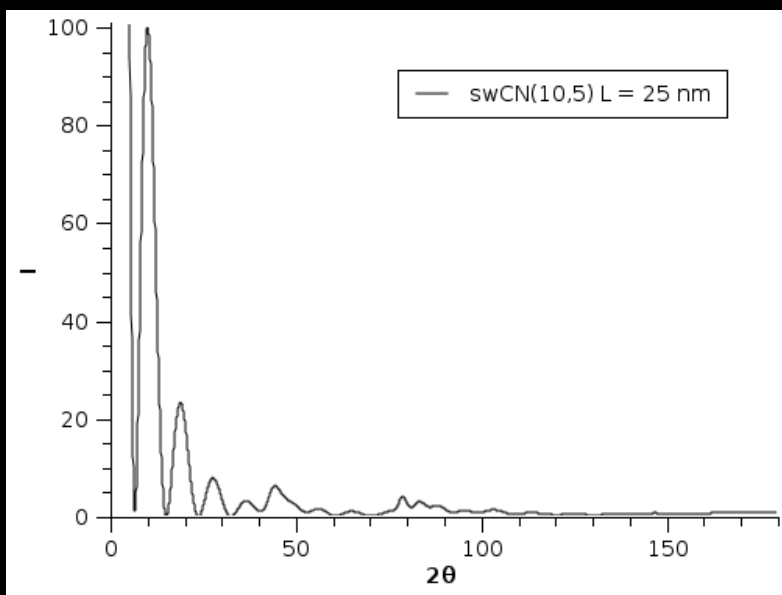K.R. Beyerlein, M. Leoni, R.L. Snyder and P. Scardi, Mat. Sci. Forum 681 (2011) 13

Debye formula: graphene
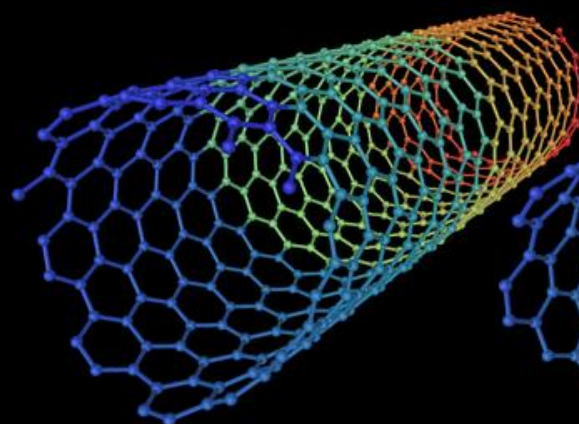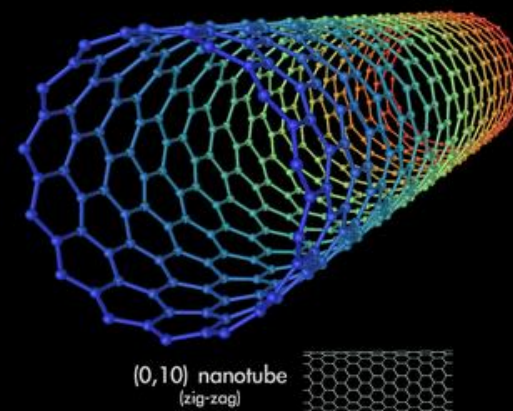

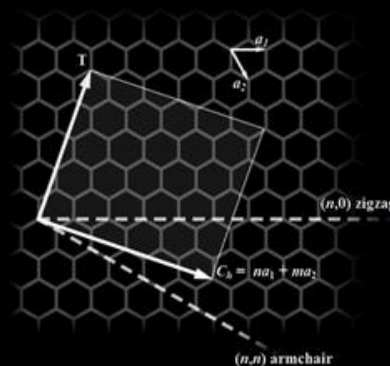graphene
(sp^2 carbon single-layer)

L. Gelisio, C.L. Azanza Ricardi, M. Leoni and P. Scardi, J. Appl. Cryst. 43 (2010) 647

L. Gelisio et al., J. Appl. Cryst. 43 (2010) 647

Debye formula: carbon nanotubes
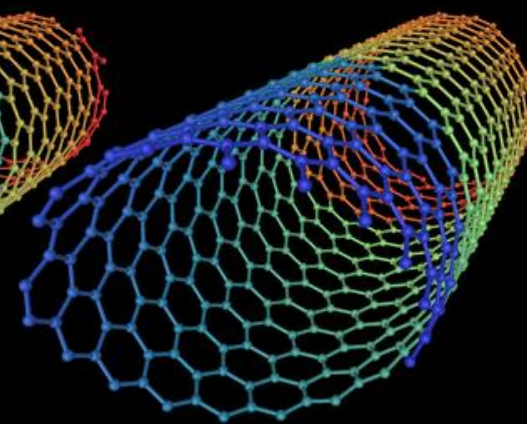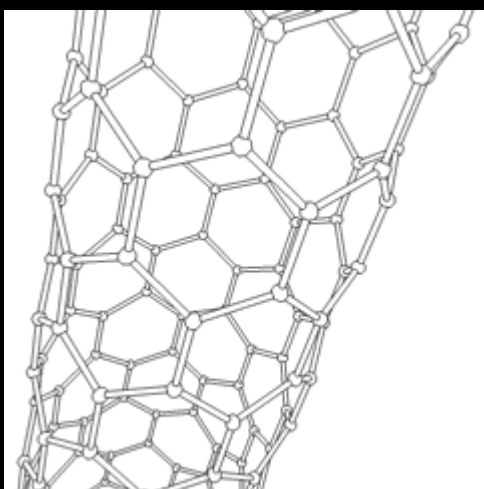
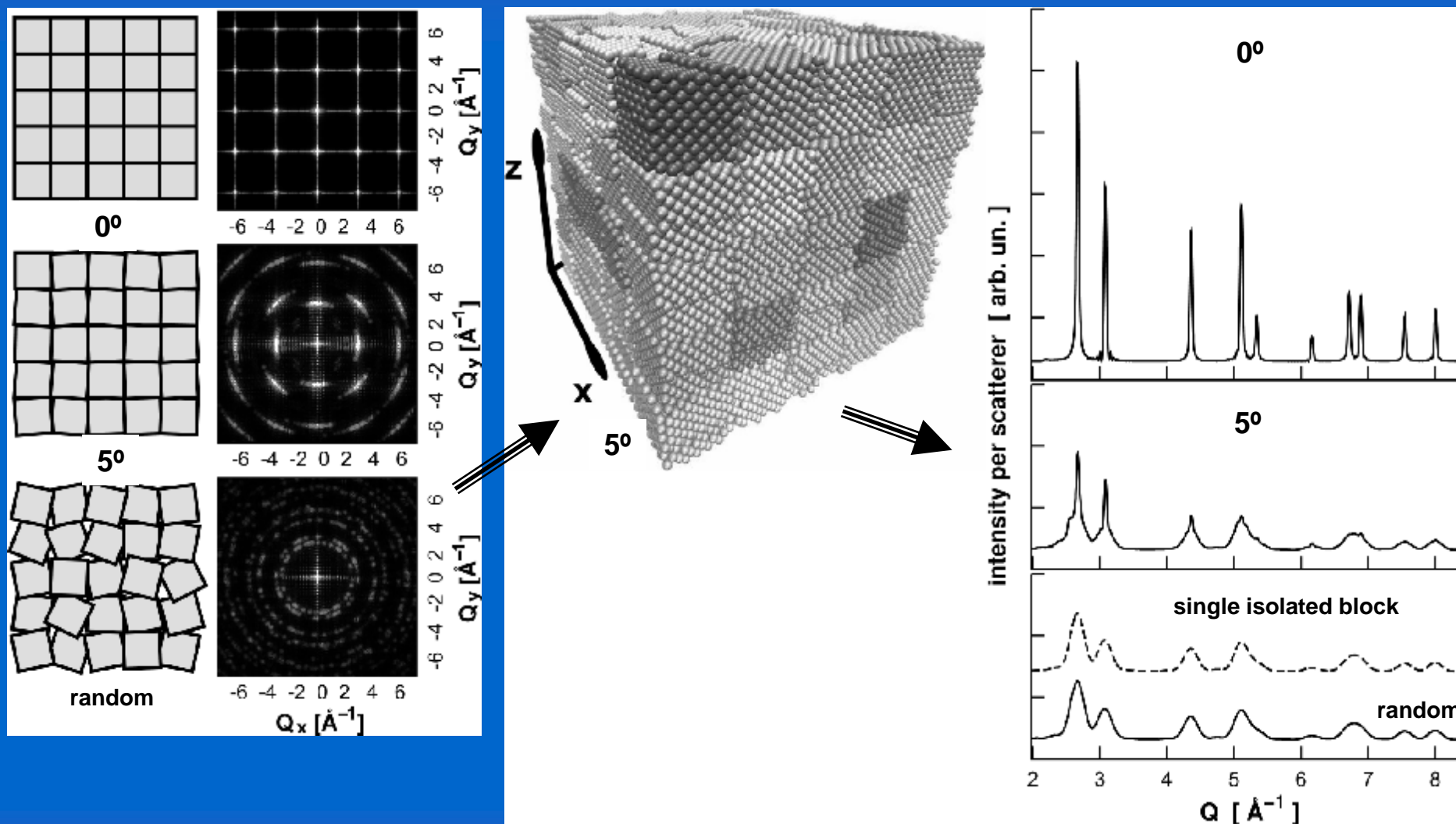## Debye formula: coherence effects on mosaic structures

L. Gelisio and P. Scardi, J. Nanosci. Nanotechnol. (2011). In press.

Debye formula: dynamical properties on nanocrystals
Temperature Diffuse Scattering (TDS)

Still

Thermalized
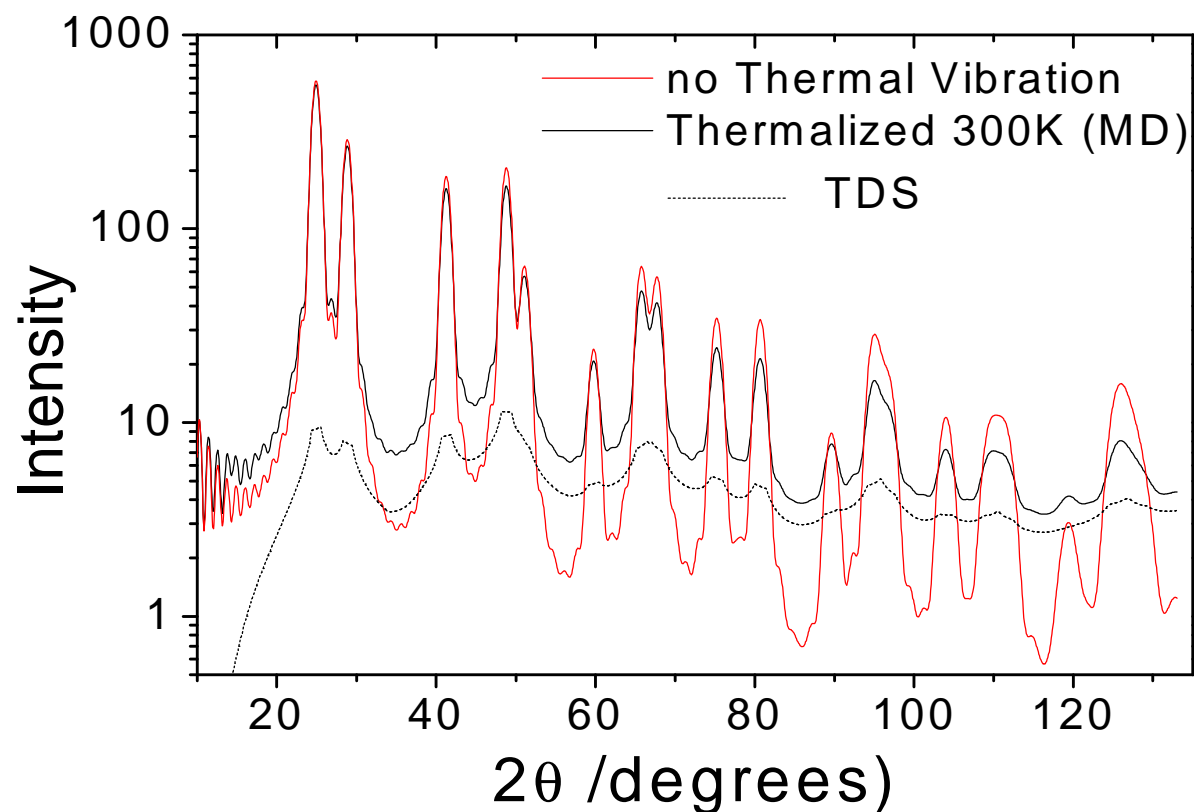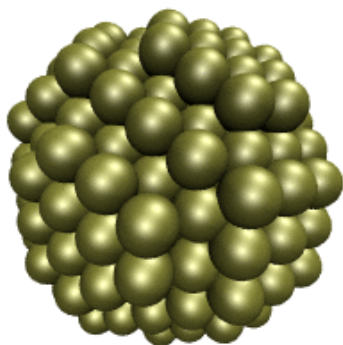
Debye formula: atomistic modelling of microstructure and plastic deformation on the nanoscale

Mean square displacement

$$< u^2 > = < u^2_{static} > + < u^2_{dynamic} >$$

static atomic disorder

thermal vibrations

32 nm
2 million atoms
200 grains
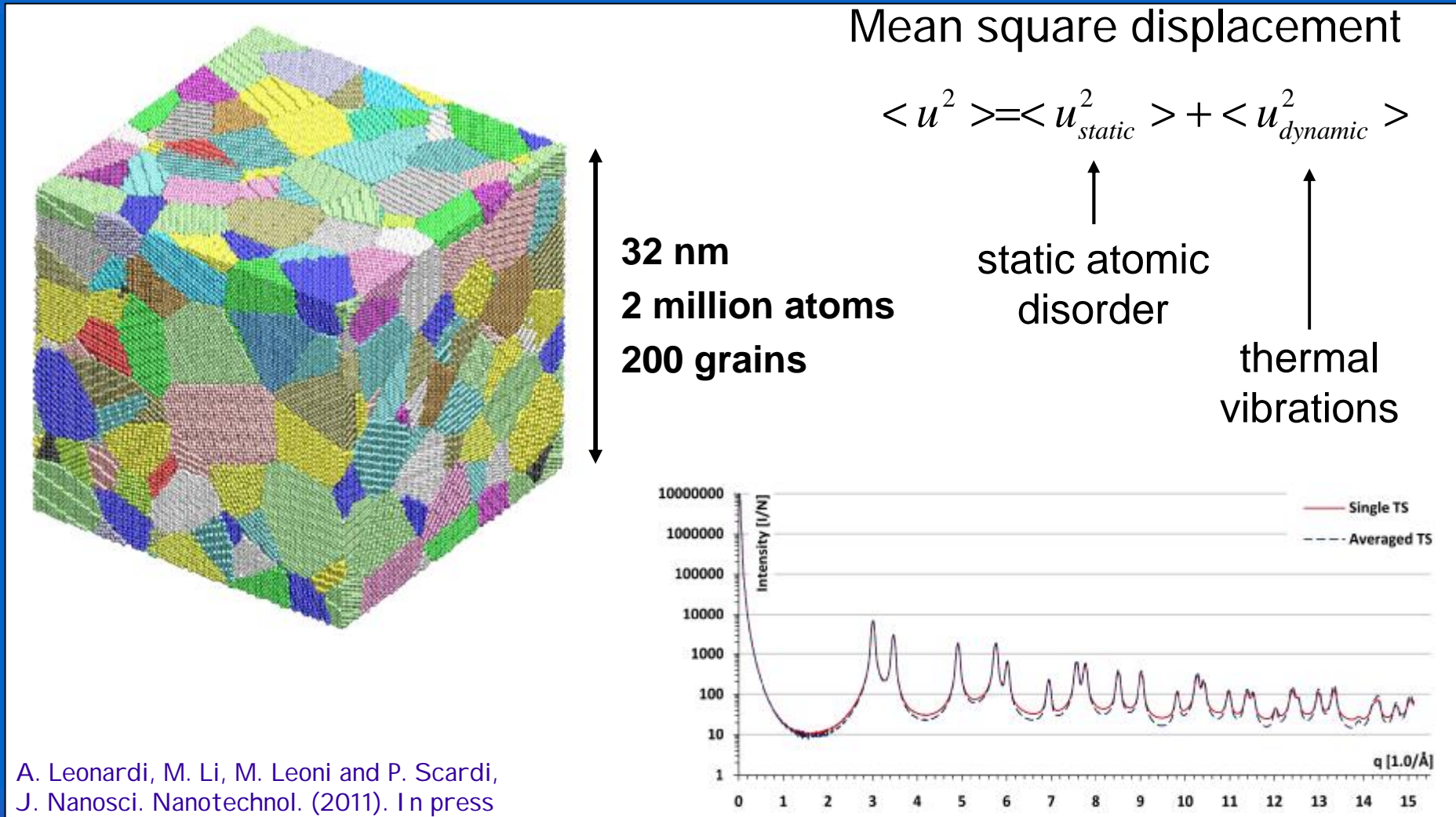
A. Leonardi, M. Li, M. Leoni and P. Scardi,
J. Nanosci. Nanotechnol. (2011). In press

QUESTIONS ??

Two possible approaches

1. Reciprocal space approach
   (Laue – Wilson)
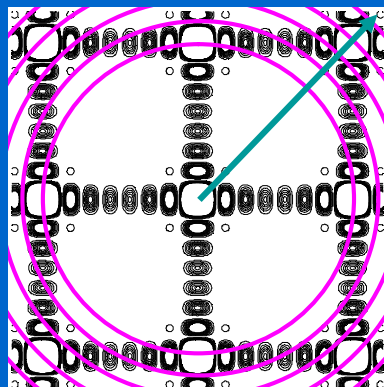
2. Direct (Real) space approach
   (Debye)

LARGE
crystal
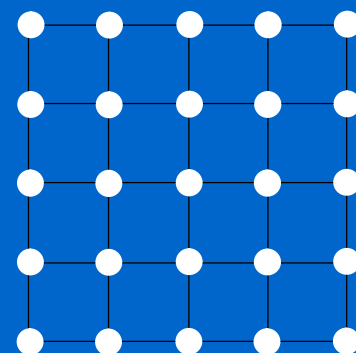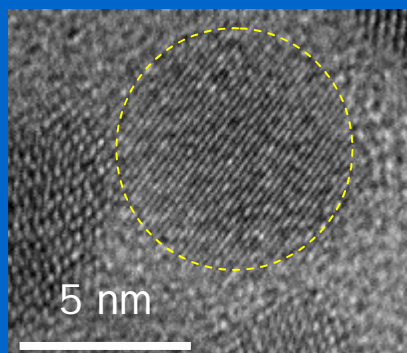
NANO
crystal
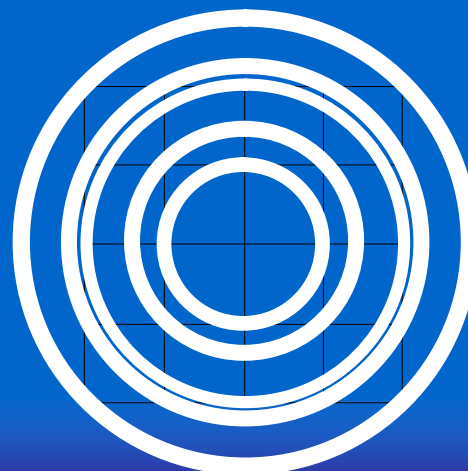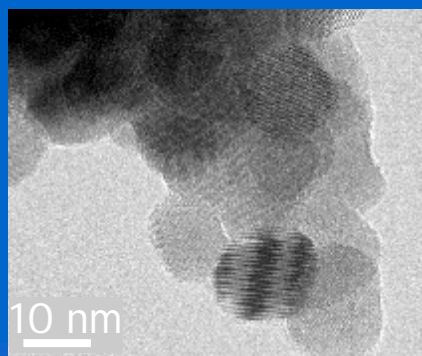
NANO
crystal
POWDER
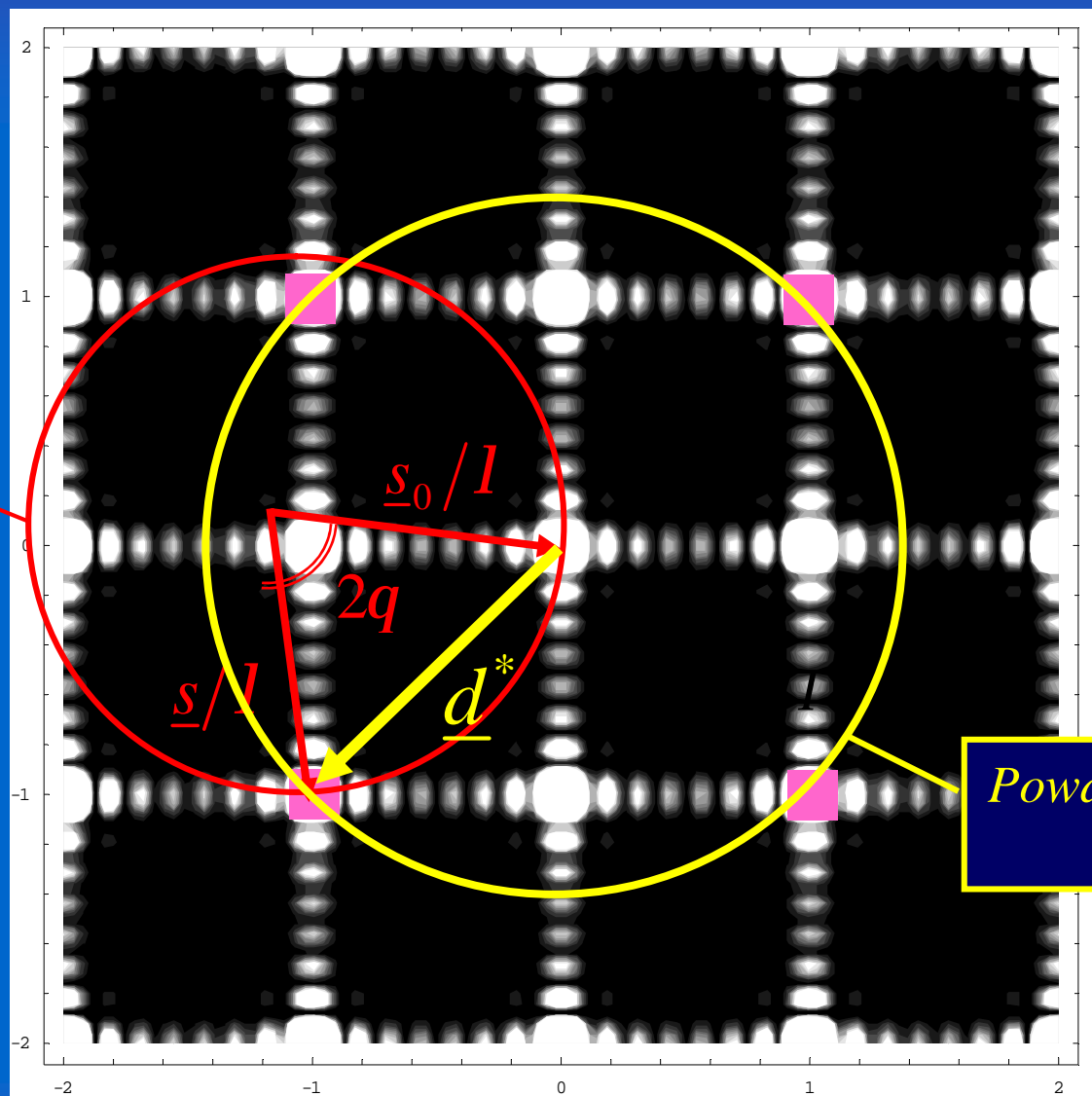
Ewald sphere
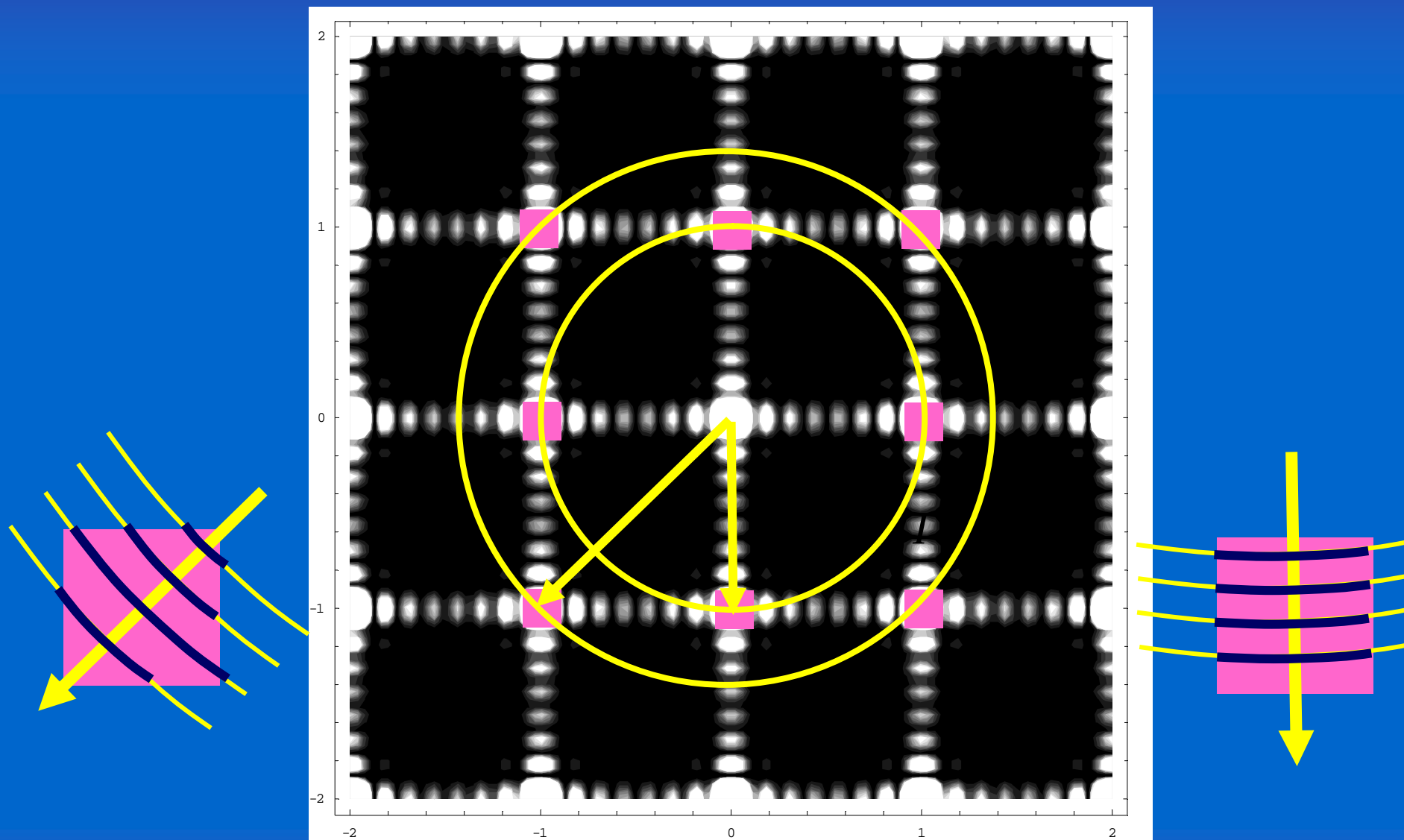
$\underline{s_0}/1$

$2q$

$\underline{s}/1$

$\underline{d}^*$

Powder Diffraction sphere
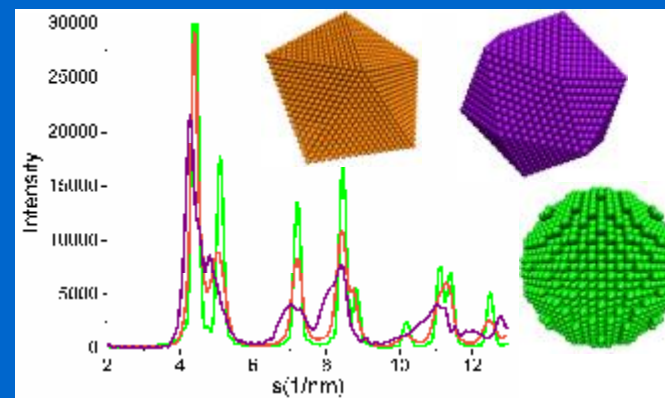
P. Scardi – Powder Diffraction & Synchrotron Radiation

Powder made of simple-shape crystallites
(one param., convex solids: sphere, cube, tetrahedron, octahedron,...)

$$b\left(d^*\right) = \frac{K_b}{D}$$

Scherrer formula (1918)

Paul Scherrer (1890–1969)

K_b , Scherrer constant, changes with crystallite shapes and (hkl)
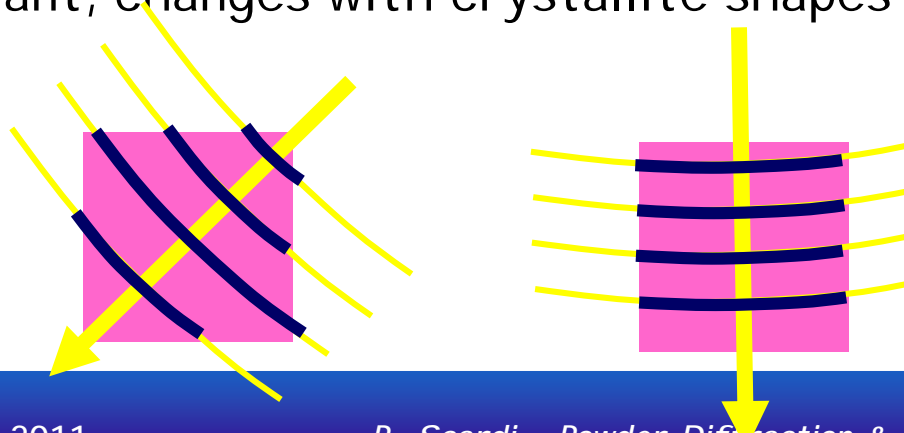
Powder made of simple-shape crystallites
(one param., convex solids: sphere, cube, tetrahedron, octahedron,…)

$$b\left(d^{*}\right)=\frac{K_b}{D}$$

Scherrer formula (1918)

Paul Scherrer (1890–1969)

K_b , Scherrer constant, changes with crystallite shapes and (hkl).

For a sphere:

$$K_b = \frac{4}{3}$$
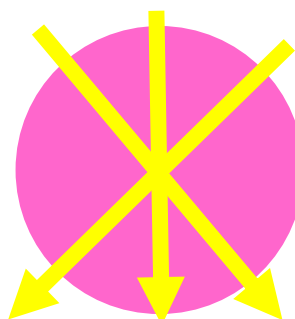
Profile information can be represented by the **Integral Breadth** β, (peak area / peak maximum). Assuming domain size effects only:

Scherrer formula

2q space
$$b(2q) = \frac{K_b l}{D \cos q}$$

recipr. space
$$b(d^*) = \frac{K_b}{D}$$
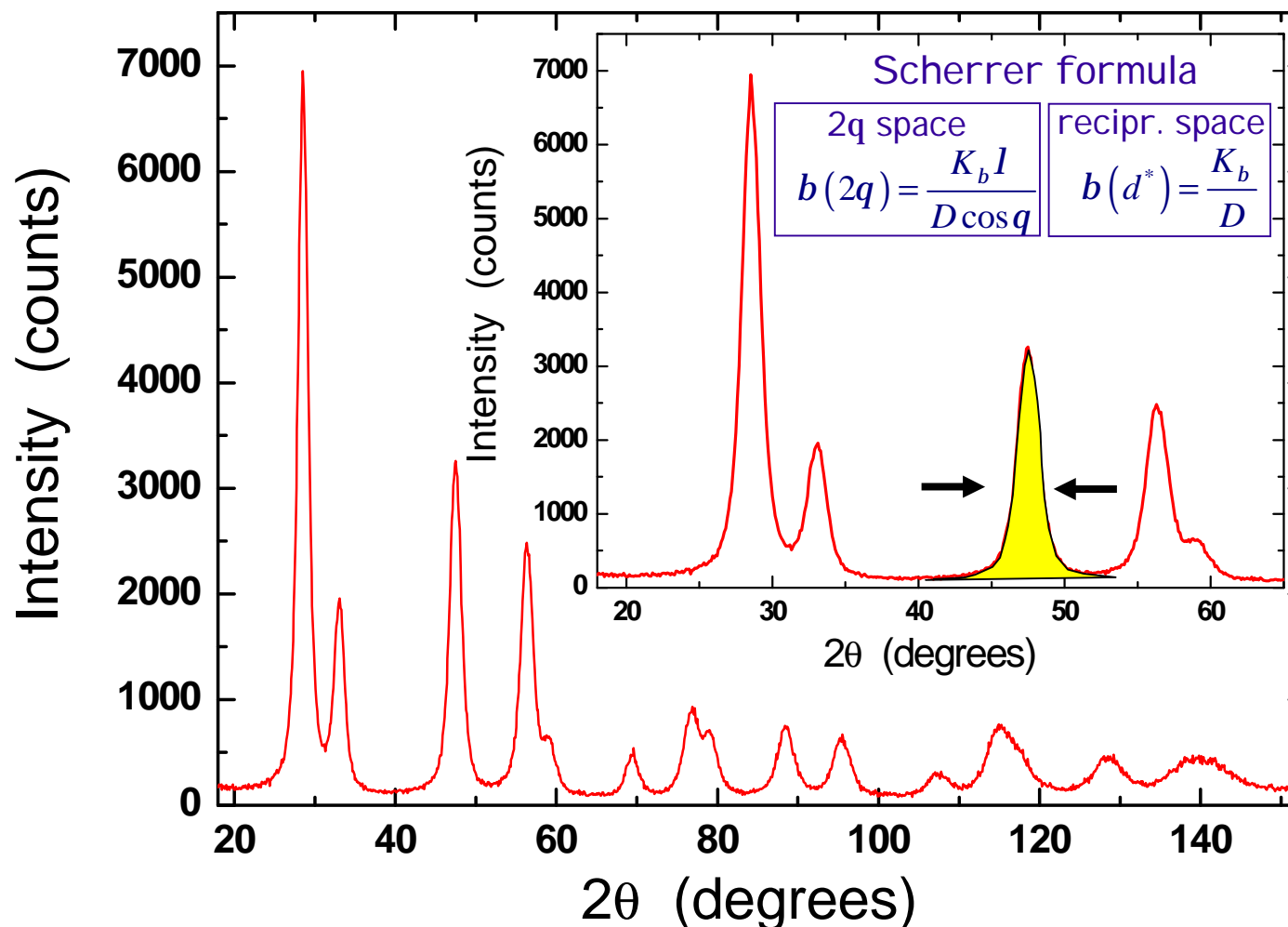
CAVEAT #1 – what is the true result of the Scherrer formula ?

For a DISTRIBUTION of crystallites
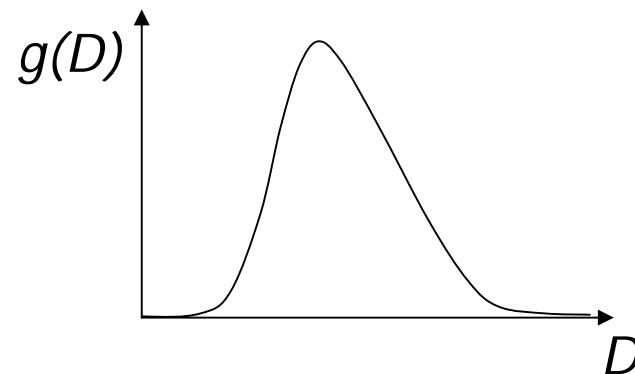
The integral breadth still provides a valid mean size value, but:

$$b\left(d^*\right) = \frac{K_b}{<D>_V} = K_b \frac{M_3}{M_4}$$

M_1 **à** *mean*

$M_2 - M_1^2$ **à** *variance*

where M_3, M_4 are 3rd and 4th moments of $g(D)$ $\left(M_i = \int D^i g(D) dD\right)$

CAVEAT #2 – what is the effect of lattice distortions ?

Quite complex: unit cells at distance L=na can be displaced and rotated.
Neglecting rotation and considering an average strain $\boxed{e = dL/L}$

$$I_c \propto |F|^2 e^{2piLd^* e(L)}$$

dL

L=n·a   L=n·a

$\underline{a}$ $\underline{a}$

undistorted   distorted
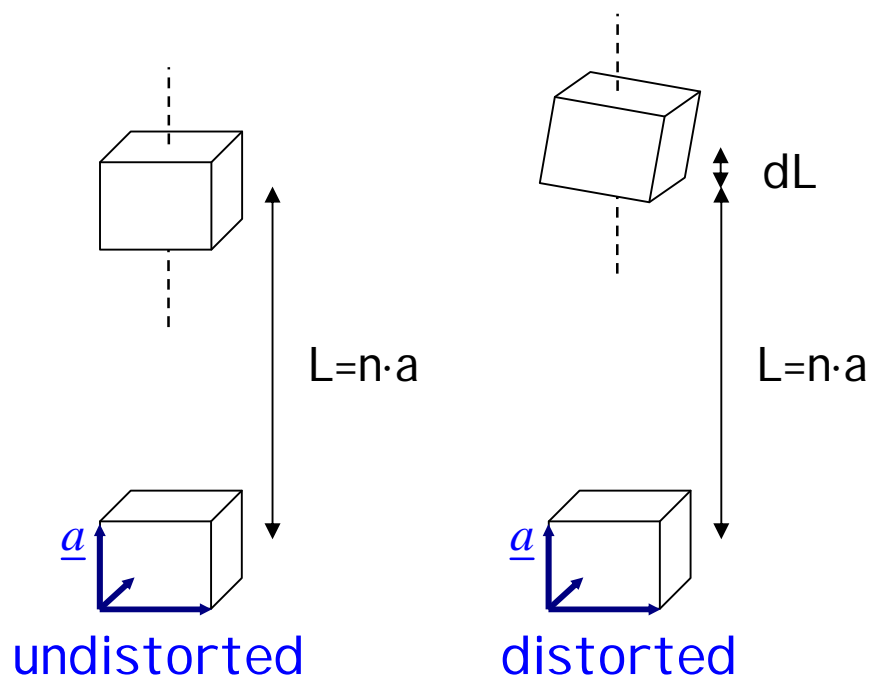
Considering both domain size and lattice distortion (microstrain) effects

(as a first order approximation):

$$b(2q) \approx \frac{K_b l}{<D>_V \cos q} + 2\left\langle e^2 \right\rangle^{1/2} \tan q$$

$$\left[b(d^*) = b(2q) \cdot \cos q / l \right]$$

Considering both domain size and lattice distortion (microstrain) effects

Williamson-Hall (WH) plot

$$b\left(d^*\right)=\frac{K_b}{<D>_V}+2e\cdot d^*$$

$$\left[b\left(d^*\right)=b\left(2q\right)\cdot\cos q/1\right]$$

β(d*) (nm⁻¹) — y-axis

d* (nm⁻¹) [=2sinθ/λ] — x-axis
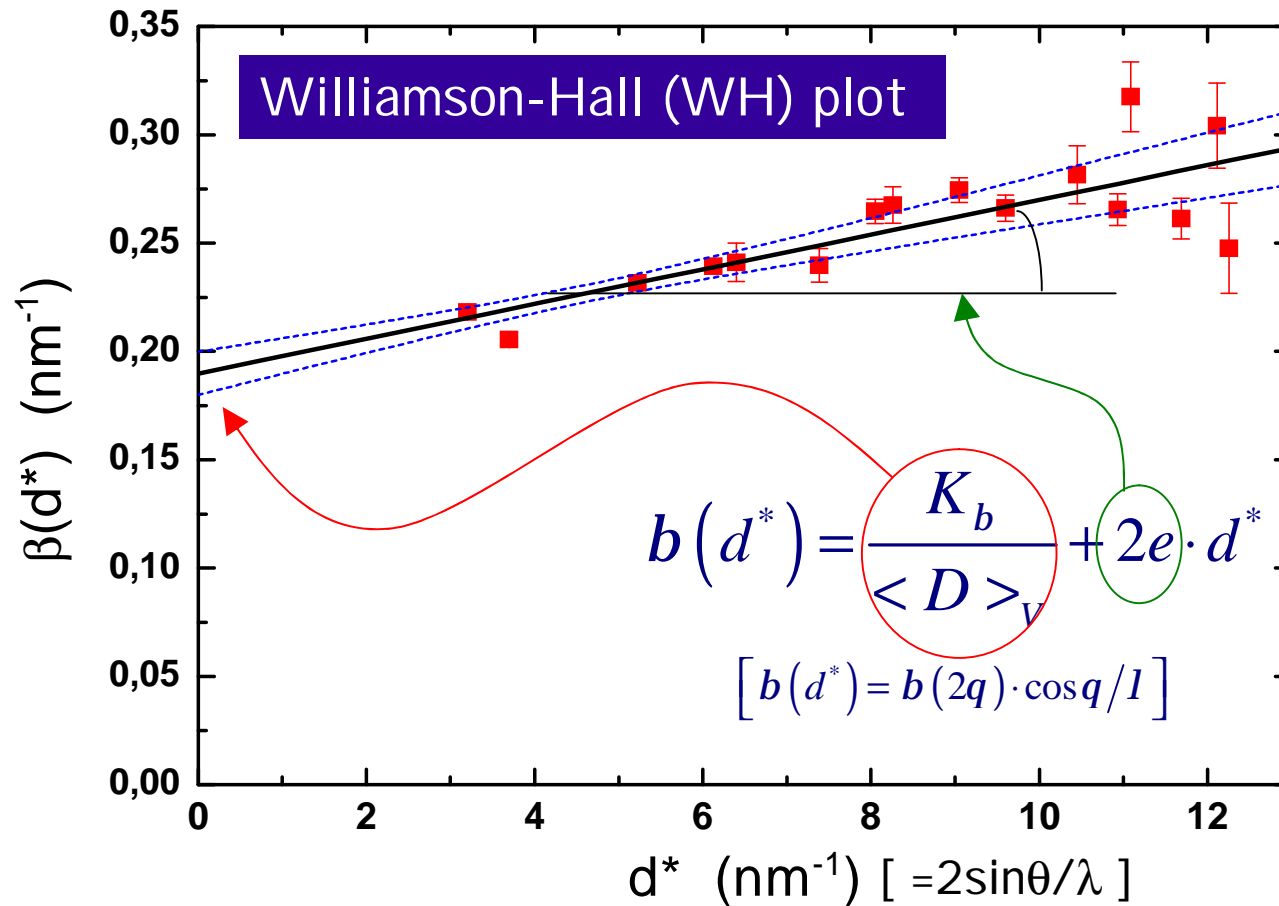
In a β(d*) vs. d* plot, intercept and slope of linear regression are related, respectively, to $<D>_V$ and e

Peak profiles invariably overlap in powder patterns. This can make it difficult to extract profile information directly from observed data
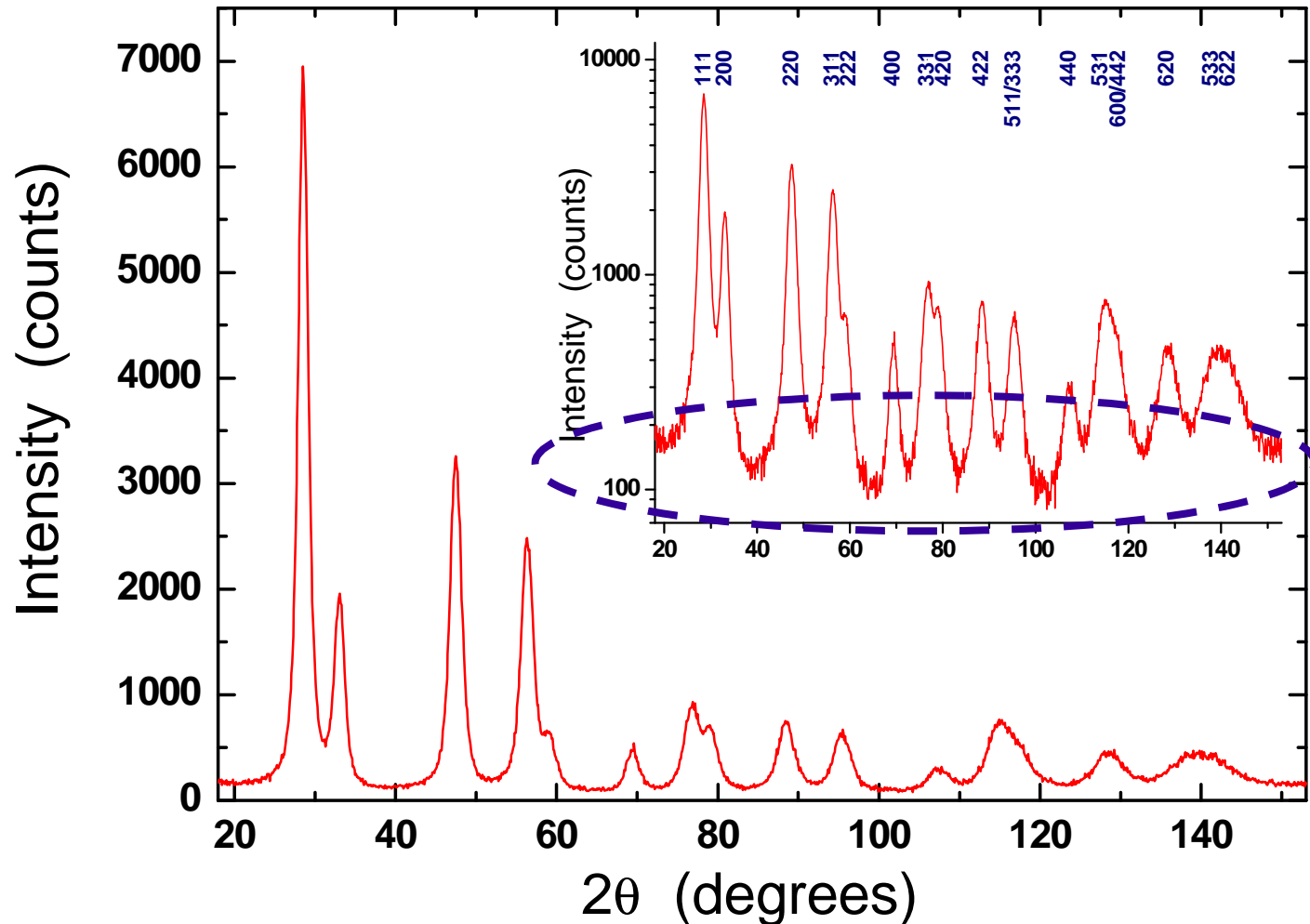
… a step forward

P. Scardi – Powder Diffraction & Synchrotron Radiation

WPPM is based on a direct modelling of the experimental pattern, based on physical models of the microstructure and lattice defects:

Diffraction Pattern	**WPPM** *Physical Model*	Microstructural Parameters

Nanocrystalline cerium oxide from xerogel, 1h @ 400°C

M. Leoni, R. Di Maggio, S. Polizzi & P. Scardi, J. Am. Ceram. Soc. 87 (2004) 1133.
P.Scardi & M. Leoni, Acta Cryst. A 57 (2001) 604. P.Scardi & M. Leoni, Acta Cryst. A 58 (2002) 190

Nanocrystalline cerium oxide
from xerogel, 1h @ 400°C
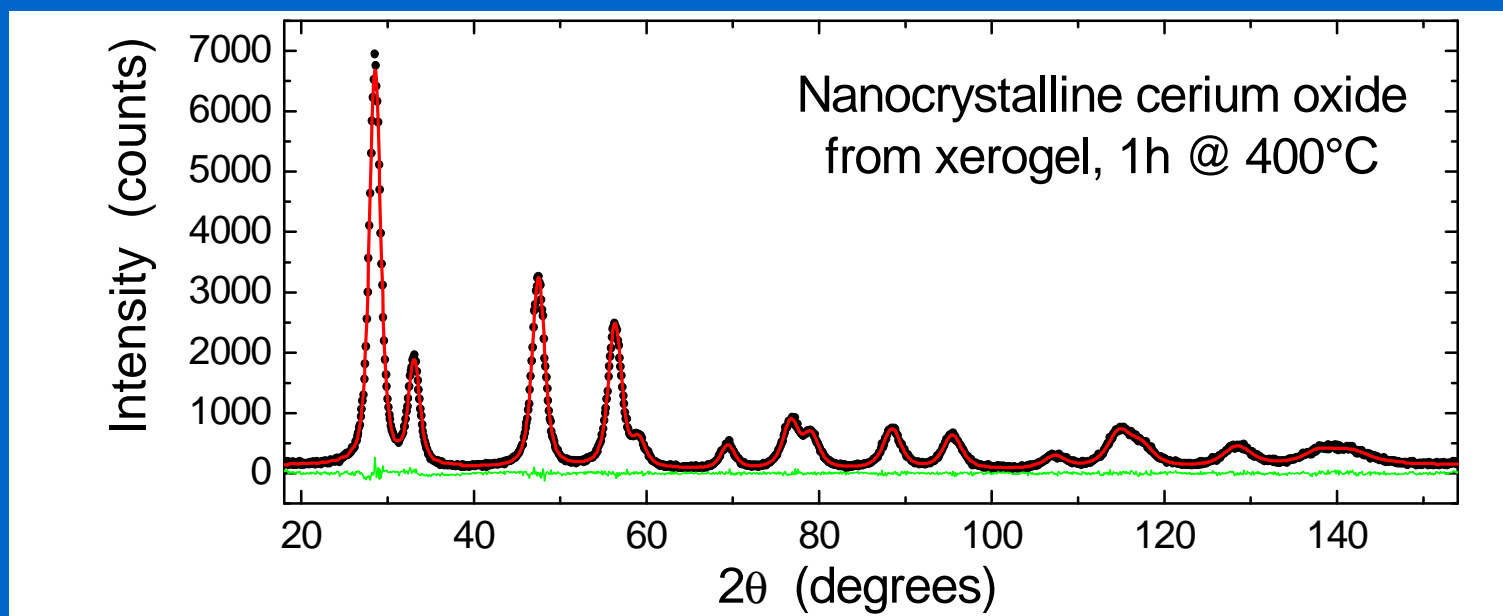
M. Leoni, R. Di Maggio, S. Polizzi & P. Scardi, J. Am. Ceram. Soc. 87 (2004) 1133.
P.Scardi & M. Leoni, Acta Cryst. A 57 (2001) 604. P.Scardi & M. Leoni, Acta Cryst. A 58 (2002) 190

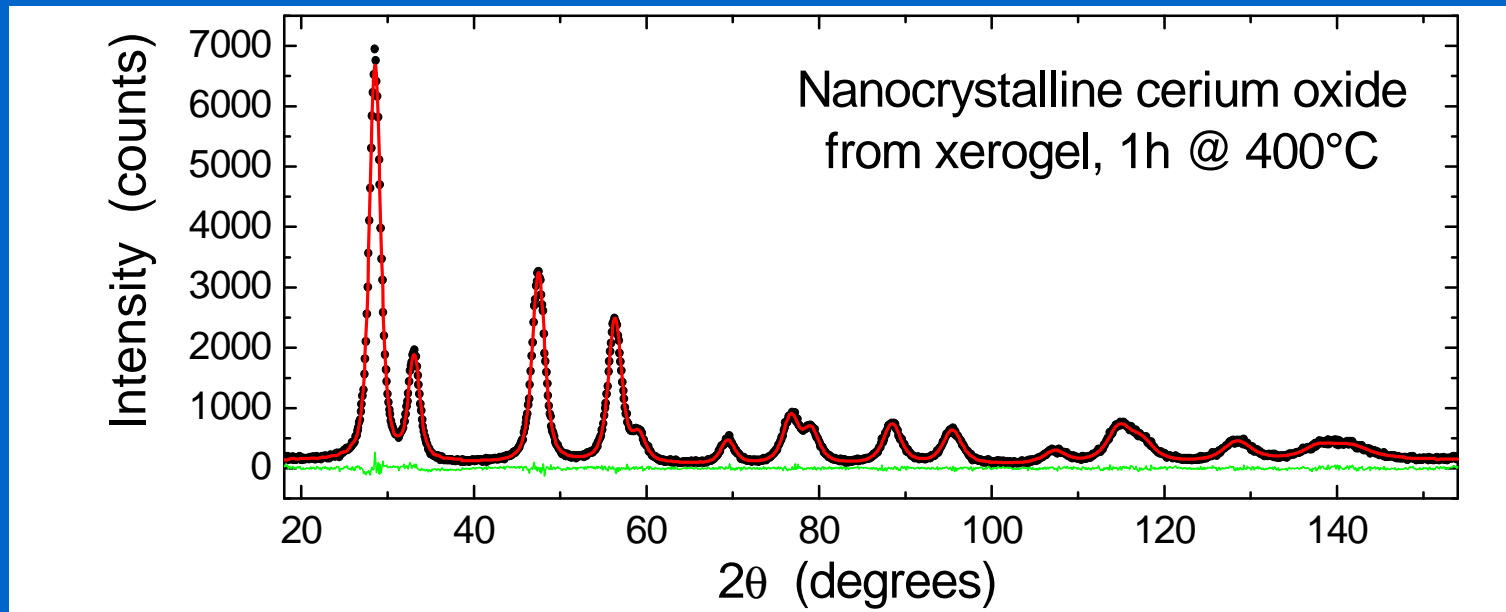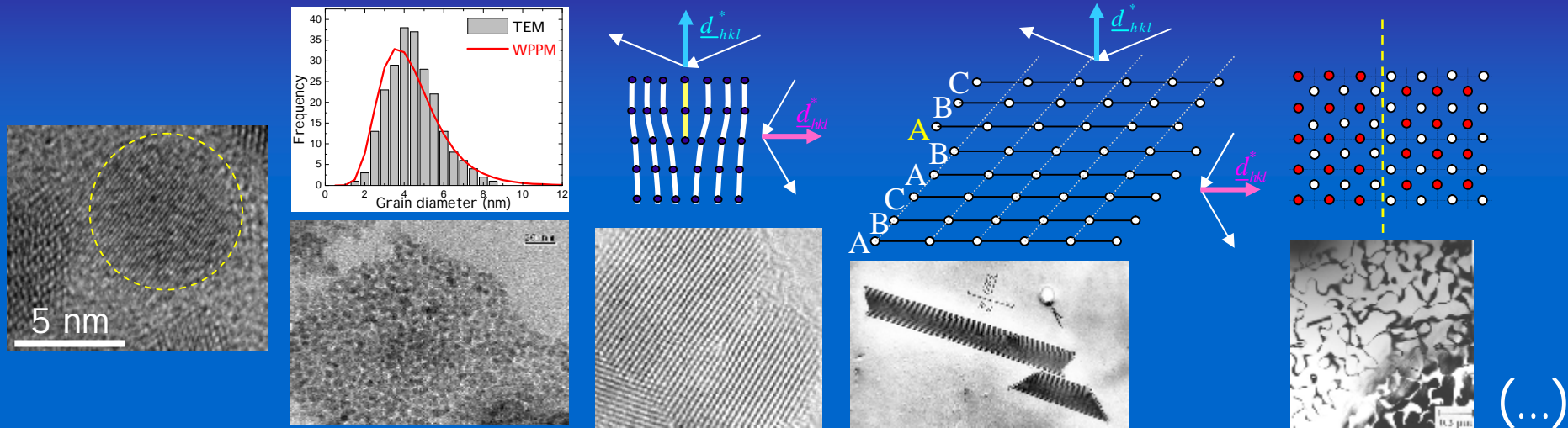*WPPM* is based on a direct modelling of the experimental pattern, based on physical models of the microstructure and lattice defects:

| Diffraction Pattern | WPPM *Physical Model* | Microstructural Parameters |

How does it work ??

So far we consider that different effects affecting the line profile simply 'add', i.e., the peak width is the sum of different components.

According to the Williamson-Hall formula,

$$b\left(d^*\right)=\underbrace{\frac{K_b}{<D>_V}}_{\text{'size'}}+\underbrace{2e\cdot d^*}_{\text{'strain'}}$$

Actually, this is not the general case ...

A diffraction peak is a **convolution** ($\otimes$) of *profile components* produced by different sources: instrumental profile (IP), domain size (S), microstrain (D), faulting (F), anti-phase domain boundaries (APB), stoichiometry fluctuations (C), grain surface relaxation (GSR), etc.

$$I(s) = I^{IP}(s) \otimes I^{S}(s) \otimes I^{D}(s) \otimes I^{F}(s) \otimes I^{APB}(s) \otimes I^{C}(s) \otimes I^{GRS}(s)...$$

$$h \;=\; g \qquad \otimes \qquad f$$

What is the difference between *convolution* and *sum* of effects ??

What is the difference between convolution and sum of effects ??
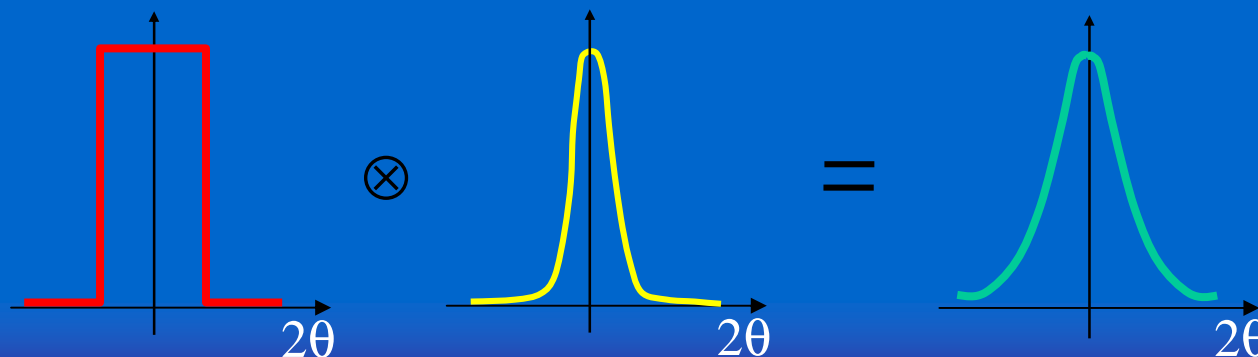
Example: let's just consider instrument (IP) and domain size (S):
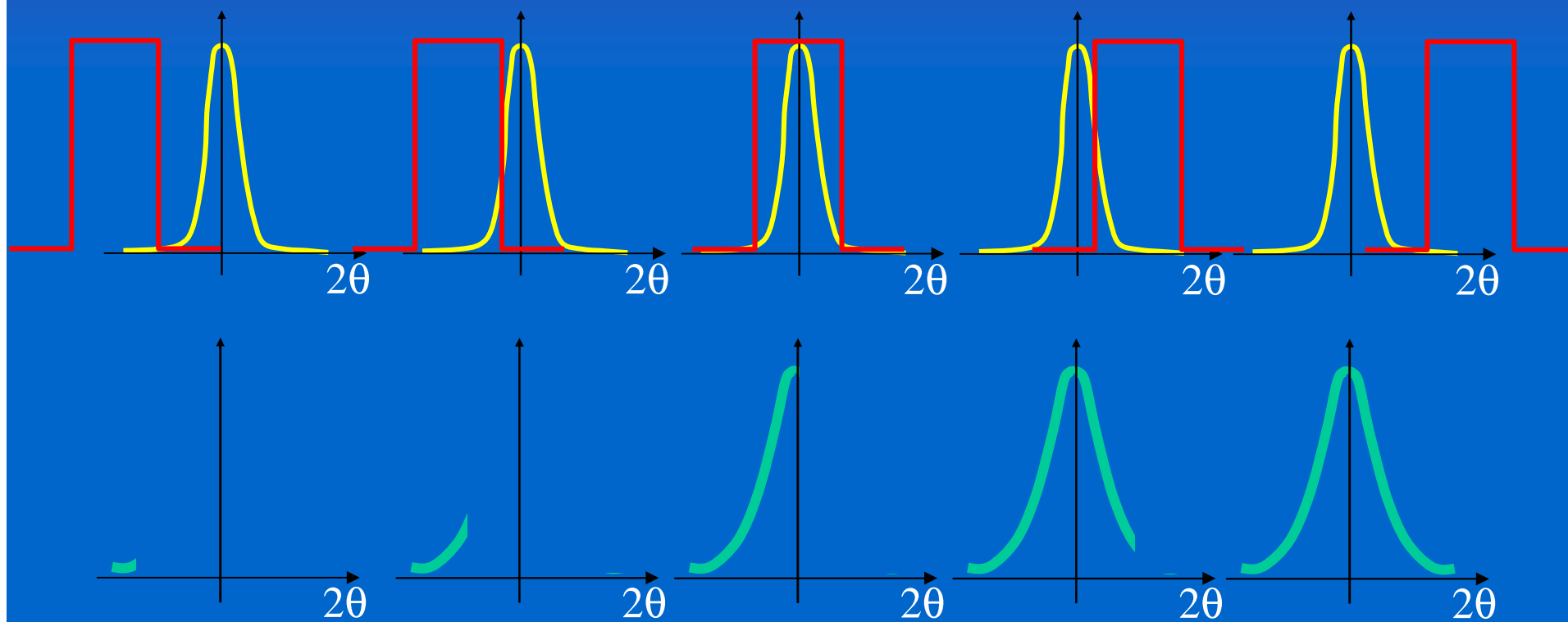
$$I(s) = I^{IP}(s) \otimes I^{S}(s)$$

$$I(s) = \int I^{IP}(t) I^{S}(s-t)\, dt$$

g profile, slit (box) function; f profile, bell-shape function (e.g. gaussian)

$$h = g \otimes f$$

A diffraction peak is a **convolution** ($\otimes$) of *profile components* produced by different sources: instrumental profile (IP), domain size (S), microstrain (D), faulting (F), anti-phase domain boundaries (APB), stoichiometry fluctuations (C), grain surface relaxation (GSR), etc.

$$I(s) = I^{IP}(s) \otimes I^{S}(s) \otimes I^{D}(s) \otimes I^{F}(s) \otimes I^{APB}(s) \otimes I^{C}(s) \otimes I^{GRS}(s)\dots$$

$$h = g \qquad \otimes \qquad f$$

the Fourier Transform of I(s) is the product of the FTs of the single profile components

The diffraction profile results from a convolution of effects:

$$I(s) = I^{IP}(s) \otimes I^{S}(s) \otimes I^{D}(s) \otimes I^{F}(s) \otimes I^{APB}(s) \otimes I^{C}(s) \otimes I^{GRS}(s)\ldots$$

the Fourier Transform of I(s) is the product of the FTs of the single profile components

$$I(s) \propto \cdot \int_{-\infty}^{\infty} C(L) \mathrm{e}^{2p\,iL \cdot s_{hkl}} \, dL$$

$$C = \prod_i A_i = T_{pV}^{IP} \cdot A_{\{hkl\}}^{S} \cdot A_{\{hkl\}}^{D} \cdot (A_{hkl}^{F} + iB_{hkl}^{F}) \cdot A_{\{hkl\}}^{APB} \cdot \ldots$$

instr. profile   domain size/shape   lattice defects / strain

P. Scardi & M. Leoni J. Appl. Cryst. 39 (2006) 24 - P. Scardi & M. Leoni, Acta Cryst. A58 (2002) 190

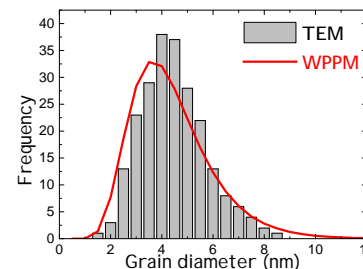$$T_{pV}^{IP}(L) = (1-k) \cdot \exp\left(-p^2 \cdot s_s^2 L^2 / \ln 2\right) + k \exp\left(-2p \cdot s_s L\right)$$

Instrumental profile
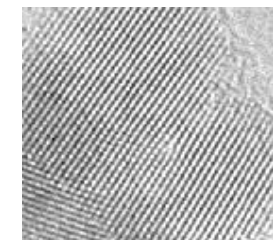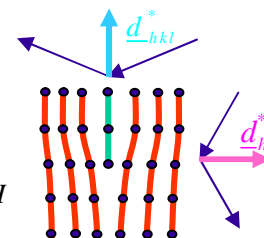
Domain size effect: m, s

$$A^S(L) = \sum_{n=0}^{3} H_n^c \cdot Erfc\left[\frac{\ln\left(L \cdot K^c\right) - m - (3-n)s^2}{s\sqrt{2}}\right] \frac{M_{l,3-n}}{2M_{l,3}} \cdot L^n$$
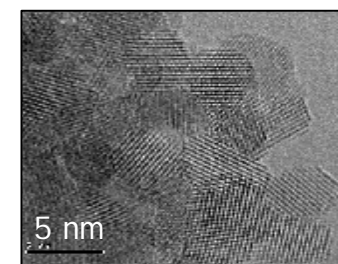
Dislocation (strain) effect: r, Re, $(\overline{C}_{hkl})$

$$A_{\{hkl\}}^D(L) = \exp\left[-\frac{1}{2}p|b|^2 \overline{C}_{hkl} r d_{\{hkl\}}^{*2} \cdot L^2 f^*\left(L/R_e\right)\right]$$

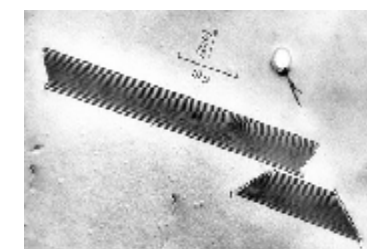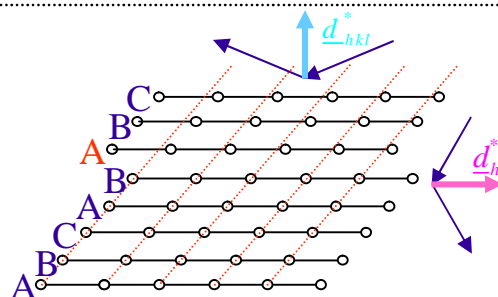$$\overline{C}_{hkl} = A + B \cdot \frac{h^2 k^2 + k^2 l^2 + l^2 h^2}{\left(h^2 + k^2 + l^2\right)^2} = A + B \cdot H$$
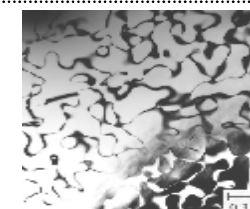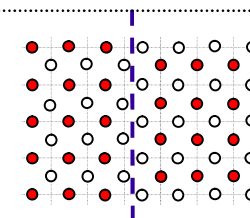
Faulting: a (def.), b (twin)

$$A_{hkl}^F(L) = \left(1 - 3a - 2b + 3a^2\right)^{\left|\frac{1}{2}Ld_{\{hkl\}}^* \cdot \frac{L_o}{h_o^2} s_{L_o}\right|}$$

$$B_{hkl}^F(L) = -s_{L_o} \cdot \frac{L}{|L|} \cdot \frac{L_o}{|L_o|} \cdot b \Big/ \left(3 - 6b - 12a - b^2 + 12a^2\right)^{1/2}$$

Anti-Phase Domains: g

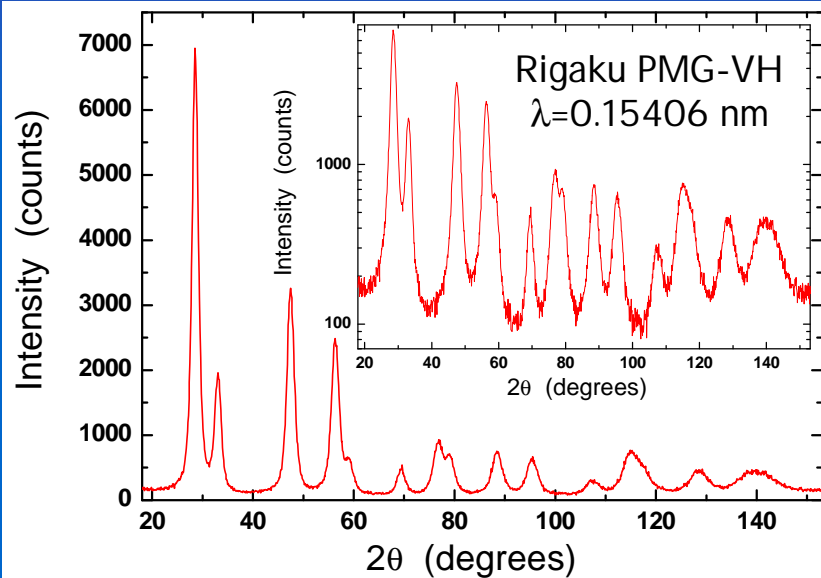$$A_{\{hkl\}}^{APB}(L) = \exp\left[-\frac{-2g\left(|h| + |k|\right) \cdot L}{d_{hkl}\left(h^2 + k^2 + l^2\right)}\right]$$
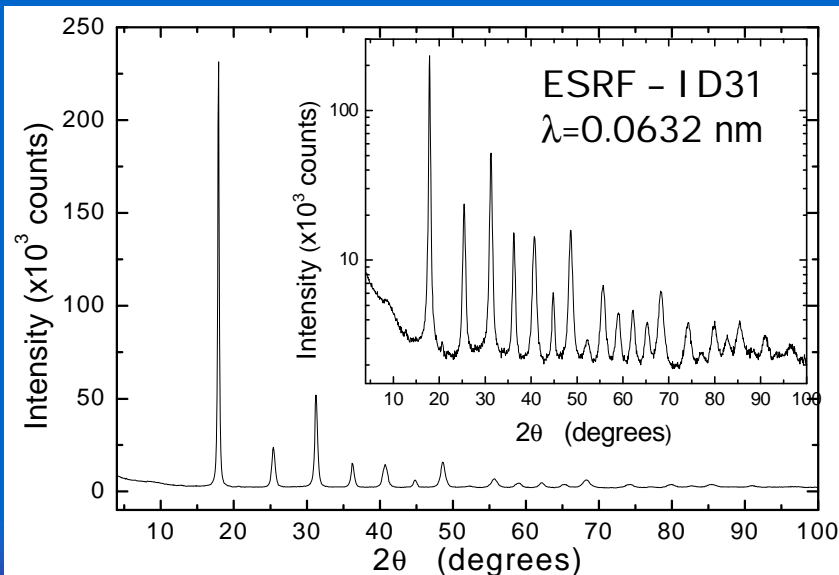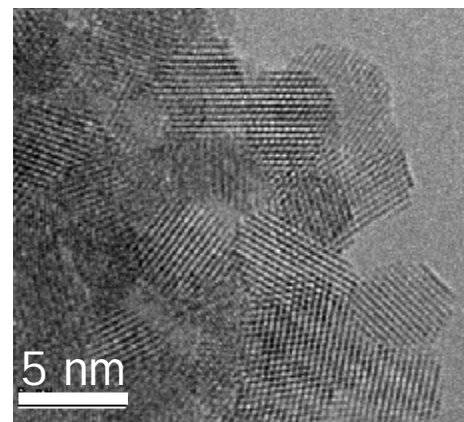
WPPM APPLICATIONS

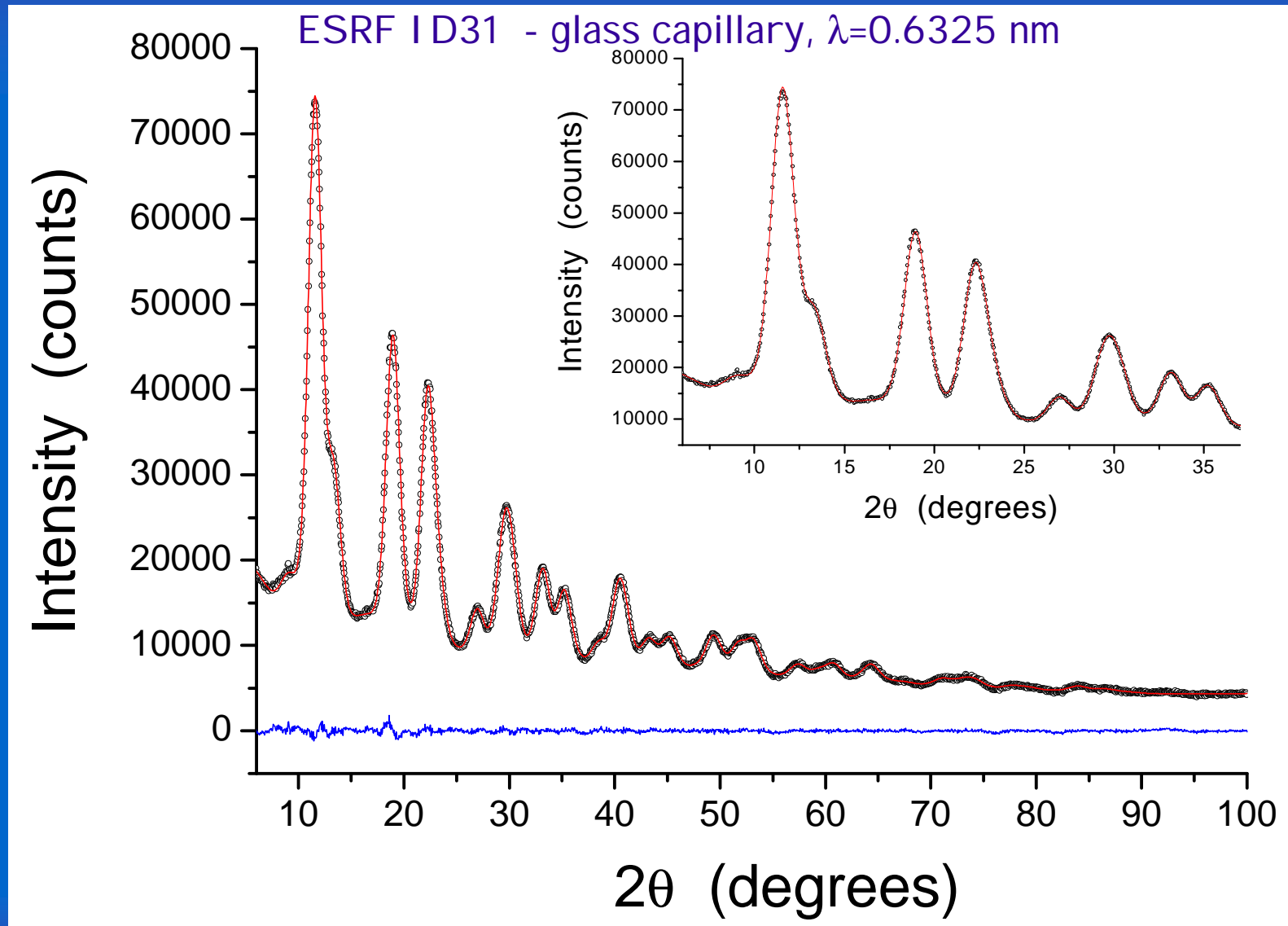## Two typical cases of study

Cerium oxide powder from xerogel
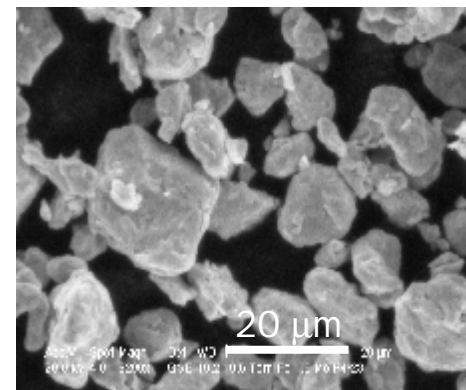
Rigaku PMG-VH
λ=0.15406 nm

5 nm

Ball milled Fe-1.5%Mo

ESRF – ID31
λ=0.0632 nm

20 µm

Xerogel obtained by vacuum-drying: broad diffraction lines of nanocrystalline fcc phase

ESRF ID31 - glass capillary, λ=0.6325 nm

Xerogel obtained by vacuum-drying: broad diffraction lines of nanocrystalline fcc phase

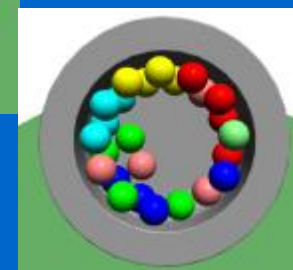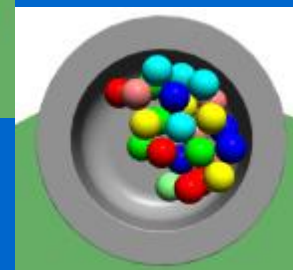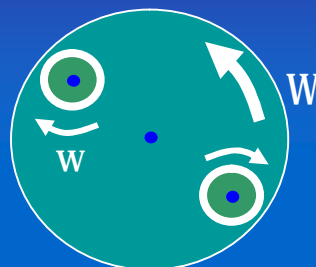ESRF ID31 - glass capillary, λ=0.6325 nm

<D>=2.25(10) nm
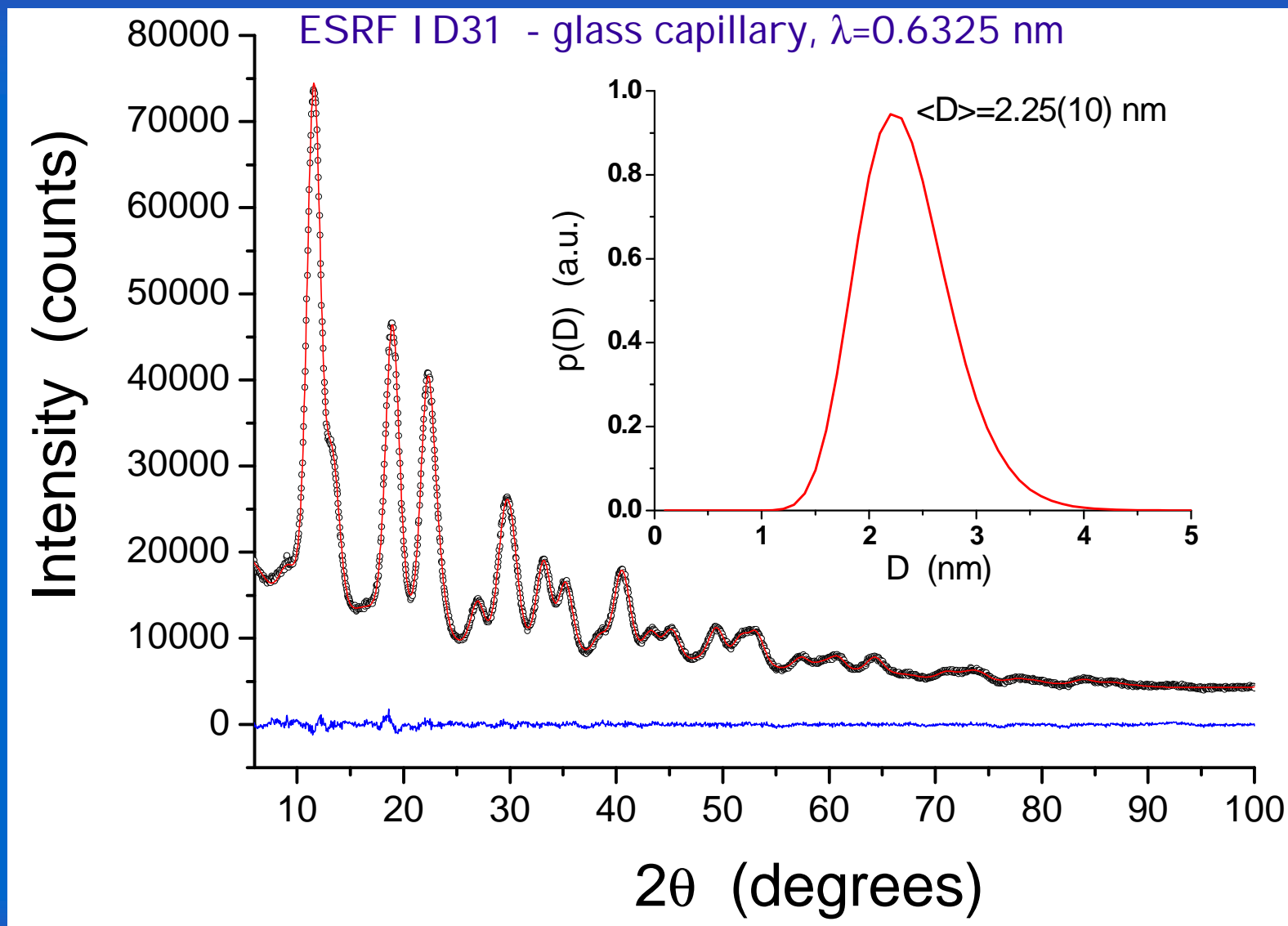
NANOCRYSTALLINE Fe-1.5%Mo POWDER
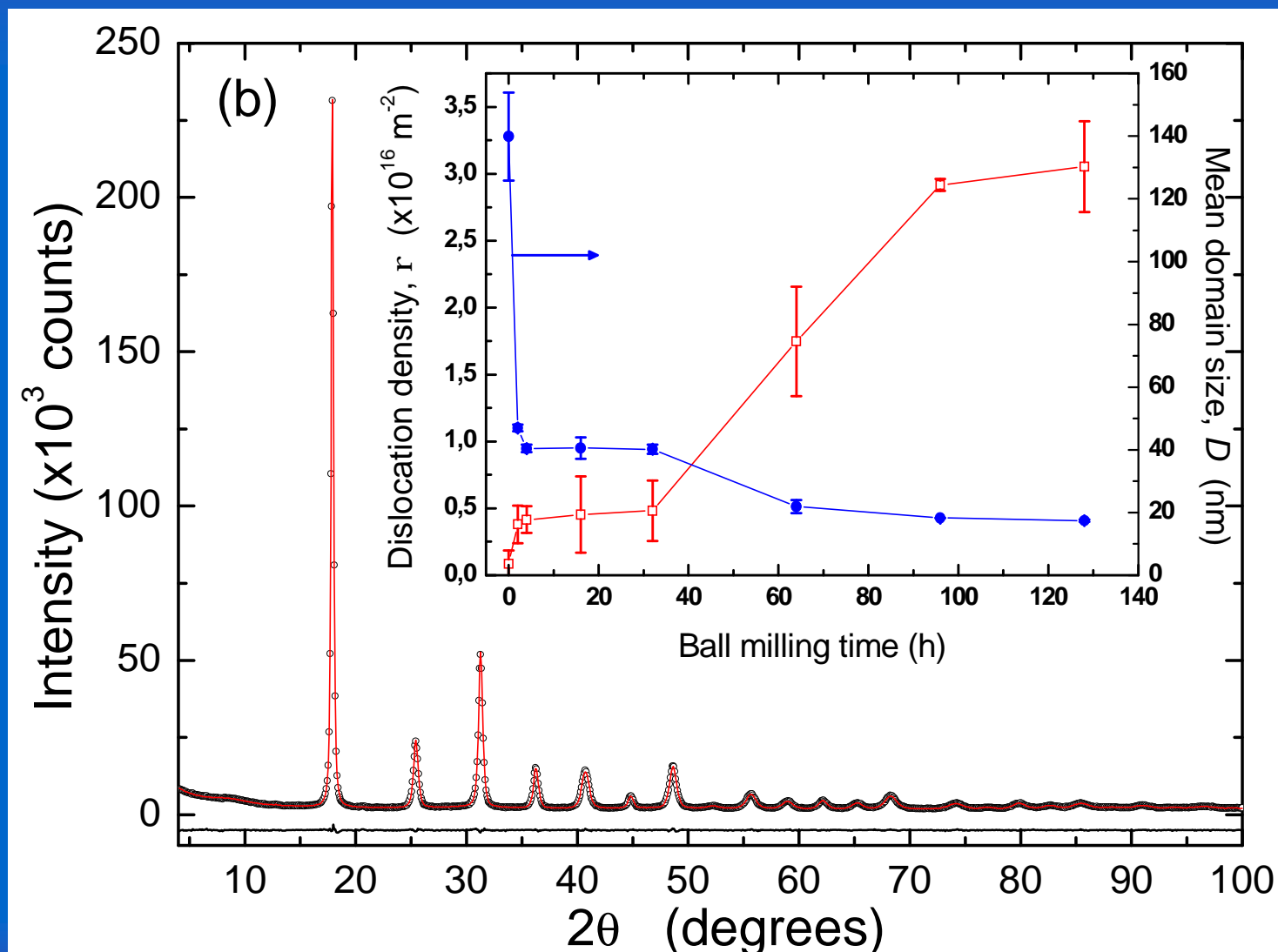
Planetary ball milling - production of nanocrystalline Fe-1.5%Mo

P. Scardi – Powder Diffraction & Synchrotron Radiation

Ball milled Fe1.5Mo (Fritsch P4) – data collected at ESRF – ID31 λ=0.0632 nm

Ball milled Fe1.5Mo (Fritsch P4) – data collected at ESRF – ID31 λ=0.0632 nm

Ball milled Fe1.5Mo (Fritsch P4) – data collected at ESRF – ID31 λ=0.0632 nm

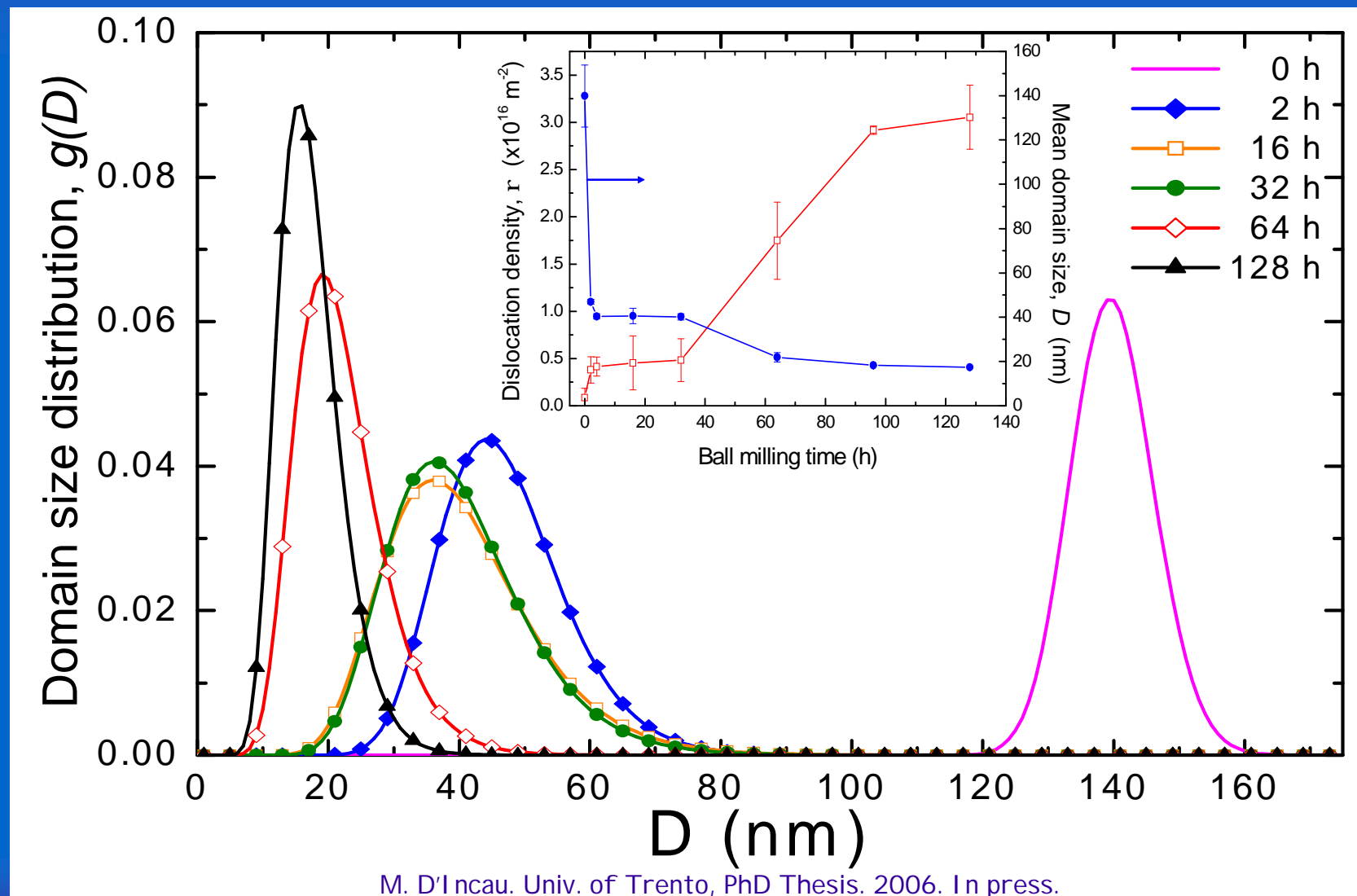Ball milled Fe1.5Mo (Fritsch P4) – data collected at ESRF – ID31 λ=0.0632 nm
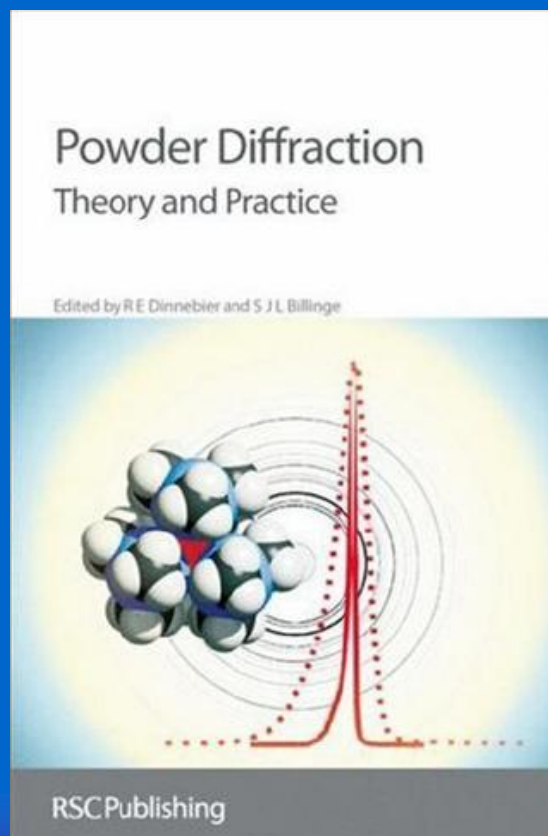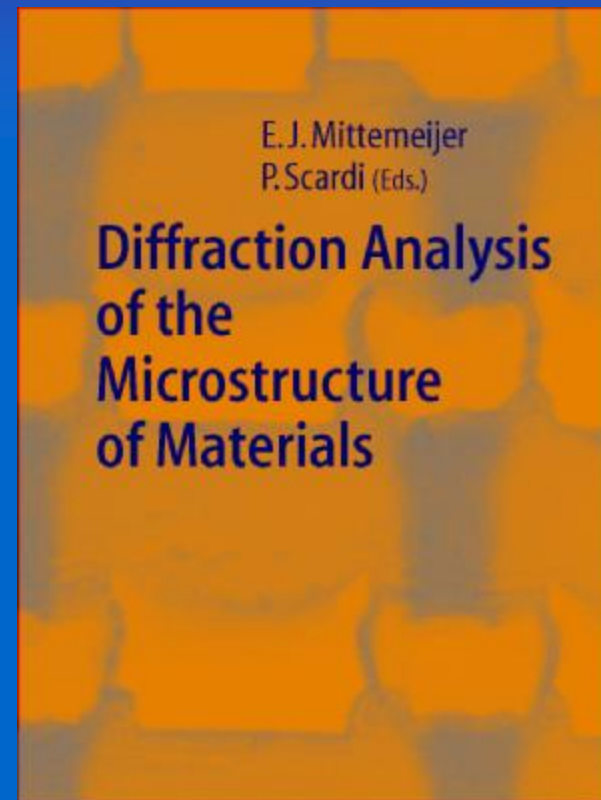In addition to mean values, WPPM provides the size distribution

M. D'Incau. Univ. of Trento, PhD Thesis. 2006. In press.

Diffraction Analysis of Materials Microstructure

E.J. Mittemeijer & P. Scardi, editors.

Berlin: Springer-Verlag, 2004.

E. J. Mittemeijer
P. Scardi (Eds.)

**Diffraction Analysis
of the
Microstructure
of Materials**

Powder Diffraction
Theory and Practice

Edited by R E Dinnebier and S J L Billinge

RSC Publishing

Powder Diffraction: Theory and Practice

R.E. Dinnebier & S.J.L. Billinge, editors.

Cambridge: RSC Publishing, 2008. Cap. XIII, p.376

Paolo.Scardi@unitn.it

P. Scardi – Powder Diffraction & Synchrotron Radiation

Powder Diffraction & Synchrotron Radiation

P. Scardi

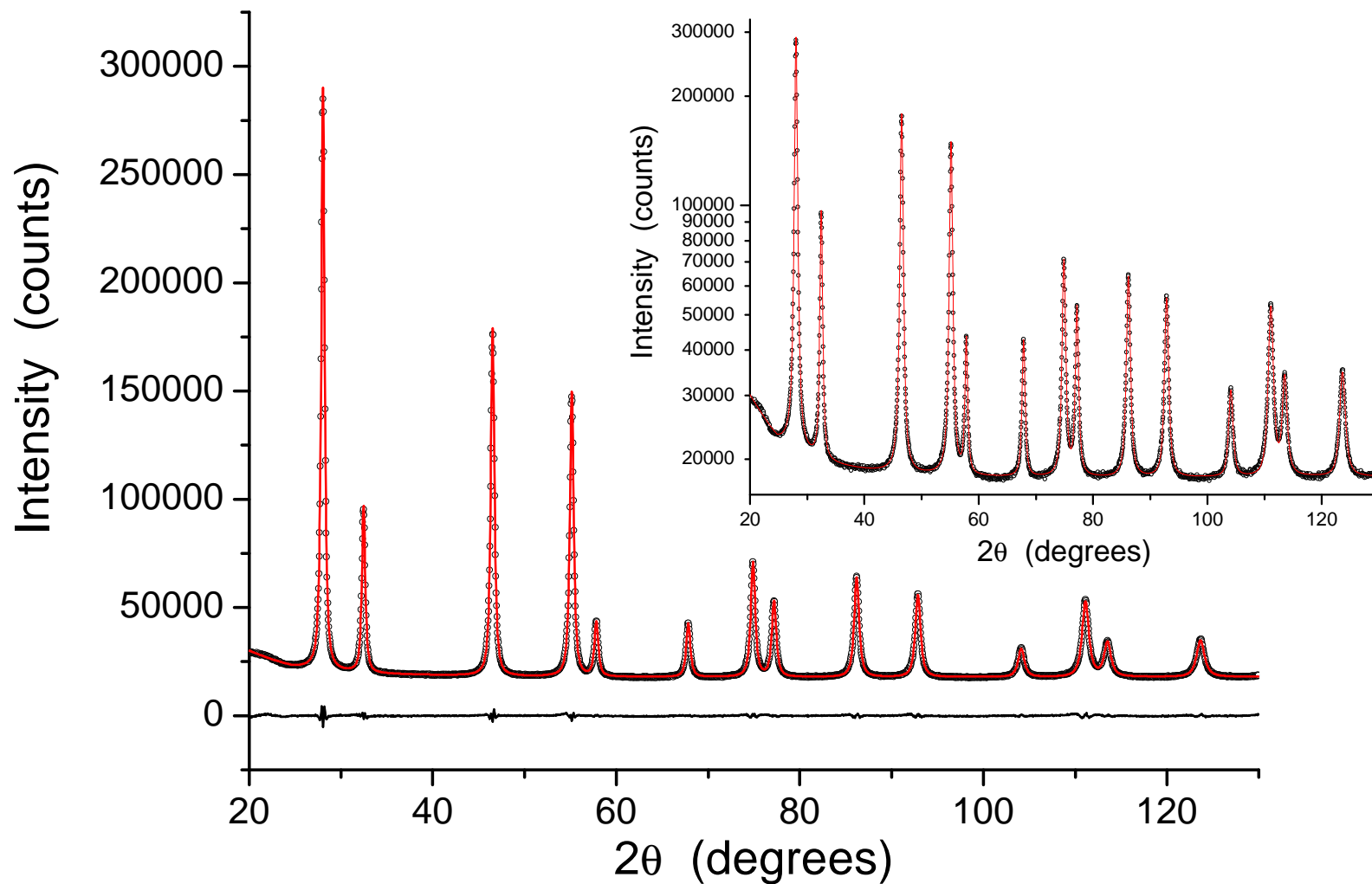*Department of Materials Engineering and Industrial Technologies*
University of Trento

XRD data collected at Campinas Synchrotron (Brasil)

ZrO$_2$-90%CeO$_2$ catalyst: nanocrystalline powder

XRD data collected at Campinas Synchrotron (Brasil)
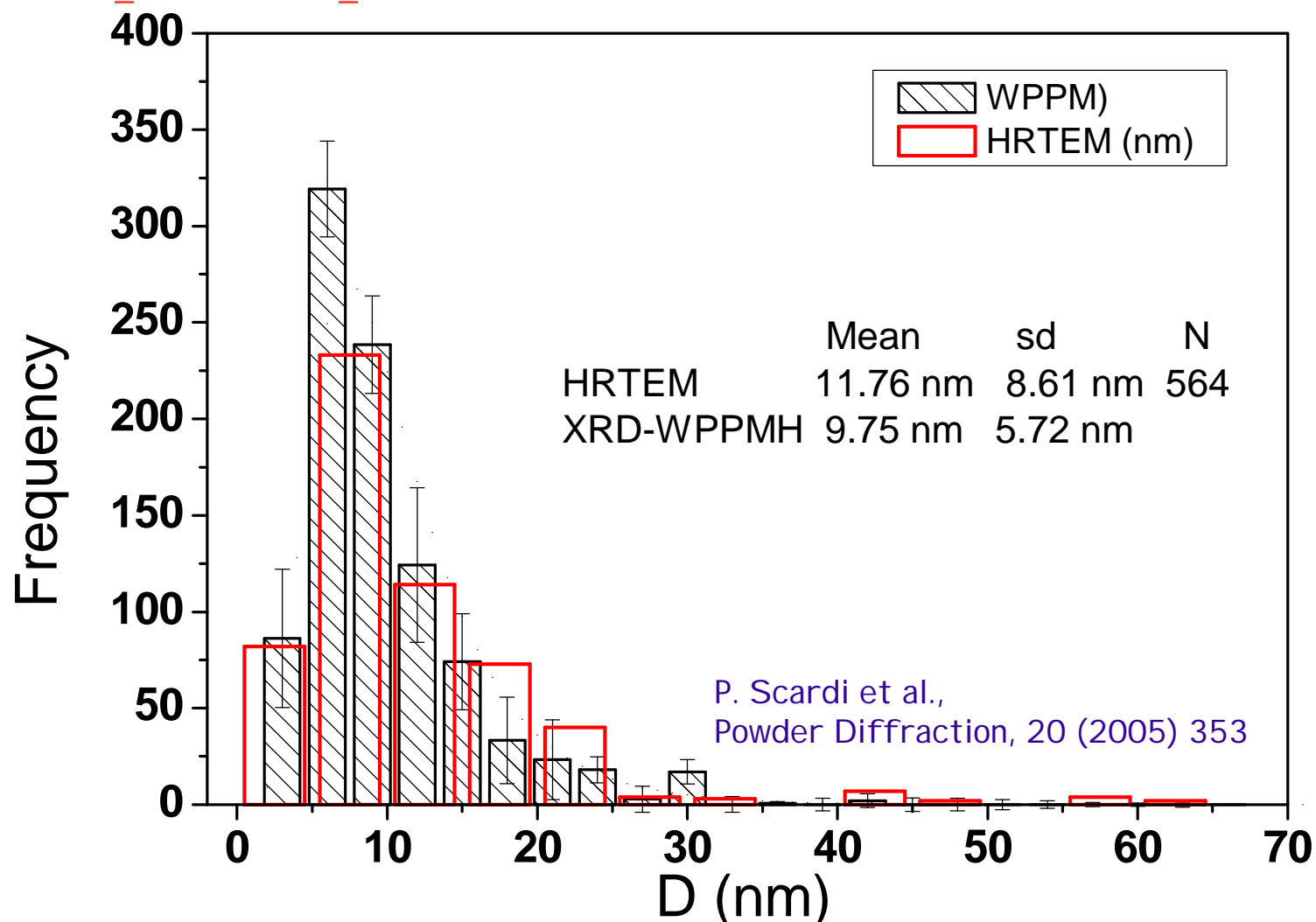
ZrO$_2$-90%CeO$_2$ catalyst: nanocrystalline powder

XRD data collected at Campinas Synchrotron (Brasil)

ZrO$_2$-90%CeO$_2$ catalyst: comparison between WPPM and TEM
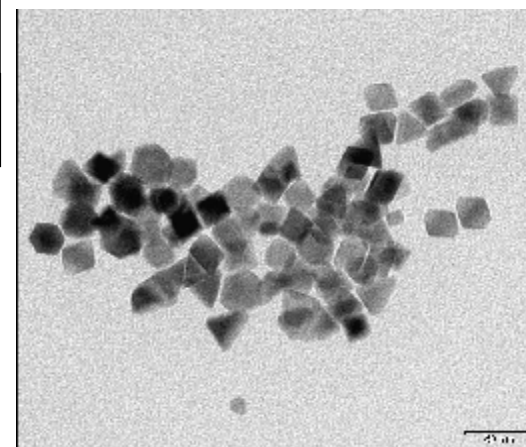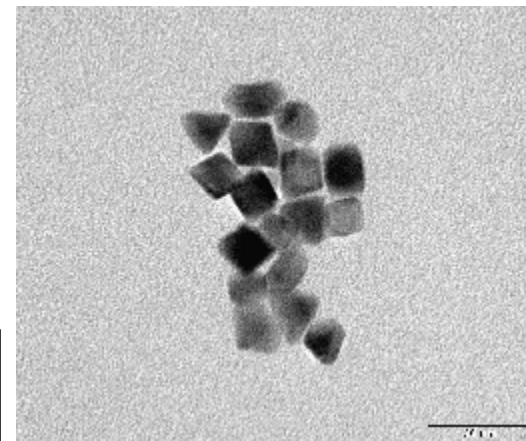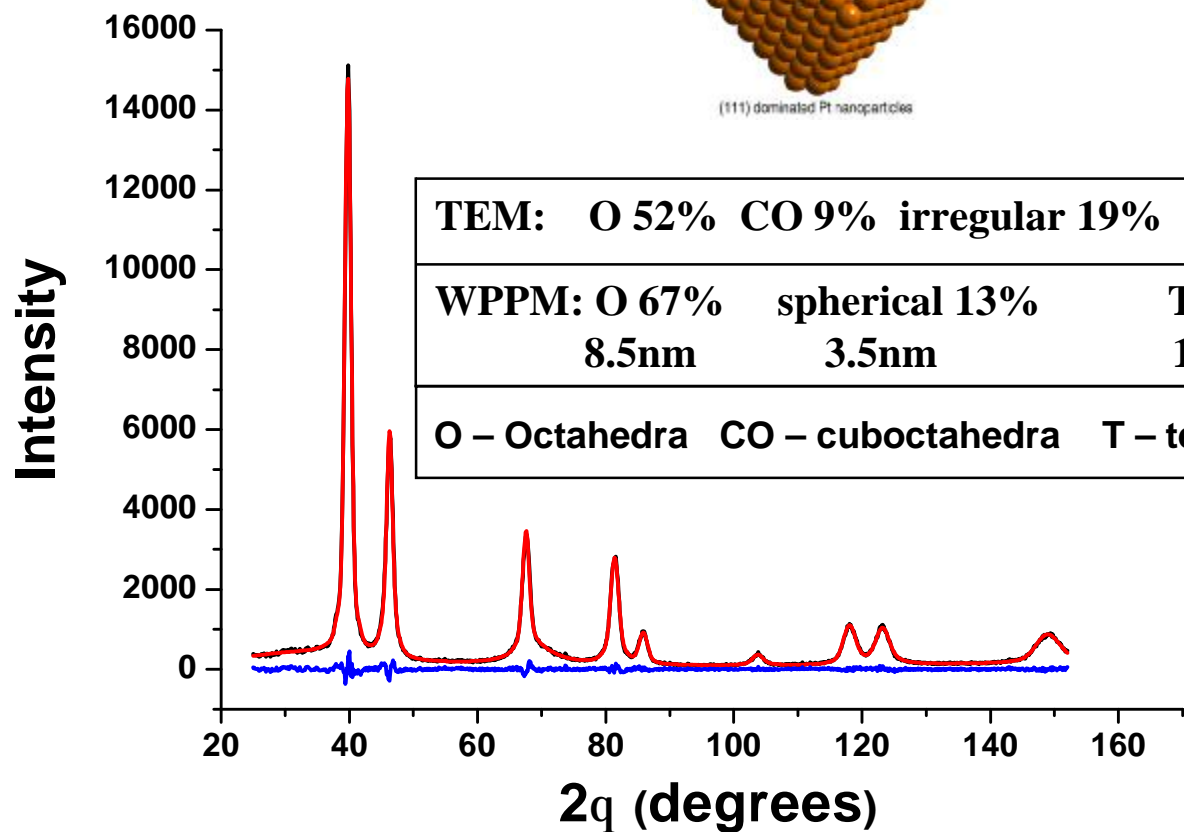

Legend:
- WPPM)
- HRTEM (nm)

	Mean	sd	N
HRTEM	11.76 nm	8.61 nm	564
XRD-WPPMH	9.75 nm	5.72 nm	

P. Scardi et al.,
Powder Diffraction, 20 (2005) 353

The quest for control of nanocrystal size and shape

preferential (111) Pt:

(111) dominated Pt nanoparticles

TEM:	O 52%	CO 9%	irregular 19%	T 21%
WPPM:	**O 67%** 8.5nm		**spherical 13%** 3.5nm	**T 20%** 17nm
O – Octahedra		**CO – cuboctahedra**		**T – tetrahedra**

K.R. Beyerlein, J. Solla-Gullón, E. Herrero, E. Garnier, F. Pailloux, M. Leoni, P. Scardi, R.L. Snyder, A. Aldaz, J.M. Feliu, Mat. Sci. Eng. A 528 (2010) 83